TECHNISCHE UNIVERSITÄT KAISERSLAUTERN

Functional and Structural Analyses of RTP1, a Rust Haustorial Protein Transferred into Host Plant Cells

Vom Fachbereich Biologie
der Technischen Universität Kaiserslautern
zur Erlangung des akademischen Grades

„Doktor der Naturwissenschaften“

genehmigte Dissertation

(D 386)

vorgelegt von

MSc. Maryam Rafiqi

Betreuer: Herr Prof. Dr. M. Hahn
Koreferent: Herr Prof. Dr. H. E. Neuhaus

Datum der wissenschaftlichen Aussprache: 27.03.2007
Erscheinungsort: Kaiserslautern

Dedication

Dedicated to my mother, who stood by me at my times of needs.

i. List of Abbreviations

ATP	adenosine triphosphate
Avr	avirulence gene or protein
bp	base pair(s)
BSA	bovine serum albumine
cDNA	complementary DNA
Col0	*Arabidopsis* ecotype Columbia0
DTT	dithiothreitol
EDTA	ethylenedinitro-N,N,N',N'-tetraacetic acid
EF2a	elongation factor 2a
ER	Endoplasmic reticulum
GFP	green fluorescent protein
GUS	β- glucoronidase
HMC	Haustorial mother cell
HR	hypersensitive response
M	molar
MCS	Multiple Cloning Site
MES	2-morpholinoethanesulfonic acid monohydrate
min	minute
mRNA	messenger RNA
MS	Murashige and Skoog medium
NLS	nuclear localization signal
OD	optical density
PAGE	poly acrylamide gel electrophoresis
PCR	Polymerase Chain Reaction
PDF1.2	the plant defensin gene
PR	pathogenicity related gene
R	resistance gene or protein
rpm	rotation per minute
RT	reverse transcriptase
RTP1	rust transferred protein 1
s	second
SDS	Sodiumdodecylsulfate
SP	Signal peptide
T3SS	type III secretion system
T-DNA	transfer-DNA
Tris	tris(hydroxymethyl)aminomethan
WT	wild type
X-Gluc	5-bromo-4-chloro-3-indolyl-α-galactopyranoside
YEB	yeast extract broth medium

Legend

RTP1	indicates the name of the gene or cDNA
sRTP1	indicates the name of the gene or cDNA, including the signal peptide
RTP1	indicates the mature protein

ii. Table of Contents

1 Introduction 1
1.1 Rust fungi 1
1.2 The haustorium: a highly specialized infection structure 2
1.3 Role of haustoria in nutrient uptake 3
1.4 Role of rust haustoria in establishing and maintaining of biotrophy 4
1.5 How do haustorially secreted proteins enter the host cell? 6
1.5.1 Type III secretion system: a nanomachine to deliver bacterial effectors 6
1.5.2 RxLR: a conserved host targeting signal within oomycetes effectors 8
1.6 Basic knowledge about RTP1 8
1.7 Goal of the thesis 11
2 Materials and Methods 12
2.1 Materials 12
2.1.1 Plant materials 12
2.1.2 Fungi 13
2.1.3 Bacteria 13
2.1.4 Plasmids 14
2.1.5 Primers 16
2.1.6 Culture media and growth conditions 18
2.2 Methods 18
2.2.1 Growth conditions 18
2.2.2 Cloning and sequencing 19
2.2.3 Constructs 19
2.2.3.1 Construction of PEST-like mutants 19
2.2.3.2 Cloning of RTP1 cDNA fragments in the plant expression vectors 20
2.2.3.3 Cloning of sRTP1 in the fungal expression vectors 20
2.2.4 Transformation 21
2.2.4.1 Bacterial transformation 21
2.2.4.2 Fungal transformation 21
2.2.5 Ethanol treatment 25
2.2.6 Histochemical GUS assay 25
2.2.7 Leaf DNA extraction for PCR analyses 26
2.2.8 RT-PCR 26
2.2.9 Quantitative PCR 26
2.2.10 Proteins extraction and precipitation 27
2.2.11 Protein deglycosylation 28
2.2.12 SDS-Polyacrylamide Gel-Electrophoresis 29
2.2.13 Coomassie blue staining of SDS-Polyacrylamide Gels 29
2.2.14 Immunoblots 29
2.2.15 Infection assays 30
2.2.16 Photography and microscopy 31
2.2.17 Bioinformatic methods 31
3 Results 32
3.1 Subcellular localization of RTP1 32
3.1.1 NLS regulated nuclear localization of RTP1 in plants 33
3.2 Stable constitutive expression of RTP1 in *Arabidopsis thaliana* 35
3.2.1 Stable expression of RTP1 in *Arabidopsis* resulted in very low number of transformants 36
3.2.2 Phenotype of *35S:RTP1* and *35S:sRTP1* expressing plants 37

3.2.3 RTP1 expression in *35S:RTP1* and *35S:sRTP1* plants. 37
3.2.4 Susceptibility of *35S:RTP1* and *35S:sRTP1* plants to pathogen infection 39
3.3 Stable inducible expression of RTP1 in *A. thaliana* 40
3.3.1 Characterization of *alcA:UidA*, *alcA:RTP1* and *alcA:sRTP1* transgenic *Arabidopsis* plants 40
3.3.2 Efficiency of the *alcA* inducible expression system 41
3.3.3 RTP1 is not detected in *alcA:RTP1* plants 42
3.3.4 *alcA:RTP1* transcript is induced with similar efficiency to *alcA:UidA* 43
3.3.5 Phenotypic consequences of RTP1 induction in agar-grown plantlets 44
3.4 RTP1 interferences with plant cells vitality 46
3.4.1 RTP1 is not detected when transiently expressed in *N. benthamiana* 46
3.4.2 *RTP1* transcript is expressed with similar efficiency as *GUS* in agroinfiltrated leaves 47
3.4.3 RTP1 is not detected when transiently expressed in many plant species including the host plant 48
3.4.4 RTP1 contains a PEST-like sequence, which does not destabilise GFP:RTP1 50
3.4.4.1 Construction of PEST mutants 51
3.4.4.2 Expression of the PEST mutants 52
3.4.5 Coexpression with RTP1 suppresses GFP expression 53
3.4.6 Identification of a functional domain in RTP1 necessary for interference with plant cell vitality 54
3.4.6.1 Construction and characterization of truncated GFP:RTP1 fusion proteins 54
3.4.6.2 Identification of functional domain in RTP1 55
3.4.6.3 Definition of the minimal functional domain of RTP1 56
3.5 Investigation of RTP1 translocation into plant host cells 57
3.5.1 RTP1 enters the plant cytoplasm in the absence of the rust pathogen 58
3.5.2 RTP1 PEST-like sequence plays a role in RTP1 reentry into plant cells 59
3.6 Establishment of a delivery model to study RTP1 translocation mechanism 60
3.6.1 Heterologous expression of *sRTP1* by *Colletotrichum lindemuthianum* 60
3.6.2 *Ustilago maydis/Zea mays* pathosystem as a model to study RTP1 delivery. 61
3.6.2.1 Efficient *in vitro* secretion of RTP1 from transgenic *U. maydis* 62
3.6.2.2 Recombinant secreted RTP1 shows similar glycosylation as native RTP1 65
3.6.2.3 Expression of *sRTP1* in *U. maydis* under control of *in planta*-induced promoter 66
3.6.2.4 *mig2-6:GFP* resulted in highly bright hyphal cytoplasmic fluorescence ... 67
3.6.2.5 Efficient secretion of RTP1:GFP during pathogenic growth of transgenic *U. maydis* hyphae 68
3.6.2.6 Evidence for RTP1:GFP transfer into plant cells 69
4 Discussion 71
4.1 What is the final target compartment for RTP1? 71
4.2 What is the biological function of RTP1 in plants? 73
4.2.1 Does RTP1 interfere with plant's defence? 74
4.2.2 Does RTP1 manipulate plant gene expression? 76
4.3 Structure-function deletion analyses of RTP1 78
4.4 What is the role of the RTP1 PEST-like sequence? 80
4.5 How does secreted RTP1 enter the plant cell? 82
4.6 RTP1 in other rust species? 87
4.7 *Ustilago maydis* as a model system to study RTP1 delivery into host cells 89
4.7.1 *U. maydis*: a suitable secretion system 90

4.7.2 Pursuing RTP1 delivery 91
5 Outlook 93
6. Summary 94
7. Appendix 96
8 References 97
9 Acknowledgements 103

1 Introduction

1.1 Rust fungi

Forming the largest group of fungal plant pathogens, rust fungi attack most cereal crops and many fruits, vegetables, forage crops, ornamental plants, and forest trees (**Fig.1**). They belong to the class Basidiomycota and the order Uredinales, and contain more than 7000 species that possess the most complex life cycles in the Kingdom Fungi (Maier et al., 2003). They may produce up to five different spore stages and may require two unrelated host plants to complete their life cycle. In rust fungi that require two host plants (heteroecious rusts), aeciospores infect only the 'alternate' host, not the host on which they were produced. For example, the wheat stem rust *Puccinia graminis* f. sp. *tritici* alternates between wheat as the primary host and barberry as the alternate host. Other rust fungi, for example *Uromyces fabae*, require only a single host plant to complete their life cycle (autoecious rusts). Rust fungi may produce either all five spore stages or a reduced number to a minimum of only teliospores and basidiospores as found in *microcyclic* rust fungi (Hahn, 2000).

Fig.1. *Uromyces fabae* sporulating on *Vicia faba* leaves

Rust infection begins with spore germination on the leaf surface, followed by the development of an appressorium. For dikaryotic spores, appressorium formation depends on a thigmotropic signal triggered by the specific topography of the host plant leaf surface (Staples and Hoch, 1987). An infection peg formed by the appressorium enters the leaf through the stoma, followed by the development of a substomatal vesicle, which extends an infection hypha, and forms the haustorial mother cell. From this latter, the haustorium is differentiated that penetrates the host mesophyll cell (**Fig.2**). Artificial membranes and etched surfaces have been used to mimic the topography of the leaf surface and induce the development of infection structures *in vitro* (Allen et al., 1991). However, the development is incomplete and haustoria are usually not formed in the absence of the host plant, except in rare cases after addition of a carbohydrate (Heath, 1990; Deising et al.,1991).

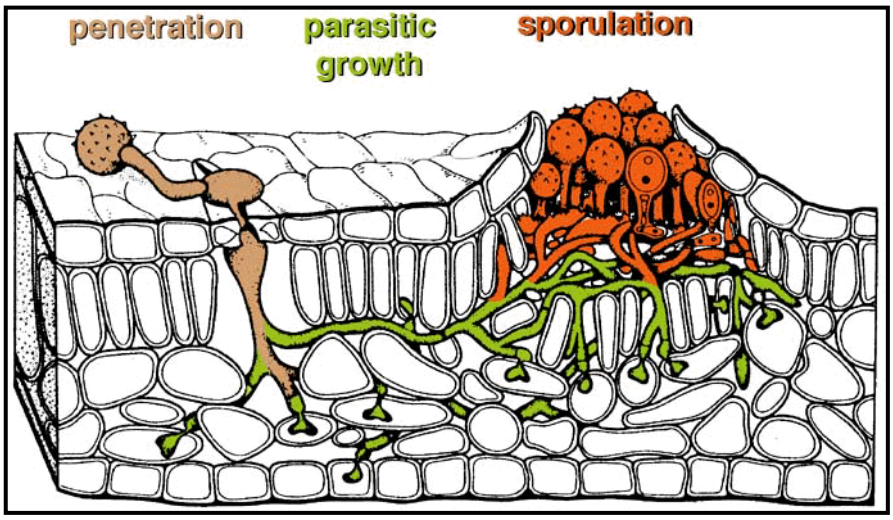

Fig.2. Schematic illustration of the dikaryotic rust infection structures formed in a host plant leaf (Hahn, 2000).

1.2 The haustorium: a highly specialized infection structure

The haustorium is a highly specialized hypha that penetrates the plant cell wall and grows inside that cell. This hyphal structure is surrounded by a plasma membrane and a haustorial wall. However, the haustorium is not located directly in the plant cell cytoplasm; instead, the plant cell membrane is invaginated and forms

an extrahaustorial membrane around the haustorium (**Fig.3**). In the interface between extrahaustorial membrane and fungal haustorial wall lays a carbohydrate-rich, gel-like layer called the extrahaustorial matrix. It has been postulated that both the rust fungus, but also mainly the host plants contribute to the formation of this compartment (Vögele and Mendgen, 2003). The extrahaustorial matrix is separated from the apoplast by the presence of a mineral-rich structure called the neckband, that connects the fungal and the host plasma membranes (Hahn, 2000). To be delivered from the haustorium to the plant cytoplasm, substances must pass successively through the haustorial plasma membrane, the extrahaustorial matrix and the plant plasma membrane.

1.3 Role of haustoria in nutrient uptake

In order to elucidate the role of haustoria in the biotrophic mode of rust nutrition, several research approaches have been initiated in the last 15 years, to isolate these hyphal structures (Tiburzi et al., 1992; Cantrell and Deverall, 1993; Hahn and Mendgen, 1992). In particular, Hahn and colleagues established a successful rust gene library approach, in which cDNAs of differentially expressed genes in isolated haustoria have been cloned (Hahn and Mendgen, 1997). They demonstrated that some of the most abundantly expressed genes in the rust haustorium encode for proteins involved in nutrition uptake and metabolism. Some of these haustorium specific proteins are: a hexose transporter (HTX1) (Voegele et al., 2001), putative transporters for amino acids (AAT1 and AAT2) (Hahn and Mendgen, 1997), enzymes involved in thiamine (vitamin B1) biosynthesis (THI1 and THI2) (Sohn et al., 2000), mannitol dehydrogenase (MAD1) (Voegele et al., 2005) and D-arabitol dehydrogenase (ARD1) (Link et al., 2005). Thus, the authors provided the first molecular evidence for the since long speculated role of haustoria in nutrient acquisition from the host plant (Mendgen, 1981).

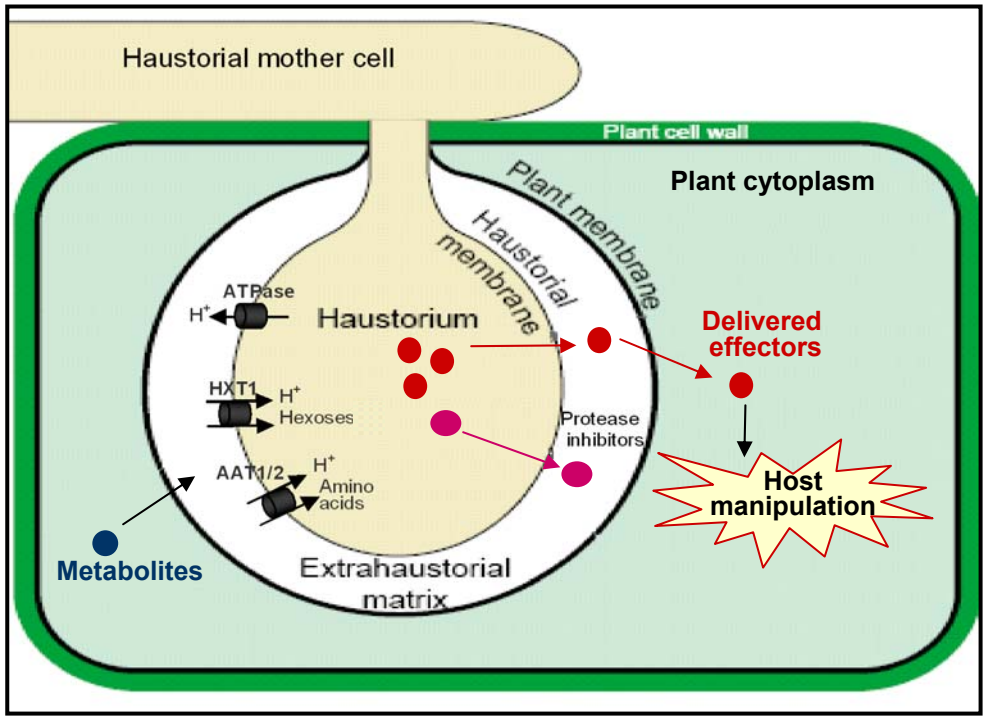

Fig.3. The host plant–rust haustorium interface. The rust haustorium penetrates the plant cell wall but not the host plasma membrane. An intensive molecular trafficking is suggested to take place in the extrahaustorial matrix. Drawing modified from Ellis et al. (2006).

1.4 Role of rust haustoria in establishing and maintaining of biotrophy

Rust fungi, like many other obligate biotrophs, are host specific and can develop compatible or incompatible associations with their host plants (Eckardt, 2006). Infection can be limited depending on the interaction between avirulence (*avr*) genes (so called because their presence hampers spread of the pathogen on resistant plants) in the pathogen and the corresponding resistance (*R*) genes in the host plant. Interaction between *R* and *avr* genes provides the basis of gene-for-gene concept (Dangl and McDowell, 2006).

There is a growing evidence that haustoria might play a major role in the virulence of rust fungi, through secretion of signal molecules that suppress host defence responses and facilitate disease development in host plants. A large-scale analysis of haustorially secreted proteins from the flax rust fungi, *Melampsora lini*, has identified 21 secreted proteins (HESP) (Catanzariti et al., 2005). Interestingly,

one of the studied genes encoding for HESP, named AvrP123-A, was found to encode a small Cys-rich secreted protein with sequence similarity to Kazal Ser protease inhibitors (**Table.1**), suggesting a possible role in pathogenesis of *M. lini* by inhibiting host proteases. Two other HESP effectors, AvrP4 and AvrM, show no similarity to known proteins in the databases, and were found to induce programmed cell death when expressed inside the plant cell, dependent on the presence of functional corresponding *R* genes *M* and *P4*. This was interpreted as these effector proteins being transferred from the haustorium into the host plant cells (Catanzariti et al., 2005). These findings corroborate the suggested role of haustoria in reprogramming plant cell defence. However, the biological function of the known rust Avr effectors (surely not to kill the host cells) is still unclear.

Table1. Cloned avirulence genes encoding for HESP from flax rust *M. lini*.

Protein	Protein size	Postulated function	References
AvrP4	95	Unknown	Catanzariti et al., 2006
AvrM	314-377	Unknown	Catanzariti et al., 2006
AvrP123	117	Similar to Kazal serine protease inhibitors	Catanzariti et al., 2006
AvrL567	150	Unknown	Dodds et al., 2004

Lately Voegele et al. (2005) provided evidence that mannitol is released from the fungal mycelium into the apoplast. The concentrations of mannitol measured in rust infected *V. faba* tissue has been found to be sufficient to quench reactive oxygen species (ROS) (Link et al., 2005). Mannitol production has been shown to be required for pathogenicity of *Cladosporium fulvum*, probably to quench ROS produced by host plant (Joosten et al., 1990). Thus it can be suggested that mannitol is secreted from the rust intercellular hyphae to suppress host defence responses involving ROS. However there is yet no direct evidence that haustoria would secrete mannitol into the extrahaustorial matrix. Another indirect evidence for the involvement of haustoria in controlling plant defence has been provided by Harder and Chong (1991). The authors highlighted differences in the morphology of extrahaustorial membranes induced by *Puccinia graminis* or *P. coronata* on oat, suggesting that formation of the fine structure of the haustorial host–parasite interface is under the

control of specific signals from the fungus. These signals may be involved in maintaining basic compatibility between the rust fungus and its host plants. However direct involvement of haustoria in suppressing plant defence is still poorly characterized (Vögele, 2006), and more work is needed to unravel molecular and cytological mechanisms used by the rust fungi to establish and maintain the biotrophic interaction with the host plants.

1.5 How do haustorially secreted proteins enter the host cell?

Despite the important progress achieved in the past years to clone rust effector proteins delivered from the haustoria to the host plant, little is known about their biochemical function, and nothing is yet understood about how they enter the host cells. To get some insights into the possible mechanisms of cell entry by rust effectors, it is important to discuss the knowledge acquired from other bacterial and fungal effectors delivered to host cells.

1.5.1 Type III secretion system: a nanomachine to deliver bacterial effectors

Interaction of bacterial pathogens or symbionts with host cells is mediated by factors that are located on the bacterial surface or are secreted into the extracellular space. The secretion systems by which these proteins are transported from the bacterial cytoplasm to the extracellular space are classified into four major types (I-IV). Type III secretion system (T3SS) or the injectisome, is maybe the most sophisticated protein-export apparatus described so far. It is found in many species of gram-negative bacteria, pathogenic for animals and plants, as well as in endosymbionts (Cornelis, 2006). Most effector proteins secreted by T3SS are destined to the cytosol of eukaryotic cells and not to the extracellular medium (**Fig.4**). More than hundred of these effectors have been identified, that exhibit a wide variety of functions including proteolysis, cytotoxicity, cell death suppression, protein phosphorylation and dephosphorylation (Mota and Cornelis. 2005). In contrast to the T3SS effectors that vary considerably, according to the particular needs of the bacteria, the secretion machinery itself is relatively conserved. While T3SS has been

intensively studied in a variety of animal bacterial pathogens (such as *Yersinia spp*., *Shigella spp*., *Salmonella spp*., *Pseudomonas aeruginosa*, enteropathogenic and enterohaemorrhagic *Escherichia coli*), *Pseudomonas syringae* is the plant pathogen in which T3SS is best-studied (Mota et al., 2005b).

In contrast to gram-negative bacteria, no T3SS has been discovered for fungal pathogens, suggesting that rust effectors secreted from the haustoria to the EHM might use another translocation mechanism to enter host plant cells.

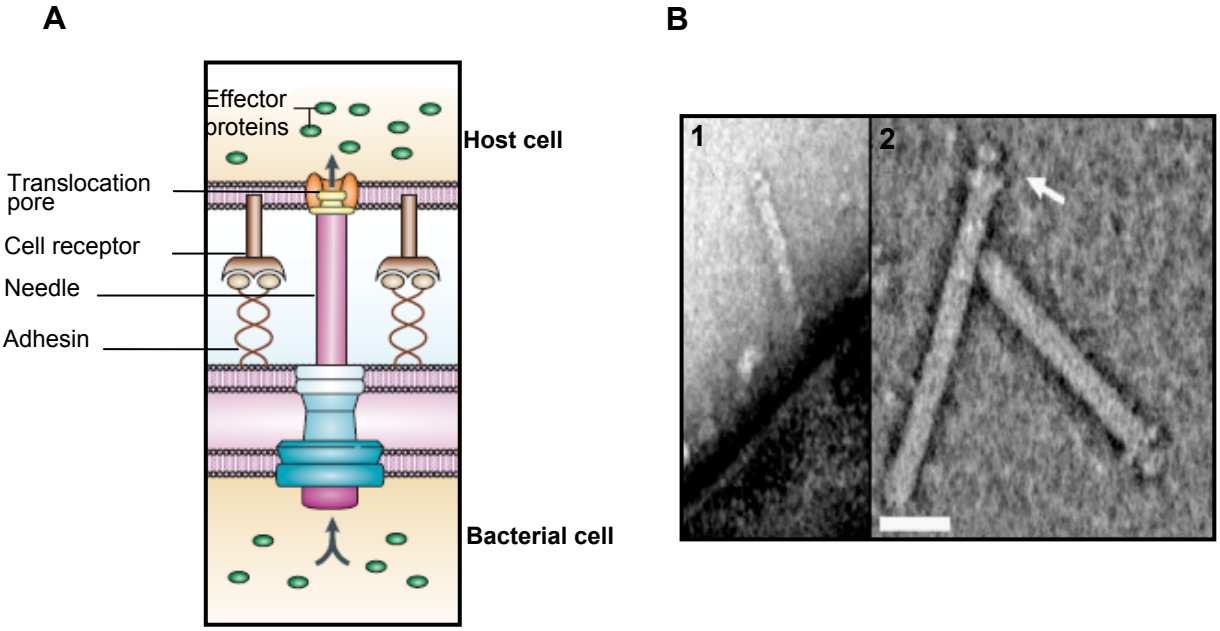

Fig.4. Needle structure of the T3SS. (**A**) Schematic presentation of the injectisome (picture from Cornelis, 2006). A close association of the bacterial cells and the target host cell occurs via contact between an adhesin and a receptor on the surface of the host cell. The bacterial and target cell membranes are separated by a gap which is bridged by the needle structure. This allows the bacterial effector proteins to be exported, in one step, from the bacterial cytosol to the cytosol of the target cell. (**B**) Structure of the tip of the T3SS needle. Transmission electron micrographs of *Yersinia enterocolitica* negatively stained with 2 % uranyl acetate (pictures from Mueller et al., 2005). **1,** Needles protrude from the cell surface and have a distinct structure at their distal end. Scale bar is 40 nm. **2,** The characteristic tip complex (white arrow) comprises a head, a neck and a base. Scale bar is 20 nm.

1.5.2 RxLR: a conserved host targeting signal within oomycetes effectors

Recently, sequence alignment of oomycete (*Hyaloperonospora parasitica* and two *Phytophthora* species) avr proteins and other secreted proteins of unknown function revealed a conserved amino acid sequence called “RxLR” motif that occurs closely following the N-terminal signal peptides. This motif which consists of the consensus sequence ‘RxLRx5-21ddEER’ is related to a protein transport motif, ‘RxLxE/Q’, that occurs in a similar location near the signal peptide in virulence proteins secreted by the malaria pathogen *Plasmodium falciparum* (Rehmany et al. 2005). During infection, malaria parasites occupy the parasitophorous vacuoles within the cytoplasm of human erythrocytes in a way that parasite and host cytoplasm are separated by two membranes, similarly to the situation of haustoria inside infected plant cells. Assays using YFP-tagged proteins expressed in *P. falciparum* have confirmed the role of RxLxE/Q motif in targeting secreted malaria effectors to the cytoplasm of the host erythrocyte across the parasitophorous vacuolar membrane (Hiller et al, 2004). However, the transport mechanism is not yet identified and it remains unclear how the host-cell-targeting signal mediates translocation of malaria effectors. A comparable function for the RxLR motif in oomycete avr proteins has been suggested. Therefore it is likely that oomycete avr proteins enter the host cell in a two-step process, involving signal peptide-mediated secretion followed by host cell uptake mediated by the RxLR motif. However, the predicted function of RxLR motif still has to be demonstrated. Unlike oomycetes secreted avr proteins, the RxLR motif has not been found in any of the identified rust fungi secreted effectors.

1.6 Basic knowledge about RTP1

Based on a differential screening of isolated rust haustoria cDNA library, a large number of *in planta*-induced genes (*PIGs*) have been cloned from *U. fabae* (Hahn and Mendgen 1997). While some of the identified haustorium-specific genes, showed (discussed above) sequence similarity to genes involved in nutrient uptake and metabolism, no function could be attributed to many other *PIGs* with no

homologues in the databases. The products of these genes might fulfil functions important for establishing and maintaining biotrophy.

PIG7 was found to be exclusively expressed in haustoria of *U. fabae* (**Fig.5**), and coding for a protein of 220 aa lacking homology in the databases. *In silico* analysis of PIG7, using Signal P software, revealed the presence of a predicted N-terminal secretion signal peptide within the first 19 aa (Kemen et al., 2005).

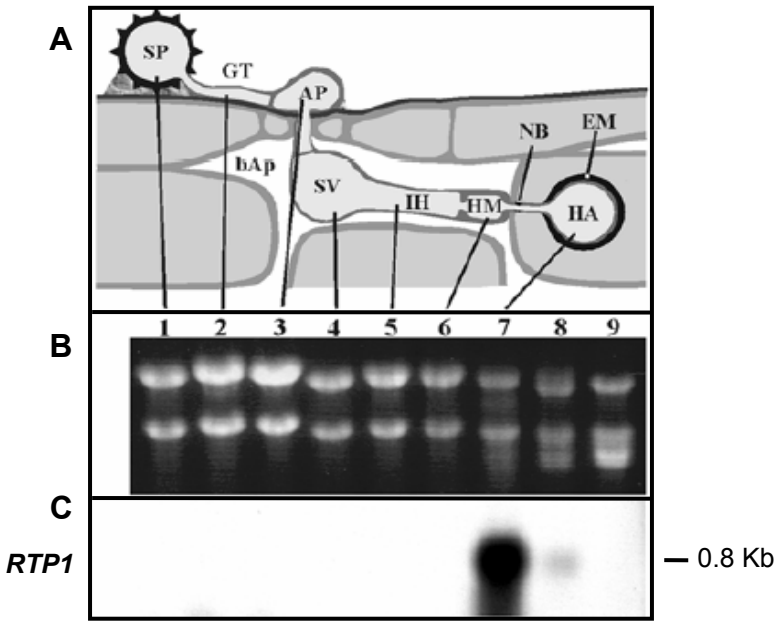

Fig.5. Haustorium-specific expression of *PIG7*. (A) Schematic presentation of *U. fabae* infection structures. **(B)** RNA gel loading control. **(C)** Northern blot hybridization. Lanes 1 to 7 corresponds to samples harvested at following stages: SP=Uredospore, GT=germ tube, AP=appressorium, SV=substomatal vesicle, IF=infection hypha, HM=haustorial mother cell, HA=isolated haustoria, lanes 8 and 9 correspond to infected and non infected leaves, respectively (Kemen et al. 2005).

In order to study in detail the localization of the PIG7 protein in rust-infected leaf tissue, and to confirm the functionality of the predicted signal peptide, His-tagged fusion proteins were made to generate polyclonal antibodies (Hempel, 2005). Immunofluorescence microscopy, using the generated antibodies, of *U. fabae* infected leaf tissue localized PIG7 not only in the extrahaustorial matrix, but also inside the infected host cell cytoplasm and nucleus (**Fig.6**). PIG7 was thus renamed

RTP1 referring to “rust transferred protein”. RTP1 was then shown to be the first rust protein to be secreted and delivered to the infected host cells. These findings have raised many questions which have been discussed throughout this work.

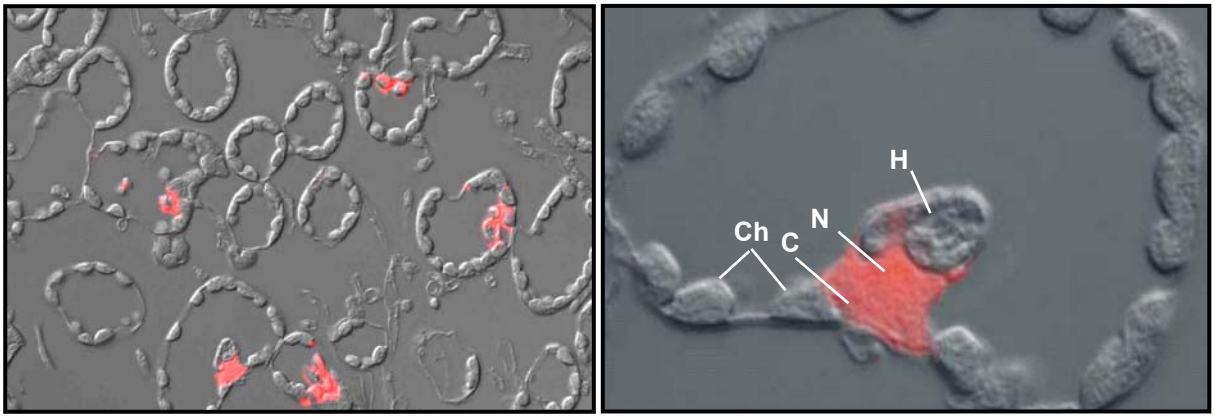

Fig.6. Immunolocalization of PIG7 (RTP1) in *V. faba* leaves infected with *U. fabae*. H: haustorium, N: plant cell nucleus, C: cytoplasm, Ch: chloroplasts (Kemen et al, 2005).

1.7 Goal of the thesis

The findings about the unusual localization of RTP1 within the rust infected host cells show that RTP1 might play an important role in the biotrophic relationship between rust haustorium and the host cells. The goal of this work was to characterize RTP1 in different aspects.

The first aspect was the subcellular localization of RTP1 within the plant cells. The immunofluorescence studies shown in **Fig.6** detected a strong signal within the plant nucleus. We wanted to know whether this is a result of specific targeting, or rather of simple diffusion into the plant nucleus. Analysis of RTP1 by different bioinformatic programs revealed the presence of a putative bipartite nuclear localization signal (**Fig.7**). The functionality of the NLS motif has been studied in this work. Second, we wanted to get insights into the biological function of RTP1 inside the host plant cell. For this purpose, RTP1 functional and structural analyses were carried out in different heterologous *in planta* expression systems. Finally, we were interested to unravel the mechanism by which RTP1 is delivered from the haustoria into host plant cells. In particular, how does RTP1 protein cross the host membrane and enter the plant cell after its secretion from the haustorium? Transient expression studies as well as the establishment of a delivery model for RTP1 have been adopted to answer these questions.

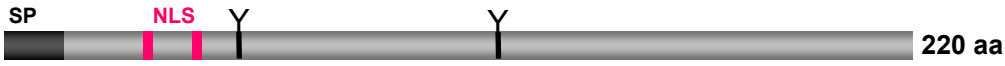

Fig.7. Schematic presentation of RTP1 structure. Analysis of RTP1 in many prediction programs revealed the presence of an N-terminal secretion signal (SP), a potential bipartite nuclear localization signal (NLS) and two potential N- glycosylation sites (marked with Y). Other sequence motifs identified during this work are shown in Chapter. 3 and 4.

2 Materials and Methods

The Materials and Methods section is subdivided into two parts. In the first part (2.1) materials used throughout this study including bacterial strains, pathogens, plant species, vectors, primers, media, buffers. The second part is reserved to describe methods applied in this work.

2.1 Materials

2.1.1 Plant materials

- *Arabidopsis thaliana:* Ecotype Columbia 0 wild type, kindly provided by Alexandra Wormit (University of Kaiserslautern), was used for *Agrobacterium,* as well as Particle bombardment-mediated transformations.

- *Nicotiana benthamiana*: Wild type plants were used for transient transformation, using particle bombardment, or *Agrobacterium*-mediated transformation of leaf tissues.

- *Vicia faba:* Wild-type seeds , variety “Hangdown” (ENZAZADEN, Haling 1e, Enkhuizen, The Netherlands) were used for transient transformation mediated by particle bombardment. *V. faba* plants were grown in soil or “Seramis” at 20°C with a 16 hours photoperiod. 5 to 6 week-old plants were used for gene delivery bombardment experiments. The plants were used for the bombardment when the first 3 “True” leaves were fully extended. Only new leaves (1-2 weeks) at the top of the plant were used.

- *Zea mays: S*eeds of the variety “Early Golden Bantam” were obtained from Prof. Jörg Kämper (MPI, Marburg) and used for infection with different strains of *Ustilago maydis*.

2.1.2 Fungi

- *Ustilago maydis:* strain SG200, kindly provided by Prof. J. Kämper (MPI, Marburg), was used for all expression studies in *U. maydis*.

- *Colletotrichum lindemuthianum*: strain UPS9 was used for expression of *oliC:sRTP1*.

- *Botrytis cinerea*: B0510 strain was used for *Arabidopsis* infection studies.

2.1.3 Bacteria

- For preparation of the plasmids, *Escherichia coli* XL1-Blue and JM105 competent cells were used (Bullock et al., 1987).

- For stable transformation of *A. thaliana* plants and transient expression of constructs in *N. benthamiana*, *Agrobacterium tumefaciens* strain GV3101 containing the helper plasmid pMP90 was used (Koncz and Schell, 1986). This strain carries resistances for gentamycin and rifampicin.

- For stable transformation of *C. lindemuthianum, A. tumefaciens* strain AGL1, carrying the hypervirulent, attenuated tumor-inducing plasmid pTiBo542*,* was used.

- For *Arabidopsis* infection studies, *Pseudomonas syringae* pv*. tomato* DC 3000 was used.

2.1.4 Plasmids

The plasmids used and generated during this study are given in Tables.1 and 2 including the characteristics.

Table.2. Plasmids used in the presented work

Plasmid	Vectors	Characteristics	Resistance Marker	Provider/reference
P123	pT7HB2.7	Contains O2*tef:eGFP:nos* cassette for expression in *U. maydis*	Carboxin	Prof. J. Kämper (MPI Marburg)
PA35	pTM1	Contains CaMV-35S promoter and OCS terminator for *in planta* expression	Amp	Hofte and chrispeels, 1992
pUC∆*alc*AN	pUC	Contains *alcA* promoter and nos terminator expression cassette	Amp	Roslan et al., 2001
pBin-∆*alcR*	pBin19	Contains *35S:alcR* expression cassette.	Km (Bacteria and plants)	Roslan et al., 2001
pCHS-GFP.	pUC18	Contains 35S:CHS-GFP:nos expression cassette.	Amp	Prof. T. Merkle, University of Bielefeld
pCB302	pBIN19	Mini binary vector for plant and fungal transformations	- Km (for bacteria) - BASTA (plants)	Xiang et al., 1999
pCambia	pUC18	Contains *35S:UidA* expression cassette	- Km (for bacteria) - Hyg (for plants)	Roslan et al., 2001

Table.3. Plasmids generated during the presented work

Plasmid	Origin	Characteristics
p123mod	p123	*2Otef* promoter replaced (using *Bam*HI and *Sph*I) by a 648bp fragment encoding *mig2-6* promoter
p123-sRTP1	p123	p123 in which *GFP* was excised and replaced by a 819bp fragment of *sRTP1*
p123-sRTP1:GFP	p123	Contains *2Otef:sRTP1:GFP* expression cassette
p123mod-sRTP1	p123	Contains *2Otef:sRTP1* expression cassette
p123mod-sRTP1:GFP	p123	Contains *mig2-6:sRTP1:GFP* expression cassette
p123mod-sRTP1$_{PESTala}$	p123	Contains *mig2-6:sRTP1$_{PESTala}$* expression cassette
p35Smod	pA35	*Bam*HI site was inserted at position 762bp in pA35
p35S-RTP1	p35Smod	p35Smod expressing *35S:RTP1*
p35S-sRTP1	p35Smod	p35Smod expressing *35S:sRTP1*
pCB-RTP1	pCB302	T-DNA containing *35S:RTP1* and *35S:bar*
pCB-sRTP1	pCB302	T-DNA containing *35S:sRTP1* and *35S:bar*

pUC∆*alc*AN-RTP1	pUC∆*alc*AN	Expressing *alcA:RTP1*
pUC∆*alc*AN-sRTP1	pUC∆*alc*AN	Expressing *alcA:sRTP1*
pBin-∆*alcR*-RTP1	pBin-∆*alcR*	T-DNA containing *35S:alcR, alcA:RTP1 and 35S:nptII*
pBin-∆*alcR*-*s*RTP1	pBin-∆*alcR*	T-DNA containing *35S:alcR, alcA:sRTP1 and 35S:nptII*
pCambia-RTP1	pCambia	T-DNA containing *35S:RTP1:UidA* and *35S:nptII*
pCambia-sRTP1	pCambia	T-DNA containing *35S:sRTP1:UidA* and *35S:nptII*
pCBhyg	pCB302	*pnos:bar* cassette has been replaced by *pnos:hyg* for fungal transformation
pCBhyg-sRTP1	pCBhyg	T-DNA containing *oliC:sRTP1* and *nos:hyg*
pGFP-UfNLS	pCHS-GFP.	Expression of GFP:RTP(36-69) fusion protein
pGFP-UfNLSx	pCHS-GFP.	Expression of GFP:RTPx(36-69) fusion protein
pGFP-UsNLS	pCHS-GFP.	Expression of GFP:UsRTP(37-64) fusion protein
pGFP-RTP1	pCHS-GFP.	Expression of GFP:RTP1(20-220) fusion protein
pGFP-UsRTP1	pCHS-GFP.	Expression of GFP:RTP1(23-229) fusion protein
pRTP-CHS-GFP	pCHS-GFP.	Expression of RTP1(20-220):CHS:GFP fusion protein
pGFP-35S-RTP1	pCHS-GFP.	Coexpression of *35S:GFP* and *35S:RTP1 cassettes*
pGFP-35S-sRTP1	pCHS-GFP.	Coexpression of *35S:GFP* and *35S:sRTP1 cassettes*
pGFP-RTP1$_{PESTala}$	pCHS-GFP.	Expression of GFP:RTP1$_{PESTala7}$ fusion protein
pGFP-RTP1$_{\Delta PEST}$	pCHS-GFP.	Expression of GFP:RTP1$_{\Delta PEST}$ fusion protein
pGFP-35S-sRTP1$_{PESTala7}$	pCHS-GFP.	Coexpression of *35S:GFP* and *35S:sRTP1 $_{PESTala7}$ cassettes*
pGFP-RTP1-1	pCHS-GFP.	Expression of GFP:RTP1(69-220) fusion protein
pGFP-RTP1-2	pCHS-GFP.	Expression of GFP:RTP1(20-176) fusion protein
pGFP-RTP1-3	pCHS-GFP.	Expression of GFP:RTP1(114-220) fusion protein
pGFP-RTP1-4	pCHS-GFP.	Expression of GFP:RTP1(69-176) fusion protein
pGFP-RTP1-5	pCHS-GFP.	Expression of GFP:RTP1(114-176) fusion protein
pGFP-RTP1-4a	pCHS-GFP.	Expression of GFP:RTP1(69-106) fusion protein
pGFP-RTP1-4b	pCHS-GFP.	Expression of GFP:RTP1(69-137) fusion protein
pGFP-RTP1-8	pCHS-GFP.	Expression of GFP:RTP1(69-106) fusion protein
pGFP-RTP1-4-1	pCHS-GFP.	Expression of GFP:RTP1(76-176) fusion protein
pGFP-RTP1-4-2	pCHS-GFP.	Expression of GFP:RTP1(69-157) fusion protein
pGFP-RTP1-4-3	pCHS-GFP.	Expression of GFP:RTP1(90-157) fusion protein

pGFP-RTP1-4-4	pCHS-GFP.	Expression of GFP:RTP1(114-157) fusion protein
pGFP-RTP1-4-7	pCHS-GFP.	Expression of GFP:RTP1(100-145) fusion protein
pGFP-RTP1-4-8	pCHS-GFP.	Expression of GFP:RTP1(113-138) fusion protein
pGFP-RTP1-4-9	pCHS-GFP.	Expression of GFP:RTP1(111-139) fusion protein
pGFP-RTP1-4-10	pCHS-GFP.	Expression of GFP:RTP1(114-137) fusion protein
pGFP-RTP1-4-11	pCHS-GFP.	Expression of GFP:RTP1(111-145) fusion protein
pGFP-RTP1-4-12	pCHS-GFP.	Expression of GFP:RTP1(100-138) fusion protein

2.1.5 Primers

The oligonucleotides were ordered online from Operon at website "http://www.operon.com" and were obtained as high purified, salt free and lyophilized. The primers were dissolved in H_2O resulting in a concentration of 100 pmol/µl and stored at –20°C.

Table.4. Oligonucleotides used in this study. Restriction sites are highlighted in bold letters, start or stop codons are underlined.

Primer name	Sequence (5'->3')
BamHI-Uf-NLS	GT**GGATCC**CTGACTTGTGACGCCTGTGT
EcoRI-Uf-NLS	TG**GAATTC**AGTATGGGCAAAGCAAGTGTCAG
Uf-NLSx-rev	GT**GGATCC**CTGACTTGTGAAGCGT
Ust-NLS rev	TC**GGATCC**GTCCCGCTTGCGAAGTATGACA
GFP-UfRTP-1	TG**GAATTC**CAACTAGTAGGCTCAGATGTG
GFP-UroRTP-2	GT**GGATCC**TCATTCRGGTATGATGAAATCC
XbaI-RTP1 for	TC**TCTAGA**ATGGGCAAAGCAAGTGTCAGC
BclI-RTP1 rev	CTC**TGATCA**CCGTTCTCCTTCGGGTATG
SP-RTP1-NcoI	TC**CCATGG**CGTCAAACCTTCGCTTAC
SP-RTP1-EcoRI	TG**GAATTC**CCCGTTCTCCTTCRGGTATG
KpnI-SP.RTP1	CT**GGTACC**AACATGGCGTCAAACCTTCGCTTACTTTTCACA
XbaI-RTP1	TG**TCTAGA**TCATTC(AG)GGTATGATGAAATCC

KpnI-RTP1	GT**GGTACC**ATGCAACTAGTAGGCTCAGATGTG
XbaI-HDEL-rev	TG**TCTAGA**TCAGAGCTCATCATGTTCRGGTATGATGAAATCC
CRTP-1-for	TG**GAATTC**TCAGAACCAGAGGGTGTCAAG
CRTP-2-for	TG**GAATTC**GCTAGAGGACTGTGAAGTGGTCATT
CRTP-3-rev	GT**GGATCC**CAGACAGCGACCTGCTAGT
CRTP-4b-rev	GT**GGATCC**ACGTAGTCACCTGGAGAA
CRTP-4a-rev	GT**GGATCC**GGTAGCAAGCAGTATTAAGCT
cRTP-4d-rev	TCT**GGATCC**TTAGCGGGAGTTAAATCGAC
cRTP-4e-for	CT**GAATTC**CTTCATCACCTCCGCTGA
cRTP4-4R	GT**GGATCC**GTCACCTGGAGAAACTTGAAGAC
cRTP4-4F	TG**GAATTC**GCCCCTTTGCTAGAGGACTGTG
cRTP4-3R	GT**GGATCC**GTAGTCACCTGGAGAAACTTGAAGAC
cRTP4-5F	TG**GAATTC**TTGCTAGAGGACTGTGAAGTGGTC
GUSA-for	ACGGCAGAGAAGGTACTG
GUSA-rev	TCACCGAAGTTCATGCCAGTC
BamHI-NES-for	GT**GGATCC**CGTACCCGCTACTTTTACTCAC
XhoI-NES-rev	CTGT**CTCGAG**CCATGGACGTTAATCAAGAGTAAGC
PDF-1	CATCATGGCTAAGTTTGCTTCCATCA
PDF-2	GTTACTCATAGAGTGACAGAGAC
PR1-1	GTAGCTCTTGTAGGTGCTCTTGTTC
PR1-2	CTTTATGTACGTGTGTATGCATGATCAC
Col-act-1	AGGATCACGAGCTCTGGCAGTACGAC
Col-act-2	ATGCCGTCCTCGTGAGGTGGCAT
BamHI-35S	CT**AAGCTT**GGATCCCAATCAGTAAATTGAACGGA
hph-EcoRI-1	CT**GAATTC**CAGCTGTGGAGCCGCATTC
PEST-mut-for	CACACTTCCGCAGCTGCAGCTGCTGCTGCAGCTCTGACCACAGTCGATTTAA
PEST-mut-rev	CTGTGGTCAGAGCTGCAGCAGCAGCTGCAGCTGCGGAAGTGTGATTAGAA
PESTdel-rev	TCTCCCGGGTGCGGAAGTGTGATTAGAA
PESTdel-for	TCTCCCGGGCTGACCACAGTCGATT

2.1.6 Culture media and growth conditions

LB-medium: 10 g/L tryptone, 5 g/L yeast extract, 10 g/L NaCl

TB-medium: 5g/L glycerol, 12 g/L tryptone, 24 g/L yeast extract, 12,54 g/L K_2HPO_4, 2,31 g/L KH_2PO_4 (pH7)

YEB-Medium: 0,5% (w/v) Beef-Extract, 0,1% (w/v) yeast extract, 0,5% (w/v) Peptone, 2 mM $MgSO_4$,

HA medium: 10g/L Malt extract, 4g/L Glucose, 4g/L yeast extract.

Solid media were prepared by adding 15 g/L agar.

Table.5. Relevant antibiotics used for growth selection

Substrate	Final concentration (µg/ml)	Organism
Ampicillin	80	*E. coli*
Kanamycin	50	*E. coli*, *A. tumefaciens*
Kanamycin	40	*A. thaliana*
Rifampicin	25	*A. tumefaciens*
Gentamycin	25	*A. tumefaciens*
Hygromycin	30	*C. lindemuthianum*
Carboxin	4	*U. maydis*

2.2 Methods

2.2.1 Growth conditions

The bacteria were maintained, cultured, stored and transformed according to standard methods (Sambrook *et al.*, 2001). Bacterial and fungal cultures were grown in acclimatised growth chambers. *A. tumefaciens* and *U. maydis* cultures at 28°C, *C. lindemuthianum* at RT and *E. coli* at 37°C.

With the exception of young seedlings germinated and selected on MS agar plates, all the other plants were grown in soil in acclimatised growth chambers, at a temperature of 22°C during the light period and 18°C during the dark period with a relative humidity of 60%. Light conditions averaged 100 µE, at 10 hours day and at 14 hours night.

2.2.2 Cloning and sequencing

Standard methods such as plasmid preparations, digestions, electrophoresis, ligations, amplifications by PCR were performed as described (Sambrook *et al.*, 1989). The sequencing was done in the Nano-Bio-Center at The University of Kaiserslautern using the ABI PRISM Dye Terminator Cycle Sequencing Ready Reaction Kit (Perkin Elmer, Warrington, UK) on an ABI Prism Sequencer 310 (Perkin Elmer, Warrington, UK).

2.2.3 Constructs

2.2.3.1 Construction of PEST-like mutants

- **Generation of *sRTP1$_{PESTala7}$***

sRTP1$_{PESTala7}$ mutant was created using the overlapping mutagenic PCR method (Horton et al., 1989). The first round of PCR was performed to amplify two PCR products with a primer-length overlap containing the PEST-like mutant residues. One of these was prepared using a mutant PEST_ala_for sense oligo and a flanking wild-type *sRTP1* primer GFP-UroRTP-2 that adds a *Bam*HI site at the 5' end of *sRTP1*; the other with a mutant PEST_ala_rev antisense oligo and a wild-type *sRTP1* primer that adds an *Eco*RI site at the 3' end of the *sRTP1*. The PCR products were purified by the Macherey-Nagel purification Kit (Macherey-Nagel GmbH and Co.KG, Düren), 1ng of the purified products were mixed and used as template in the second round of amplification, in which the wild-type *sRTP1* primers were used (**Fig.24**). The presence of desired mutations was verified by sequencing.

- **Generation of *RTP1$_{\Delta PEST}$***

RTP1$_{\Delta PEST}$ was generated by fusing a 197bp *EcoRI-SmaI RTP1$_{(58-246bp)}$* and a 400bp *Sma*I-*Bam*HI *RTP1$_{(268-660bp)}$* fragments into *Eco*RI-*Bam*HI sites of pCHS-GFP. The resulting construct was *GFP: RTP1$_{\Delta PEST}$* , in which the longest contiguous PEST-like residues in RTP1 were in frame deleted and replaced by *Sma*I restriction site. The Mutation was confirmed by restriction digest analyses and by sequencing.

2.2.3.2 Cloning of RTP1 cDNA fragments in the plant expression vectors

The coding sequences were amplified, from *U. fabae* or *U. striatus* EST library in lambda phages, by PCR using primers flanking either full length *sRTP1* or studied fragments within *sRTP1* sequence (**Table. 2**). All primers were designed adding restriction sites on each, for cloning purposes. After restriction digests, amplified PCR fragments were inserted into the MCS of corresponding plasmids.

- Primers used to amplify *RTP1* fragments used for GFP fusion studies in pCHS-GFP, were extended with *Eco*RI and *Bam*HI.
- Primers used to amplify *RTP1*, *sRTP1* and *sRTP1*$_{PESTala7}$ for coexpression analyses were extended with *Kpn*I and *Xba*I, the resulting fragments were cloned into p35Smod.
- Primers used to amplify *RTP1* and *sRTP1* for the inducible expression in *Arabidopsis* were extended with *Bam*HI and *Eco*RI, the resulting PCR product were ligated to pUC∆*alc*AN

To coexpress *RTP1*, *sRTP1* or *sRTP1*$_{PESTala7}$ with *GFP*, *35S:RTP1*, *35S:sRTP1* and 35S:sRTP1$_{PESTala7}$ cassettes were digested from p35S:RTP1, p35S:sRTP1 and p35S:sRTP1$_{PESTala7}$, using *Eco*RI and *Bam*HI and ligated to pCHS-GFP. To express *RTP1* and *sRTP1* in *Arabidopsis* under the control of *alcA* promoter, *alcA:RTP1* and *alcA:sRTP1* expression cassettes were digested from pUC∆*alc*AN-RTP1 and pUC∆*alc*AN-sRTP1, respectively, and inserted into the MCS of the binary vector pBin-∆*alcR*. The resulted plasmids were named pBin-∆*alcR*-RTP1 and pBin-∆*alcR*-*s*RTP1.

2.2.3.3 Cloning of sRTP1 in the fungal expression vectors

To constitutively express *sRTP1* in *C. lindemuthianum*, PCR amplified *sRTP1* was fused to *oliC* promoter in pLob1mod using *Bam*HI and *Nco*I. *oliC:sRTP1* expression cassette was than cut and blunt ligated end into the MCS of binary vector pCBhyg. To express sRTP1 and *sRTP1:GFP* under *o2tef* promoter in *U. maydis*, PCR amplified fragments were cloned into p123 using *Nco*I-*Not*I and *Nco*I, respectively. To express GFP, *sRTP1* and *sRTP1:GFP* under *mig2:6* promoter in *U. maydis, o2tef*

promoter in p123, p123:sRTP1 and p123:sRTP1:GFP, respectively, was excised and replaced by *mig2-6* promoter using *Bam*HI-*Sph*I. All constructs were confirmed by restriction digests and sequencing. To generate *mig2-6:sRTP1*$_{PESTala7}$, *sRTP1*$_{PESTala7}$ was amplified by overlapping PCR and fused to *mig2-6* in p123mod using a *NcoI* restriction site.

2.2.4 Transformation

2.2.4.1 Bacterial transformation

Transformation of *E. coli* was done with heat shock, and transformation *AGL1* strain of *A. tumefaciens* was done with electroporation, as described in Sambrook et al ., 1989. *GV3101* strain of *A. tumefaciens* was transformed using the freeze-thaw method (Chen *et al.*,1994), competent cells were thawed and incubated for 5 minutes on ice with about 1 µg of plasmid DNA. The cells were then frozen again in liquid nitrogen, thawed at 37°C for 5 minutes, then incubated with 1 ml of YEB medium for 2 hours. Transformants were selected on YEB plates containing appropriate antibiotics.

2.2.4.2 Fungal transformation

- **Transformation of *C. lindemuthianum***

A. tumefaciens strain carrying pCBhyg-sRTP1 was grown O/N in liquid minimal medium (Hookaas et al., 1979) with appropriate antibiotic. Bacteria were diluted 1:20 in minimal medium supplemented with 200µM acetosyringone and grown until OD_{600}=0.5 to1. *Agrobacterium* cells were then collected by centrifugation, washed and resupsended in induction medium (minimal medium supplemented with 0.5%[w/v] glycerol, 200µM Acetosyringone and 40mM MES, pH 5.2) at a concentration of 2. 10^7cells/ml. O/N grown UPS9 conidia (in 3% mal extract) were collected by centrifugation washed and resuspended in residual medium at a concentration of 10^6cells/ml. 100µl of *Agrobacterium* cells were mixed with 100µl conidia, and placed over a cellophane membrane placed on solid induction medium

at RT. After 2 days cocultivation, cellophane membrane was transferred onto selection medium (HA plates containing 50µg/ml Hygromycin). Finally single isolate transformants were selected and analysed for infection and for *sRTP1* integration by PCR and RT-PCR.

- **Transformation of *U. maydis***
    - **Protoplasts preparation**

A 50ml culture of *U. maydis* was grown, in YEPS medium, O/N at 28°C to a cell density of 5 x 10^7/ml (OD 0.6 to 1.0), cells were collected by centrifugation for 7 min at 2500g. The cells were then washed with SCS buffer, resuspended in SCS containing 5mg/ml Novozym 234, and kept at RT until protoplasts had formed (~10-20min). Then, 10ml of SCS was added, and the suspension was centrifuged at 1100g at RT for 10min. This washing step was repeated two times with SCS and once with STC. Finally the protoplasts were resuspended in 500µl ice-cold STC buffer at a concentration of 2x10^8/ml and kept at 0°C.

SCS-buffer
20 mM NaCitrat pH 5.8
1.0 M Sorbit

STC-buffer
10 mM Tris/HCL pH 7.5
1.0 M Sorbit
100 mM $CaCl_2$

- **Protoplasts transformation**

For protoplasts transformation, 3-5µg of linearised plasmid DNA, in a maximal volume of 10µl, was mixed with 1µl of Herparin (15µg/µl) (SIGMA H3125) before to add 50µl of the previously prepared protoplasts. After 15 minutes incubation on ice, 500µl of PEG3350 (40% w/v in STC) was added, followed by incubation, for 15 min, on ice. The mixture was then poured on freshly prepared gradient plates (10ml bottom agar overlaid with 5ml of Top agar)

Bottom agar
10ml of 1.5% agar in YEPS
1M sorbitol
4µg/ml carboxin

Top agar
ml of 1.5% agar in YEPS
1M sorbitol

- **PEG transformation of tobacco BY-2 Protoplasts**

Protoplasts were prepared from dark-grown BY-2 cells three days after subculture using the protocol described by Merkle et al. (1996). Transient transformation of the protoplast was done using the PEG-mediated transformation method described by Negrutiu *et al.* (1987).

- **Biolistic transformation of *V. faba* leaves**

  - **Preparation of DNA-coated Tungsten microcarriers**

Comercial M-10 tungsten powder from Biorad (spherical particles 0.7µm in diameter), was washed with distilled water, sterilised with 70% (v/v) ethanol, and suspended in 50% glycerol (600 mg/ml). Plasmid DNA was precipitated onto the tungsten particles as previously described by Sambrook et al (1989) with minor modifications:
20µg plasmid DNA were added to 4 µl tungsten particles stock solution, and the volume was completed with water to 60 µl under low agitation. Next 30 µl $CaCl_2$ (stock 3 M) and 5 µl spermidin (stock 4.5 M) were added and homogenized. The mixture was kept 3 min under agitation (vortex) and for an additional 10 to 20 min without agitation. DNA coated particles were centrifuged two seconds at maximum speed, rinsed carefully with 150µl 70% ethanol (to remove the free $CaCl_2$ and spermidin). The washing step was repeated with 150µl 100% ethanol and the coated particles were then resuspended in 40µl 100% ethanol to facilitate rapid drying of the coated particles onto the launching surface. After soft agitation to disperse the particles, 9µl of suspended particles was loaded in the front end of a bullet-like plastic macrocarrier. Hence, approximately 600µg of tungsten coated with 5µg of plasmid DNA was used to bombard each plant leaf. After deposition on the macrocarrier, care was taken to allow ethanol to evaporate. Total drying is important to avoid damage of plant leaf tissue and to insure the quality of the particle dispersion and penetration into the samples.

  - **DNA coated microcarriers bombardment**

A biolistic particle helium acceleration device (constructed by Eigenbau der Metallwerkstatt der TU. Kaiserslautern) was used . The bombardment was done under a pressure of 5 bar and a partial vacuum in the chamber corresponding to a reading value of at least 0.8bar. Under these conditions, the coated tungsten

particles were extruded through a small orifice to shoot the epidermal layers of the plant leaf placed on 1% agar plates and positioned at ~102 mm from the macrocarrier assembly (second level from the bottom). After the vacuum has returned to atmospheric pressure, bombarded plant material was removed and kept in a hermetic box at 26°C for 18-22 h with sufficient moisture to prevent it from drying out.

- **Agroinfiltration of *N. benthamiana* leaves**

Agrobacterium-mediated transient expression was performed essentially as described by Van der Hoorn et al. (2000) with minor changes. Cultures containing recombinant *Agrobacterium* carrying the different binary plasmids were resuspended to a final OD_{600} of 1 and infiltrated into tobacco leaves in the presence of 200 µM acetosyringone.

- ***A. thaliana* transformation**

A. thaliana plants were transformed by floral dipping method (Clough & Bent, 1998). GV301 Colonies containing the appropriate plasmids "flower-dip" transformation: colonies were inoculated into 25 ml YEB liquid medium supplied with MgSO4, Rifampicin and Kanamycin. The culture was shaken O/N at 28°C. Four times 12.5 ml of this inoculum was added to 800 ml YEB liquid medium supplied with MgSO4, Rifampicin and Kanamycin, and the cultures were shaken for 24 h at 28oC. The cells were harvested by centrifugation for 30 min at 4000 rpm and RT, and resuspended in infiltration medium (for 2 l: 4.4 g MS salts, 6.4 g Gamborg`s B5 basal medium with minimal organics, 100 g sucrose, 1.0 g MES pH 5.7 with KOH and 2µl of 10 mg/ml benzyladenin. 0.05 % Extravon was added after autoclaving). The OD was adjusted to a value of 2.

The *A. thaliana* plants to be transformed were grown for 2 month at 10h light daily. The flowers were removed 3 days prior to transformation to enhance the development of new flowers. Fully developed flowers showing petals (white) were removed prior to transformation, since they were already too old. The plants were dipped headlong into the bacterial suspension for 10s to cover most of the flowers.

The plants were covered with a plastic bag for one day for recovering and left growing for seed maturation.

The seeds of the transformed plants were collected and either sown on soil and selected for BASTA resistance, or surface sterilized as follows: Two hundred mg seeds (~100,000 seeds) were incubated with 70% ethanol for 30s, 20% sodium hypochlorite for 10 min. The liquid was removed and the seeds were washed three times in sterile water and dried on the sterile bench. For germination, the sterilized seeds were distributed on 13.5 cm diameter agar plates (0.8 % phytoagar, 0.44% MSMO [Murashige and Skoog Minimal Organics including Nitsch vitamins, Duchefa cat. no.M0256] and 2% sucrose, 0.05% MES and 40g/ml kanamycin). To control germination rate, an aliquot was distributed on agar plates without kanamycin. The plates were incubated for two weeks at 10h daily light.

2.2.5 Ethanol treatment

The roots, of 4 to 5 weeks-old (soil grown) *Arabidopsis* plants were drenched in 2% ethanol (v/v) solution, the plants were then put in a plant propagator and covered to prevent ethanol evaporation. After 24 hours, the remaining ethanol solution was drained. Agar-grown seedlings were induced by transfer into new agar plates supplemented with 2% ethanol added after autoclaving.

2.2.6 Histochemical GUS assay

GUS staining was performed according to Jefferson *et al.* (1987) with a few alterations. Plant material was incubated in 0.05% (w/v) X-Gluc (Roth) in 0.1M sodium phosphate buffer with 3% sucrose, 5µM ferrocyanide, 5µM ferricyanide (pH 7). Vacuum infiltration was applied for 30 minutes and the sample was incubated at 37°C.

2.2.7 Leaf DNA extraction for PCR analyses

Two to three medium sized leaves were cut by forceps and placed in an Eppendorf tube containing 400 µl of Edwards extraction buffer (200 mM Tris pH 7.5; 250 mM NaCl; 25 mm EDTA; 0.5% SDS). Tissues were ground with pestles and the tubes were centrifuged at 14,000 rpm for 5 minutes at room temperature and 300 µl of the supernatant was transferred to a clean eppendorf tube. Equal volume of isopropanol was added and incubated for 5 minutes at RT. The tubes were centrifuged at 14,000 rpm for 5 minutes at RT. Pellets were washed with 300 µl of 70% ethanol three times and then air-dried. Pellets were resuspended in 30 µl of distilled water and stored at 4° C.

2.2.8 RT-PCR

An aliquot of 0.1g (FW) of plant leaf or fungal hyphae material was homogenized by grinding in liquid nitrogen and the powder was used to extract RNA with RNeasy Plant Mini Kit (Quiagen). The yield was assessed via spectrophotometer (c[µg/ml]=OD260 x dilution factor x 40) and viewing aliquots on a agarose gel. The RNA was treated with DNase (DNA-free, Ambion), and 2 µg of RNA was used for cDNA synthesis, which was then used as a template in the Semi-quantitative PCR. For controlling equal loading we amplified *Ef-2a* (with primers provided by T. Reinhold, University of Kaiserslautern) or actin fragments in the same PCR. All RT-PCR reactions were repeated at least twice.

2.2.9 Quantitative PCR

For quantitative analysis, cDNA samples were subjected to quantitative real-time PCR. For this purpose, cDNA (1µl) was mixed with 1µl forward and reverse primers each for *GUS* or *RTP1* (10 pmol/µl), distilled H_2O (8µl), and 10µl absolute iQ SYBR Green Supermix (Biorad) in 96-well PCR plates. The mix was briefly spinned down

and the plates were sealed with optical tape. The PCR was performed using the iQ5 real-time PCR detection system according to the following profile:

Activation I		95.0 °C	15 min
Cycles:			
(50X)	Denaturation	95.0 °C	15 s
	Anealing	58.0 °C	25 s
	Elongation	72.0 °C	40 s
Final denaturation		95.0 °C	1 min
Final renaturation		58.0 °C	1 min
Melting curve		+0.5 °C	10 s

Measurement of fluorescence was carried out during the elongation phase (mean value) for quantification and during the melting curve (with measurements being performed for each temperature) for analysis of the product identity.
Initially, the primers (*GUS* and *RTP1*) were validated for use in the quantitative system by serial dilution of a sample (1, 0.1, 0.01, 0.001, 0.0001) using the above-mentioned protocol. Both GUS and RTP1 (**Fig.9**) primers proved to be useful for quantitative real time PCR, since both amplified one product only and remained linear over several orders of magnitude.

2.2.10 Proteins extraction and precipitation

Proteins were isolated from plant leaves by grinding in liquid nitrogen and subsequent transfer of the sample to extraction buffer preheated at 60°C (125mM Tris/HCl, pH 6.8, 4% SDS, 200µM phenylmethylsulfonyl fluoride, 100mM dithiothreitol [DTT]), followed by incubation at 100°C for 10 min. After centrifugation, the protein solutions were mixed with four volumes of acetone and incubated for 1 h at -20°C. The precipitated proteins were pelleted by centrifugation and the pellet was washed with ethanol, air dried and resuspended 1% extraction buffer.

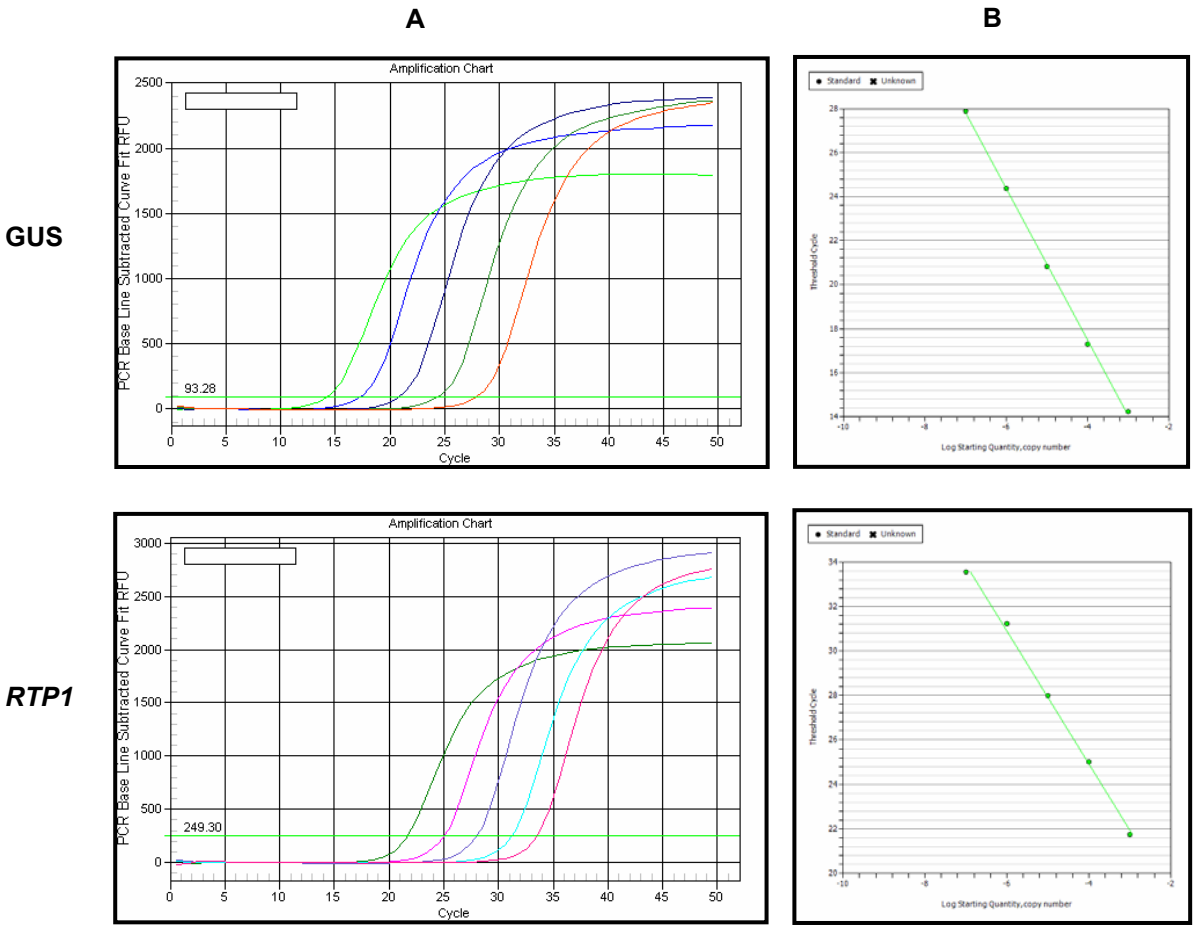

Fig.8. Validation of primers for quantitative real-time PCR. Random cDNA sample was serially diluted (1 to 0.0001) and subjected to quantitative real-time PCR, using GUS and RTP1 genes specific primers. (**A**) The fluorescence increase resulted in threshold cycles which showed a clear concentration dependency. (**B**) This allowed subsequent quantification of PCR products.

2.2.11 Protein deglycosylation

30µl protein samples were treated with 3,000 units of Endo H_f (New England Biolabs GmbH, Frankfurt) according to the manufacturer instructions. The deglycosylation reaction was incubated O/N at 37°C, dried in speedvac and resolved in SDS-sample buffer. After this treatment, native or deglycosylated fractions were submitted to 10% SDS PAGE followed by Western blotting with anti-RTP1 antibodies.

2.2.12 SDS-Polyacrylamide Gel-Electrophoresis

SDS-Polyacrylamide gels were performed with BioRad SDS/PAGE Mini Protean II apparatus. The samples were mixed with 4x Sample buffer (0.6 M Tris-HCl pH 6.8, 10% (w/v) SDS, 50 % (v/v) Glycerol, Trace bromophenol blue). Samples were boiled at 95°C for 5 min and loaded on an SDS PAGE consisting of a lower separating and an upper stacking gel with the following composition: Separating gel (6 ml for mini gels): 25 % (v/v) separating gel buffer (1.5 M Tris/HCl pH 6.8, 0.4 % SDS), 8-12 % (v/v) bisacrylamide, 0.075 % (w/v) ammonium persulfate and 0.05 % (v/v) TEMED (N,N,N`,N`-Tetramethylethylenediamine). Ammonium persulfate and TEMED cause polymerization of the gel and were added at last. Stacking gel (3 ml for mini gels): 25 % stacking gel buffer (1.5 M Tris/HCl pH 8.8, 0.4 % SDS), 4.5 %(w/v) bisacrylamide, 0.06 % ammonium persulfate and 0.05 % TEMED.

2.2.13 Coomassie blue staining of SDS-Polyacrylamide Gels

Gel was incubated by gentle shaking in stain solution (0.25 % Serva Blue R in Destain solution) for one hour to O/N. For destaining gel was incubated in destain solution (40 % ethanol, 10 % acetic acid) until the color of the gel equaled the color of the solution. Then the Destain solution was exchanged for fresh one.

2.2.14 Immunoblots

Proteins were transferred to nitrocellulose membranes (0.2 μm trans-blot transfer medium from Bio-Rad) from SDS PAGE gels in a trans-blot cell (Serva) by using 25 mM Tris/HCl/192 mM glycine/33% (v/v) methanol (pH 8.3). The blots (6 cm x 8 cm) were rinsed twice in PBS and “blocked” in 3 % BSA in PBS (0.8 % NaCl, 0.02 % KCl, 0.144 % Na2HPO4, 0.024 % KH2PO4, pH 7.4) for 60 min. The blots were rinsed twice and washed once for 15 min and three times for 5 min PBS. A 1:10000 dilution of polyclonal anti-RTP1 antibodies (in PBS containing 3 % BSA), The blots were incubated on a revolving wheel for 1 – 2 hours at RT and washed again as described above. a 1:1000 dilution of anti-rabbit serum (anti-rabbit IgG- peroxidase conjugated

monoclonal antibodies, Sigma). Finally, the membrane was washed a few times with PBS buffer and protein bands were detected via chemiluminescence, by incubating the membrane in enhanced chemiluminescence reagents for 1min. The membrane was then exposed to X-ray films (X-omat AR5, Kodak) for 1s-20min and finally, the films were developed by AGFA Curix 60.

- **Chemiluminescence reagents**

400 µl Luminol (5 mM in DMSO; Luminol: 3-amino-phthalazinedione)
400µl PIP (paraiodophenol 50 mM in DMSO)
400 µl Hydrogen peroxide (20µl 30%Hperoxide in 1m H_2O)
2.8 ml Glycine buffer (Glycine 50mM, pH 10.25)

- **Estimation of molecular weights in immunoblots**

We routinely used prestained molecular weight markers from Fermentas (Pre-stained Protein Ladders) to approximate the molecular weight of blotted crossreacting bands.

2.2.15 Infection assays

- ***C. lindemuthianum***

Conidial suspensions were obtained by scraping 6-day-old malt agar petri dish cultures in sterile water. The conidia were recovered by centrifugation at low speed (300*g*) and were rinsed twice with sterile water before use. Conidia were then used at a concentration of $5x10^6$ conidia/ ml to drop inoculate the lower surfaces of excised cotyledons. Inoculated samples were placed on wet filter paper inside petri dishes to maintain high humidity and incubated at 22°C.

- ***U. maydis***

U. maydis strains were grown O/N at 28°C in complete medium (Holliday, 1974). Sporidia were collected by centrifugation, washed twice, adjusted to a cell density of 5×10^7/mL in distilled water and used to inoculate 7 to 10 day-old maize plantlets.

Inoculation was performed by injection of approximately 200 to 400 µL sporidial suspension through the stem, using a 26-gauge needle.

2.2.16 Photography and microscopy

Whole mount GFP photographs were taken with a Zeiss Stemi SV6 dissecting microscope with a NIKON digital camera and images were processed with Paint shop version 5.0.

2.2.17 Bioinformatic methods

Similarity searches were performed using the BLAST (Basic Local Alignment Search Tool) tool at http://www.ncbi.nlm.nih.gov/blast/. PEST sequence prediction analyses https://emb1.bcc.univie.ac.at/toolbox/pestfind/pestfind-analysis-webtool.htm.
Intracellular targeting and protein domains predictions were done using PROSITE prediction server at http://www.expasy.ch/prosite/ and CBS prediction server at http://www.cbs.dtu.dk/index.shtml.

3 Results

3.1 Subcellular localization of RTP1

The nucleus of all eukaryotic cells from protozoa to mammals is delimited by a specialized double membrane, the nuclear envelope that is perforated by nuclear pore complexes (NPC). Free diffusion of molecules smaller than 10nm in diameter can occur through NPCs sites, whereas trafficking of macromolecules from the cytoplasm to their final destination in the nucleus, is subjected to a selective regulation. Karyophilic proteins are equipped with a nuclear localization signal (NLS) which is recognized by a receptor α subunit of a heterodimeric cytoplasmic receptor termed importin. The protein/receptor complex is actively transported through the NPC and, once in the nucleus, the complex dissociates and the receptor returns to the cytoplasm (Corbett and Silver,1997).

The intracellular localization of RTP1 is important for understanding the function of this protein in the cell and for the location of the compartment where its function occurs. The immunofluorescence data with *U. fabae* infected broad bean leaves have detected a strong RTP1 signal inside the host plant cytoplasm and nucleus (Kemen et al., 2005; **Fig.6**). Furthermore, the prediction of a putative bipartite nuclear localization signal in the N-terminal domain of RTP1 (**Fig.9**) prompted us to check whether this secreted fungal protein was targeted to the plant nucleus.

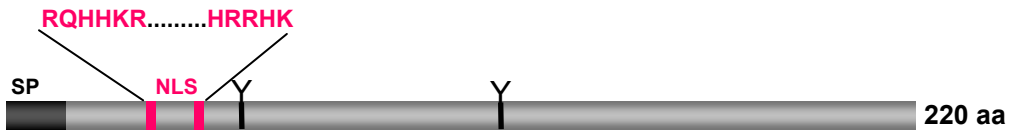

Fig.9. Schematic presentation of the bipartite NLS predicted in RTP1.

3.1.1 NLS regulated nuclear localization of RTP1 in plants

To investigate the subcellular localization of RTP1 protein in living plant cells, and to test the functionality of the predicted bipartite NLS, an enhanced version of GFP (mGFP4) was used as a reporter. As previously reported (Corbett and Silver, 1997) and expected due to its small size, expression of GFP alone results in cytoplasmic and nuclear fluorescence. For GFP to act as a convenient marker for analysis of RTP1 localization, it was desired that it does not diffuse into the nucleoplasm. For this reason, the cytosolic enzyme chalcone synthase (CHS) was fused to the N-terminal of GFP in order to increase the size of the reporter protein up to 72.3 kDa, which would make it bigger than NPC size limit. RTP1p lacking the first 20aa corresponding to the signal peptide was then fused in frame to the carboxyl-terminus of CHS-GFP fusion protein. The resulting construct GFP:RTP1 was transiently transfected into tobacco BY2 cell protoplasts and monitored for GFP expression by fluorescence microscopy 18 h post-transfection.

As shown in **Fig.10B(1),** protoplasts transiently expressing CHS-GFP show fluorescence both in the cytoplasm and the nucleus, apparently due to passive diffusion through NPC. Diffusion of GFP to the nucleus despite its size that should be bigger than the exclusion limit of the NPC might have resulted from the passive overexpression of the reporter construct and the sensitivity of the expression system displaying even very low diffusion activity. Unexpectedly, GFP:RTP1 did not show any fluorescence even after repeated transformations. The same results were obtained when RTP1 was N-terminally fused to CHS-GFP, resulting in RTP1-CHS-GFP, where CHS served as a spacer between RTP1 and GFP (not shown). The absence of GFP fluorescence in protoplasts transformed with full-length RTP1 expressing constructs will further be discussed in chapter 3.

To check whether RTP1p was targeted to the plant nucleus, a truncated protein RTP(36-69), lacking the N-terminal (aa 1-35) and the C-terminal (aa 70-220), and including the putative bipartite NLS (RQHHKR X_9 HRRHK) was generated. RTP(36-69):GFP fusion protein showed green fluorescence exclusively in the nuclei of transfected protoplasts (**Fig.10A**) indicating the functionality of the predicted NLS.

To further validate this finding, three basic aa were replaced by site-directed mutagenesis within the first core of the bipartite NLS (RQ**DQ**K**L** X_9 HRRHK) within the truncated protein RTP(36-69). This construct localized both to the cytosol and nuclei of all transfected protoplasts, similar to GFP reporter control. Taken together, these data establish that RTP1 is specifically targeted to the plant nucleus, and that the intact bipartite NLS in RTP1 is required for this specific targeting.

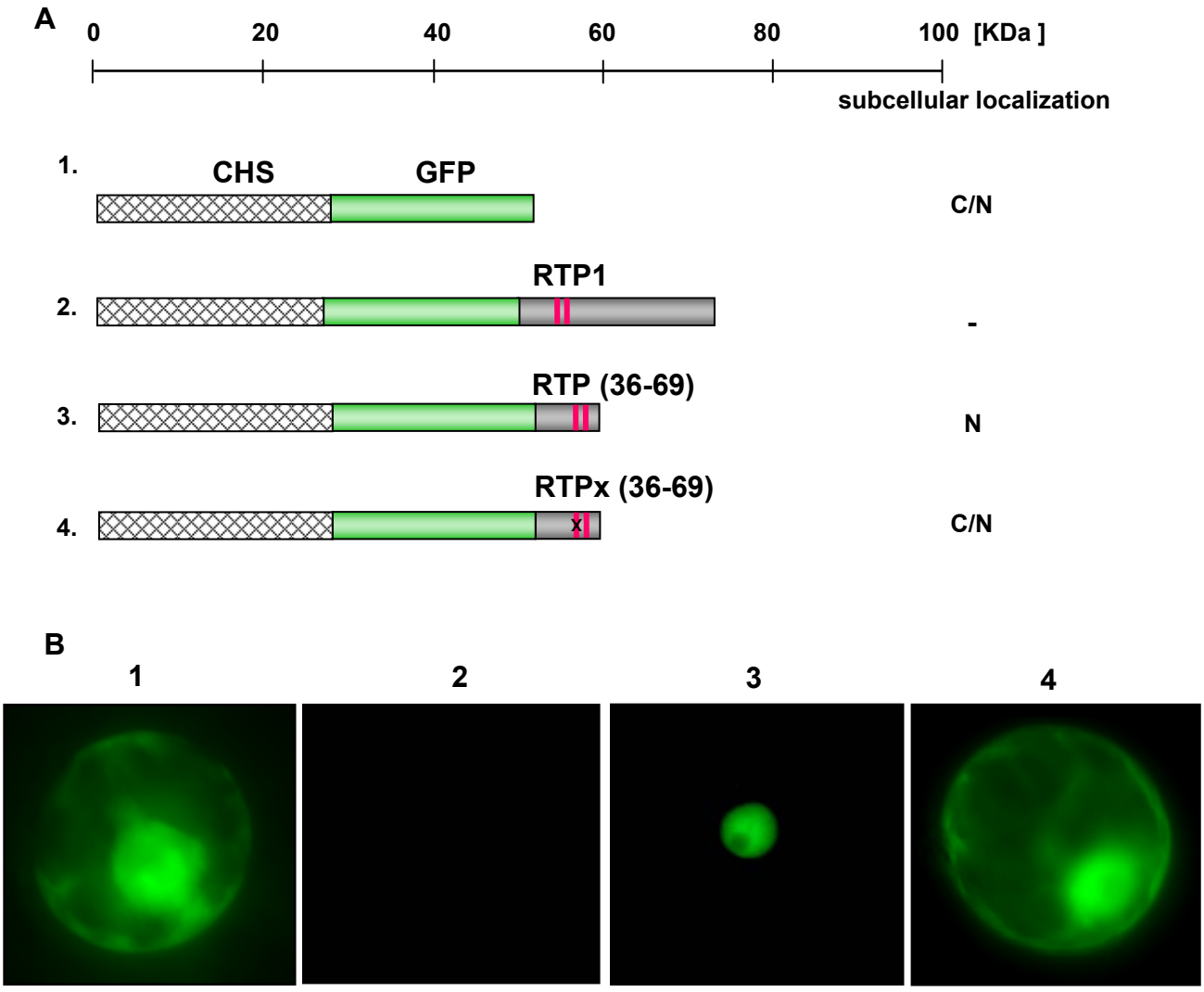

Fig.10. Subcellular localization of GFP-RTP1 constructs in BY2 protoplasts. (**A**) Fusion protein constructs used for the localization studies. RTP (36-69) refers to RTP1 truncated protein containing the predicted NLS (RQHHKR X_9 HRRHK), RTPx(36-69) designates the same truncated protein with amino acid exchanges within the first core the bipartite NLS. CHS: Chalcone synthase, GFP: Green fluorescence protein. The subcellular localization pattern of each protein is indicated on the right. C, cytoplasmic, N, nuclear; C/N, both cytoplasmic and nuclear, -, absence of GFP fluorescence. (**B**) Pictures of tobacco protoplasts transfected with the constructs shown in (A).

3.2 Stable constitutive expression of RTP1 in *Arabidopsis thaliana*

As no efficient transformation procedure is available for *Vicia faba,* the host plant of *Uromyces fabae,* stable expression of *RTP1* in the model plant *Arabidopsis thaliana* was initiated, to investigate the intrinsic function of RTP1 within rust infected plant cells. For this, the binary vector pCB302, allowing *Agrobacterium tumefaciens*-

mediated transformation was used. Two sets of T-DNA plasmids were constructed, one containing the entire open reading frame (=s*RTP1*) and another one corresponding to the mature RTP1 that excluded the signal peptide leader sequence but included an additional ATG start codon (=*RTP1*).To ensure constitutive and high level expression *in planta*, all constructs were placed between the strong viral *35S* promoter and a *nos* termination sequence (**Fig.11**). The complete expression cassette was cloned into the binary plasmid pCB302 (see Materials and Methods), which confers resistance to gluphosinate (Basta) in transgenic plants. The resulting constructs were transformed into *Arabidopsis* by flower dipping method.

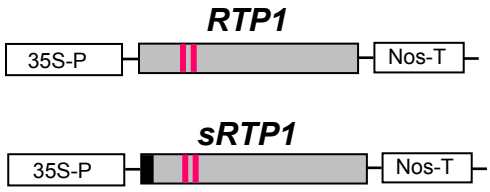

Fig.11. Constructs for stable expression of *RTP1* in *A. thaliana*

3.2.1 Stable expression of RTP1 in *Arabidopsis* resulted in very low number of transformants

Seeds generated from transformation with pCB302-*RTP1* were selected for transgenic 35S:*RTP1* plants. Of 15,000 seedlings screened in the T1 generation, only three plants were resistant to gluphosinate. This indicated a very poor transformation efficiency. RTP1 expression could therefore be partially lethal during *Arabidopsis* seed production and/or germination. In the case of seeds generated from pCB302-*sRTP1*, expression of the full-length *sRTP1* cDNA including the signal peptides resulted in 7 resistant T1 plants among 10,000 seedlings. This indicated a slightly higher transformation efficiency in comparison with the results got from pCB302-*RTP1*. However, the transformation efficiency overall is low as *Arabidopsis* (Col-0) has a transformation frequency of nearly 1%. The three 35S:*RTP1_T1*, and the 7 35S:*sRTP1_T1* transgenic lines were allowed to self and set seeds, and homozygous lines were selected in the T3 generation based on uniform herbicide resistance.

3.2.2 Phenotype of *35S:RTP1* and *35S:sRTP1* expressing plants

When comparing the phenotypes of T1 transgenic *Arabidopsis* plants with those of the wild-type plants, considerable growth retardation of *35S:RTP1* plants was observed. All three *35S:RTP1_T1* plants exhibited a smaller phenotype than the wild-type plants, both the basal rosette and the flowering stems were retarded in growth. Because of the delayed development of the transgenic plants, they had a much younger appearance, including lighter green leaves (**Fig.12**). Flowering and seed set appeared quite normal. However, this growth phenotype was not transmitted to subsequent generations, since the T2 progeny derived from selfed T1 lines showed a mixture of retarded and normally growing plants, whereas T3 generation plants looked like wild-type plants grown under long day conditions. In the case of *35S:sRTP1* plants, all transformants were similar to wild type control plants.

3.2.3 RTP1 expression in *35S:RTP1* and *35S:sRTP1* plants.

Reverse transcriptase-PCR was performed to detect *RTP1* transcript in 6 different T2 transgenic *35S:RTP1* and *35S:sRTP1* lines. PCR reactions were performed with the same quantity of cDNA for all samples and carried out for 25 cycles. *RTP1* and *sRTP1* transcripts were detected in all the analysed lines except the WT (**Fig.14**). In control experiments, analysis of the constitutively expressed Ef-2a-specific transcripts generated similar amounts of PCR products in all plant samples indicating equal efficiencies of the RT-PCRs. To verify the presence of RTP1 protein in the T2 transgenic plants, total proteins were extracted and analysed by western blotting using polyclonal antibodies raised against RTP1. However, no detectable amount of RTP1 protein could be recovered, even after repeated attempts (data not shown).

Fig.12. Growth phenotype of four-week-old RTP1 transgenic and WT plants. Cultivation was performed under short day conditions.

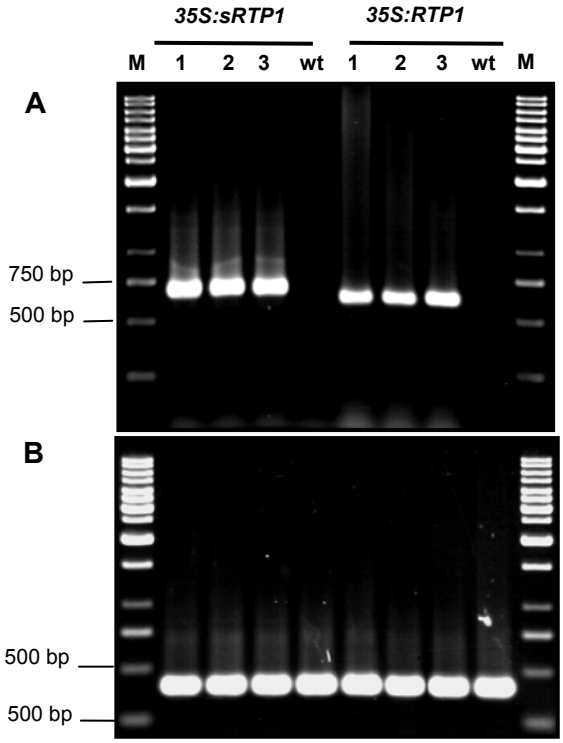

Fig.13. Semi-quantitative RT-PCR to detect *sRTP1* and *RTP1* transcripts in transgenic *Arabidopsis* lines. (**A**) Amplification of *sRTP1* (660 bp) and *RTP1* (600 bp) transcripts in three different *35S:sRTP1_T2* and *35S:RTP1_T2* lines, using gene specific primers. M:1kb DNA ladder. (**B**) Amplification of *Ef-2a* transcript in analysed plants.

3.2.4 Susceptibility of *35S:RTP1* and *35S:sRTP1* plants to pathogen infection

To determine whether RTP1 modulates plant defence responses, the transgenic *Arabidopsis* plants were analysed for their susceptibility to the bacterial pathogen *Pseudomonas syringae pv. tomato* and the fungal pathogen *Botrytis cinerea.* Five-week-old soil-grown wild-type, *35S:RTP1* and *35S:sRTP1* plants were infiltrated with bacterial suspensions containing 10^8 cfu/ml virulent DC300 strain. All infected leaves showed water-soaked symptoms similarly during the first 2 days, as a result of an aggressive growth of the bacteria (Katagiri et al., 2002). Later, tissue necrosis and chlorosis were observed in all infected leaves and no significant difference between the transgenic and WT *Arabidopsis* plants was observed (not shown). Similar results were obtained when the susceptibility of the plants to the necrotrophic pathogen *Botrytis cinerea* was analysed. Four-week-old plants grown in soil were inoculated with 6µl suspension droplets containing 10^5 spores/ml of *B. cinerea* conidia, and the progress of the infection was followed. *35S:RTP1* and *35S:sRTP1* plants showed similar infection symptoms when compared to the WT plants (**Fig.14**). These results suggest that RTP1 is unlikely to affect susceptibility of *Arabidopsis* to necotrophic and hemibiotrophic pathogens.

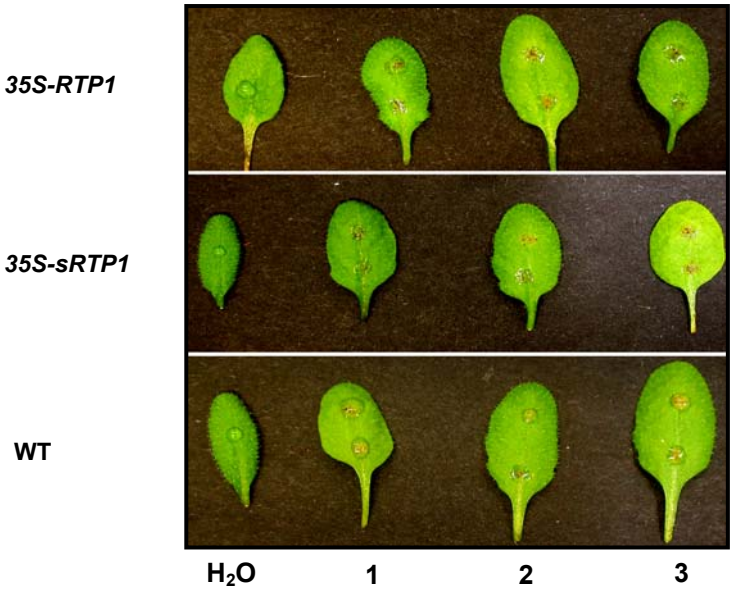

Fig.14. Response of *Arabidopsis* lines to infection with *B. cinerea*, 5 days post inoculation. The necrotic lesions were similar on all analysed lines. Leaves of 4 to 5 week-old plants were drop-inoculated with conidia of *B. cinerea* B05.10 strain (1, 2, 3), drops of water were used as negative control (H_2O). The experiment was repeated twice with similar results.

3.3 Stable inducible expression of RTP1 in *A. thaliana*

Constitutive expression of *35S:RTP1* and *35S:SPRTP1* in *Arabidopsis* (as described above) resulted in very low number of transformants, indicating that it likely causes a deleterious effect in plants. This makes it difficult to directly relate RTP1 function with the observed phenotype. In order to circumvent the problem of low transformation efficiency and to elucidate the function of RTP1 in plants, a regulated gene-expression system was adopted. The most frequently used inducible systems are those regulated by the inducers tetracycline, Cu^{2+}, dexamethasone and ethanol (Zuo and Chua, 2000). The *alc* regulon which is derived from the filamentous fungus *Aspergillus nidulans* was chosen, essentially because of its simplicity. This system employs a transcription factor, AlcR, which in presence of ethanol, binds to *alcA* promoter and activates gene expression (**Fig.15**). The ethanol inducible system presents several advantages. First it is originated from from *A. nidulans* and therefore no putative plant homologues of the AlcR protein could efficiently activate the *AlcA* promoter as *Arabidopsis* and *A. nidulans* are phylogenetically very distinct. Second the *alc* regulon allows controlled spatial and temporal induction of gene expression in plants (Maizel and Weigel, 2004). Third, ethanol has a low toxicity for plant and is inexpensive.

3.3.1 Characterization of *alcA:UidA*, *alcA:RTP1* and *alcA:sRTP1* transgenic *Arabidopsis* plants

Agrobacterium-mediated transformation was used to generate plants that were expressing either *UidA* (encoding β-glucoronidase, GUS), RTP1 or sRTP1. Transformants (T1) were selected on kanamycin containing medium. The transformation efficiency was about 0.5% for *alcA:UidA* and *alcA:sRTP1*, and about 0.2% for *alcA:RTP1*. T2 plants were selected from T1 seed groups exhibiting 3:1 segregation for kanamycin sensitivity. A third round of selection on kanamycin resulted in homozygous individuals (T3). These plants and their progeny (T4) were used for further characterization. No viability, fertility or morphological phenotypic differences to the wild type were observed for any of the transformants during the selection procedure.

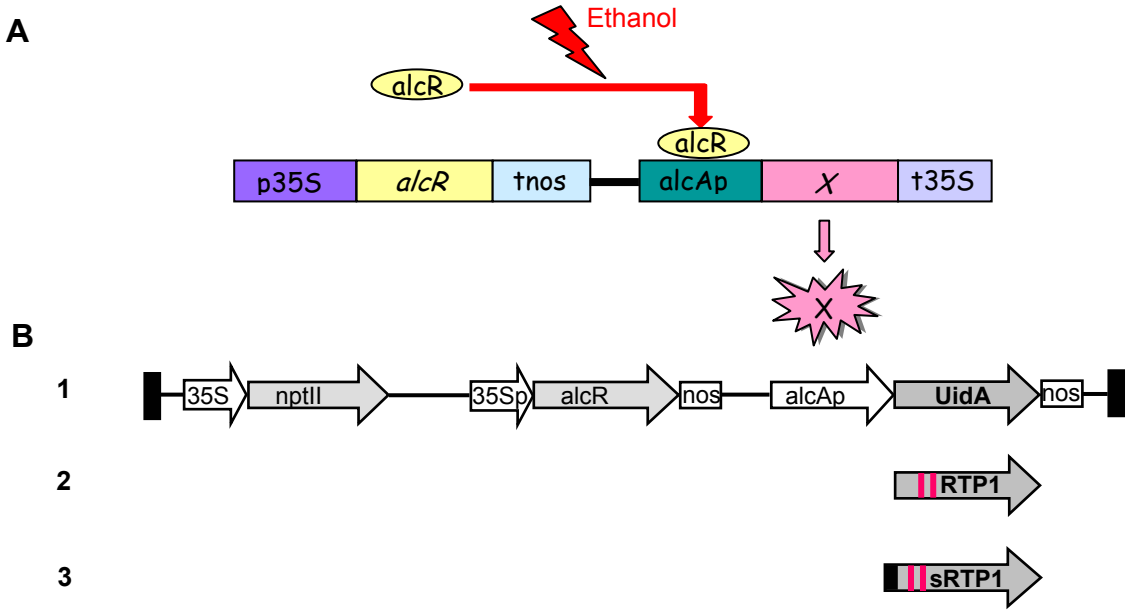

Fig.15. **Schematic presentation of *alcA* system functional components.** (**A**) In the presence of ethanol, the transactivator protein alcR binds alcA promoter, which is linked to a gene of interest. The chimeric target promoter comprises the regulatory sequences of the *alcA* promoter and a core promoter region (a TATA box and a transcription start site) of the 35S plant-expressible gene promoter (Caddick *et al*., 1998). (**B**) The *alcA*-based ethanol inducible expression T-DNA constructs used for *A. thaliana* transformation. (1) *CaMV35S* promoter is fused to *alcR*. The *GUS* reporter gene (*UidA*) was placed under control of a*lcA* and introduced into pΔalcR binary vector. The black bars represent left and right borders of the T-DNA. As a selective marker the nptII gene for kanamycin resistance was used. (2) and (3) these constructs are similar to (a) except for *UidA* which is replaced by *RTP1* and *sRTP1* respectively.

3.3.2 Efficiency of the *alcA* inducible expression system

As a first step, *alcA:UidA* transgenic plants were used to determine whether the responder cassettes are activated after ethanol induction. To this end, 4 to 6-week-old soil grown *alcA:UidA_T3* plants from 6 different lines were screened for GUS activity after induction with 2% ethanol solution by root drenching (see materials & methods). GUS activity was detected by X-GLUC (5-bromo-4-chloro-3-indolyl-β-D-glucuronide) staining. The first GUS positive spots were already visible one day after induction, and robust GUS activity was detected starting from the second day in roots, shoots and inflorescence of all tested plants (**Fig.16A**). GUS activity was maintained over the two-weeks period following the induction, before it disappeared completely from plant tissue. No GUS activity was observed prior to induction.

Collectively, the above data indicate that the *alcR*-mediated GUS expression occurs in a highly responsive manner.

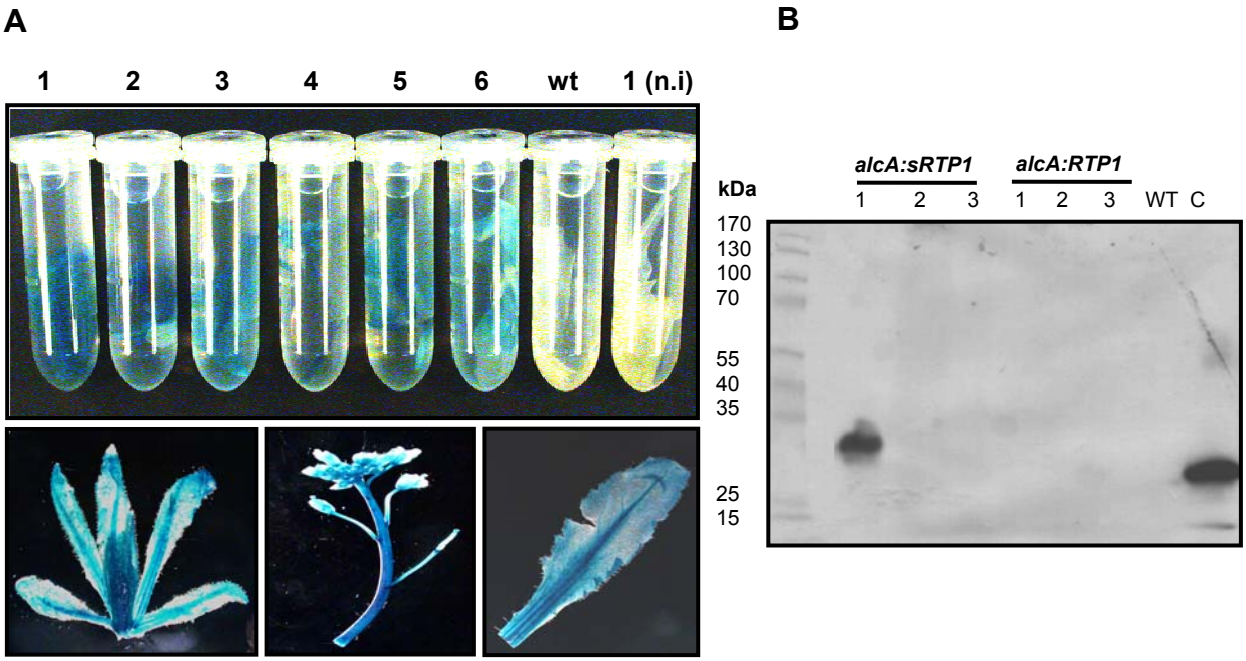

Fig.16. Response to ethanol induction in *alcA* Arabidopsis plants. (**A)** Histochemical localization of GUS activity in 6 different (T3 and T4) *alcA:UidA* 4 to 6-week-old plants. Dark blue precipitates were detected in all induced plants , but not in wild type or in non induced plants (n.i). (**B**) Western blot analysis of RTP1. Equal amounts of crude soluble protein extracts (~150µg) were loaded and fractionated by 10% SDS-PAGE, blotted, and probed using S844 anti-RTP1 antibody, C: purified RTP1 expressed in *Escherichia coli* (used as positive control).

3.3.3 RTP1 is not detected in *alcA:RTP1* plants

Three soil grown independent homozygous (T3 and T4) from *alcA:RTP1* and *alcA:sRTP1* plants (4 to 6 weeks old) were chosen and analysed for detection of RTP1 by western blotting of whole-cell extracts. In the case of *alcA:sRTP1* plants, the anti-RTP1 antibodies recognized a well stained single protein band in only one of the analysed plants. In contrast, there was no cross-reaction with proteins from *alcA:RTP1* plants, expressing the mature RTP1. The protein detected in one of the *alcA:sRTP1* plants, has a size in the SDS gel of about 32 kDa, which is close to the predicted size for RTP1 protein (25 kDa) detected in *U. fabae* infected *V. faba* leaves (**Fig.16B**). Despite repeated attempts and use of higher amount of extracted proteins

(250 µg), RTP1 protein could not be detected in any other of the ethanol-inducible, RTP1 expressing plants. *alcA:UidA* plants, used to check the induction efficiency, always showed high expression of GUS activity in all experiments.

3.3.4 *alcA:RTP1* transcript is induced with similar efficiency to *alcA:UidA*

To evaluate the levels of *RTP1* transcripts after induction with ethanol solution, total RNAs were prepared from 4-week-old plants of three independent *alcA:RTP1* lines. RNA was extracted 24 and 48 hours after induction. Accumulation levels of the *RTP1* transcript were analysed by quantitative real-time reverse transcriptase (RT)-PCR, and compared to *GUS* transcript levels in three independent *alcA:UidA* lines (**Fig.17**).

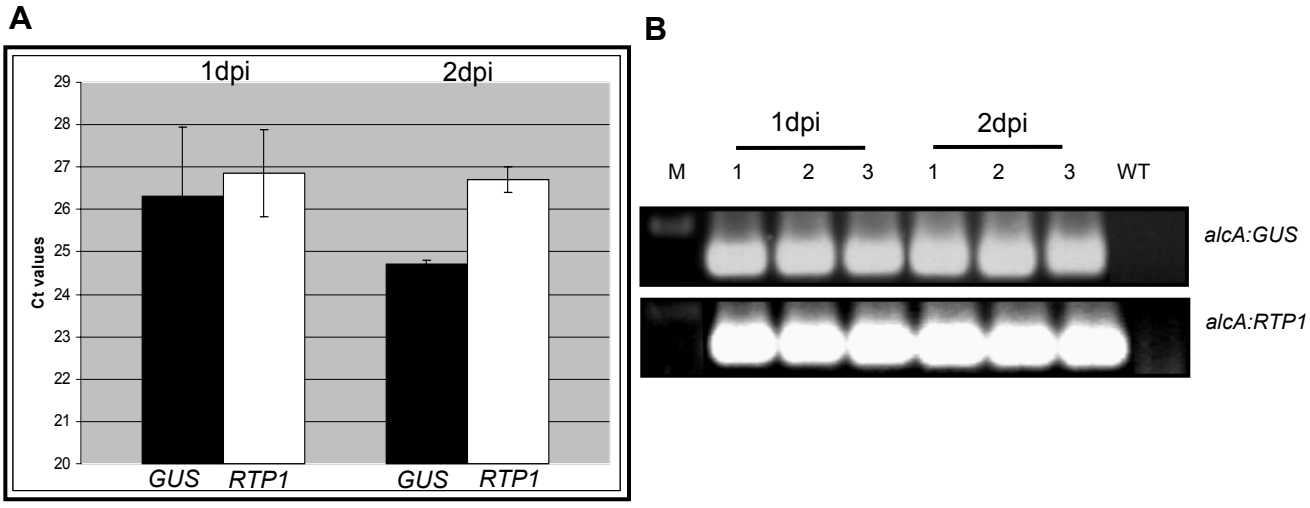

Fig.17. Real-time PCR to quantify *RTP1* transcript abundance in *alcA:RTP1* plants. (**A**) Ct values using cDNA templates derived from *alcA:UidA* and *alcA:RTP1* plants using *GUS* and *RTP1* genes specific primers, respectively. (**B**) Agarose gel electrophoresis showing *GUS* (346bp) and *RTP1* (340bp) products from the quantitative real-time PCR. M:1-kb DNA ladder.

The results showed that the accumulation of *RTP1* transcript in *alcA:RTP1* plants was similar to *GUS* transcript levels in *alcA:UidA* plants. However, when comparing transcript levels between the first and the second day post induction, the accumulation of *GUS* transcript, but not of *RTP1* transcript, increased after 2 days. This is explained by the Ct values which essentially didn't change in the 2dpi for

RTP1 transcript, while they decreased with about two cycles in the case of *GUS,* showing 4-fold increased amount of *GUS* transcript. Collectively, these data show that the expression of both *alcA:RTP1* as well as *alcA:UidA* was efficiently induced one day after application of ethanol. Additionally, this experiment provided evidence for a slight increase of *GUS* transcript accumulation in the second day after induction, which was not observed for the *RTP1* transcript.

3.3.5 Phenotypic consequences of RTP1 induction in agar-grown plantlets

The effect of *RTP1* and *sRTP1* induction on plant viability and phenotype was investigated by visual assessment of induced agar-grown plantlets and induced soil grown plants grown to maturity. Application of ethanol to 4 week-old soil-grown plants did not reveal any phenotype of any transformant type. However, when 2 week-old plantlets, grown on agar-based medium, were induced, *alcA:RTP1* plantlets were significantly weakened in further growth (**Fig.18**). This phenotype was observed in multiple transgenic lines, and was studied in detail in two homozygous lines (*alcA:RTP1_T3*, lines RTP1-4 and RTP1-7). Application of ethanol was found to have a significant effect on the *alcA:RTP1* transgenic lines starting one day after induction. However the difference between *alcA:RTP1* and *alcA:UidA* control plantlets became more distinguishable after 8dpi. Thus, plant growth appears to be weakened by *RTP1* expression.

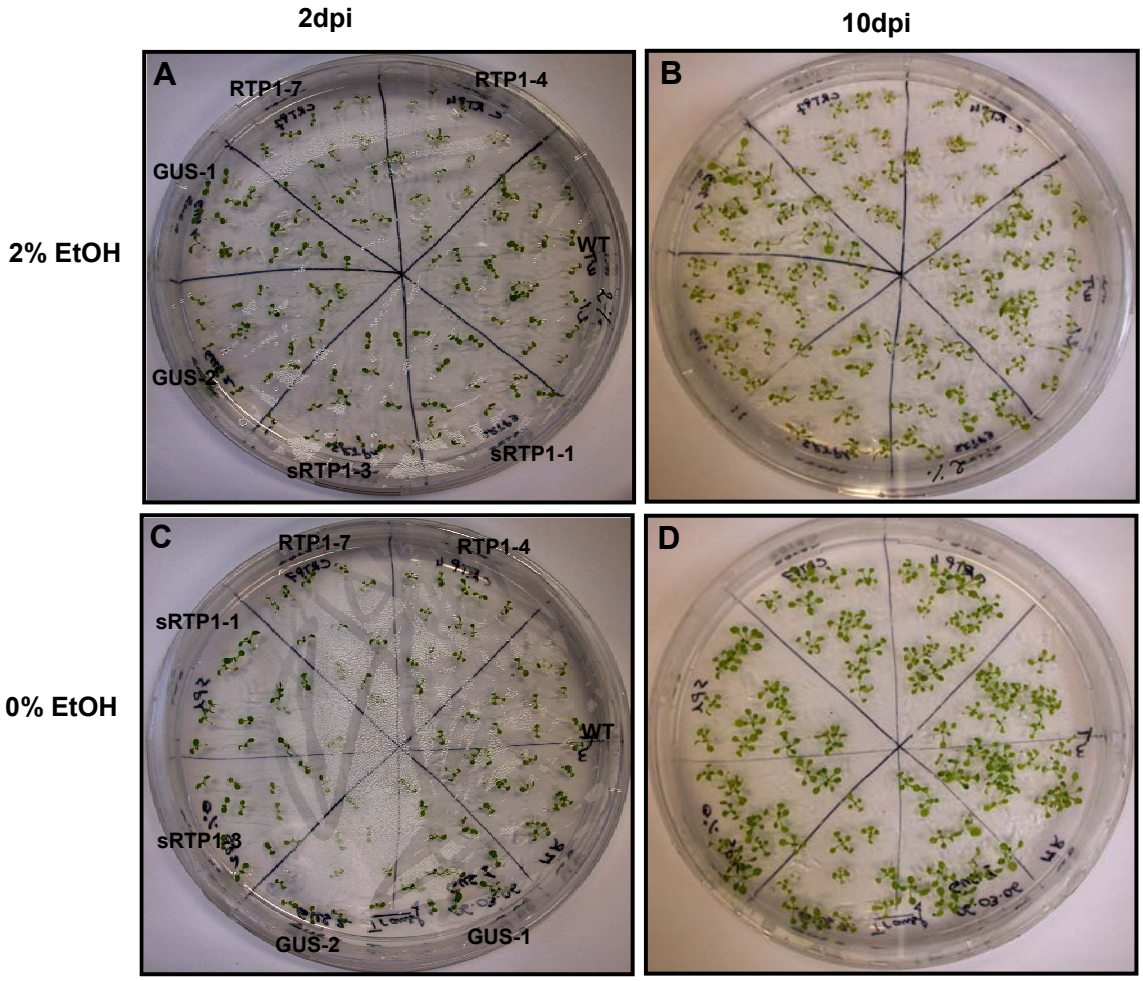

Fig.18. Phenotype of ethanol induced *alcA Arabidopsis* agar-grown plantlets. 10 day-old wild type (WT), homozygous *alcA:RTP1* (lines RTP1-4 and RTP1-7) and *alcA:UidA* (lines GUS-1 and GUS-2), and heterozygous *alcA:sRTP1* (lines sRTP1-1 and sRTP1-3) were induced by transfer into agar-medium supplemented with 2% ethanol. (**A**) and (**B**) images were taken 2 and 10 dpi, respectively. (**C**) and (**D**) control plates; the plantlets were transferred into agar-medium without ethanol.

3.4 RTP1 interferences with plant cells vitality

The ability of RTP1 to interfere with plant vitality and gene expression, as observed with *A. thaliana* plants and tobacco BY2 cells, might indicate that the activity of this protein is functional in a wide variety of plant species. To verify this unexpected finding, interaction of RTP1 with plant vitality and gene expression was further tested in the model plant *Nicotiana benthamiana* as well as in the rust host plant *V. faba*. For this purpose, transient expression assays of RTP1 by agroinfiltration (*N. benthamiana*) and particle bombardment transformation (*V. faba*) was used.

3.4.1 RTP1 is not detected when transiently expressed in *N. benthamiana*

Transient expression of genes through infiltration of *A. tumefaciens* into leaf tissue (agroinfiltration) has been found to be a quick and easy method to study genes of interest (Kapila et al.,1997; Rossi et al., 1993). This method has been chosen to transiently express RTP1 in tobacco leaves. *RTP1* was cloned into a binary vector containing an intron-containing β-glucuronidase (GUS) reporter gene (pCAMBIA 1301) to create RTP1:GUS fusion protein, *GUS* alone was used as a control (**Fig.19A**). Both constructs contained the 35S promoter of Cauliflower mosaic virus to drive transcription and the nopaline synthase terminator of *A. tumefaciens*. The resulting constructs were introduced into *A. tumefaciens*, and transient transformation was carried out by agroinfiltration of 4 to 6 weeks old *N. benthamiana* leaves. The activity of GUS (as a reporter protein) in agroinfiltrated leaves tissue was assayed by histochemical staining of leaf discs 48, 60 and 72 hours after agroinfiltration. Strong blue staining was detected in all *GUS* expressing leaf discs, but in any disc from leaves infiltrated with strains harbouring pCambia-*RTP1* (**Fig.19B**). However, western analysis, using S844 antibodies against RTP1, failed to detect RTP1 signal in protein samples harvested from the agroinfiltrated leaves. No macroscopic symptoms at infiltration sites were observed in the leaves for any of the used constructs.

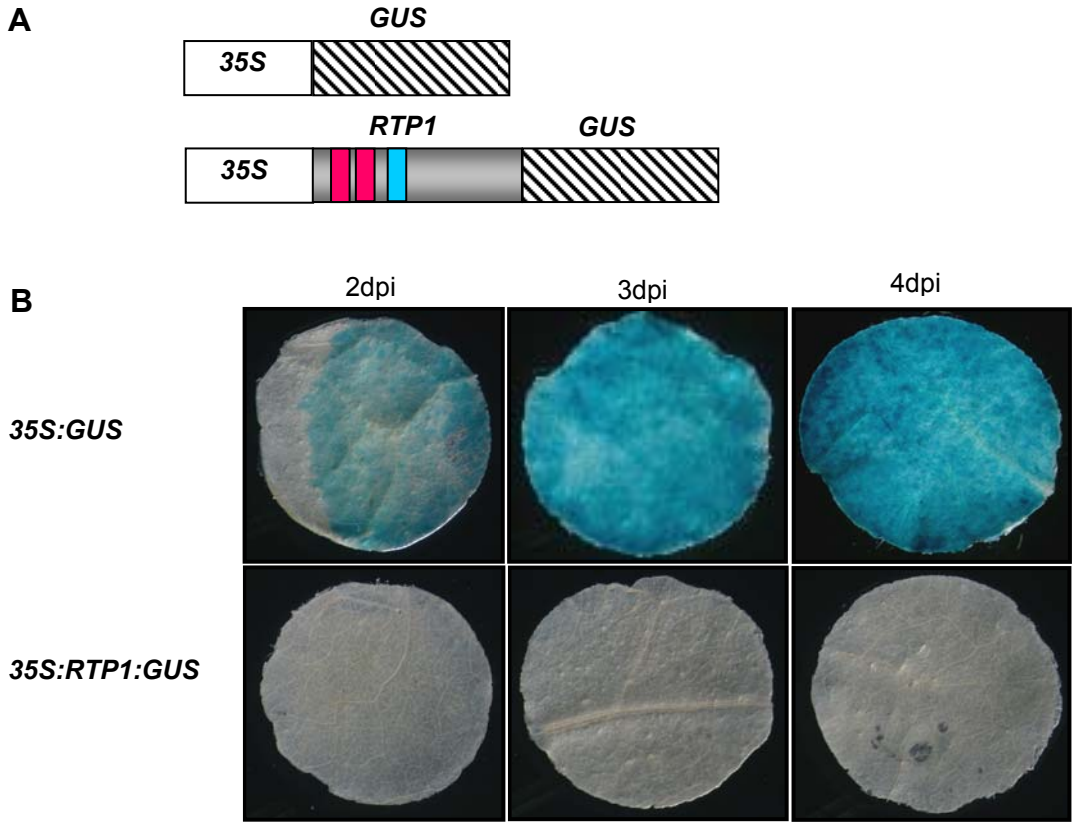

Fig.19. **Transient expression studies with agroinfiltrated leaves of *N. benthamiana***. (**A**) Schematic representation of the constructs introduced into tobacco plants leaves via pCambia binary vectors carried in *A. tumefaciens*. (**B**) Histochemical staining for GUS activity in the agroinfiltrated plant leaves. A representative set of leaves discs are shown. Leaves expressing *35S:GUS* alone showed a high level of GUS stain that increased upon a time, with the maximum being achieved 3 and 4dpi. No GUS activity could be detected in leaves infiltrated with *35S:RTP1:GUS* expressing construct.

3.4.2 *RTP1* transcript is expressed with similar efficiency as *GUS* in agroinfiltrated leaves

Although no RTP1 protein could be detected in the agroinfiltrated tobacco leaves, It was interesting to know whether the transcript itself is expressed. Total RNA was prepared from leaves of three different tobacco plants, transiently expressing either *35S:GUS* or *35S:RTP1:GUS*, one and two days after agroinfiltration. Real-time PCR was then used to quantify the levels of *GUS* mRNA in both sets of agroinfiltrated tissues using *GUS*-specific primers. Real-time RT-PCR analyses revealed no significant difference between *RTP1:GUS* transcript and the

external control *GUS* transcript abundance. This is shown by the Ct values which were similar in all samples (**Fig.20**). These results are very similar to those obtained from the ethanol inducible expression of *RTP1* in *A. thaliana* (Chapter 3. 3), which hints to a slight decrease in *RTP1* transcript when compared to the *GUS* transcript in *GUS* expressing plants, as an external control. This difference in mRNA levels remains, however, not significant.

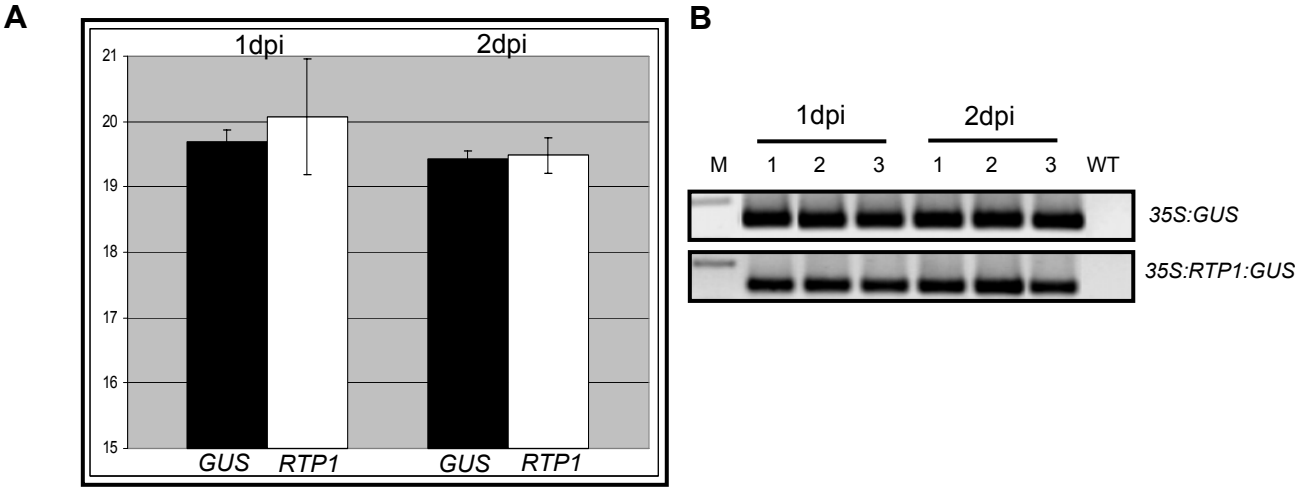

Fig.20. Real time RT-PCR to quantify *RTP1* transcript abundance in agroinfiltrated tobacco leaves. (**A**) Ct values with *GUS* specific primers using cDNA templates derived from *35S:GUS* and *35S:RTP1:GUS* expressing leaves. (**B**) Agarose gel electrophoresis showing the *GUS* (346bp) product from the quantitative real-time RT-PCR. M:1-kb DNA ladder.

3.4.3 RTP1 is not detected when transiently expressed in many plant species including the host plant

V. faba, as many other legumes, is among plants for which genetic transformation has not yet convincingly been reported (Somers et al., 2003). This is mainly because of the restricted host range of *A. tumefaciens* and the regeneration problems of *V. faba in vitro* tissue culture and protoplast transformation. However, transient gene expression technology by particle bombardment, used to deliver DNA into plant cells, has been used successfully for transient transformation studies in *V. faba* (Klein et al. 1987). In addition, this transformation method has been efficiently

used for the molecular analyses of cereal-powdery mildew interaction (Panstruga, 2004). During the presented work, particle bombardment has been found to be reliable and with reproducible results. This tool was therefore used to quantitatively study *RTP1* transient expression in epidermal cells of *V. faba* leaves.

The plasmid p*GFP:RTP1*, which expresses a *GFP:RTP1* cDNA fusion under the control of the strong *35S* promoter, was used for transient expression studies. This vector initially was constructed to study the subcellular localization of RTP1 in tobacco BY2 protoplasts, and was found to suppress GFP fluorescence (Chapter 3. 1). To test whether this construct will show the same results when expressed in host plant cells, this plasmid was transfected *V. faba* leaf cells via particle bombardment. The cells transfected with the plasmid encoding GFP alone showed, as expected, fluorescence in both the cytosol and the nucleus of the cells (**Fig.21**). The GFP:RTP1 fusion construct mostly didn't result in transformants except some rare cases where it showed GFP fluorescence located in the plant nucleus. Similar results were obtained when different plant species were bombarded (onions epidermal cells, BY2 tobacco cells, *A. thaliana* and *N. benthamiana* leaves). Alltogether these data support that RTP1 is likely to be active in many plant species and is not restricted to the host plant.

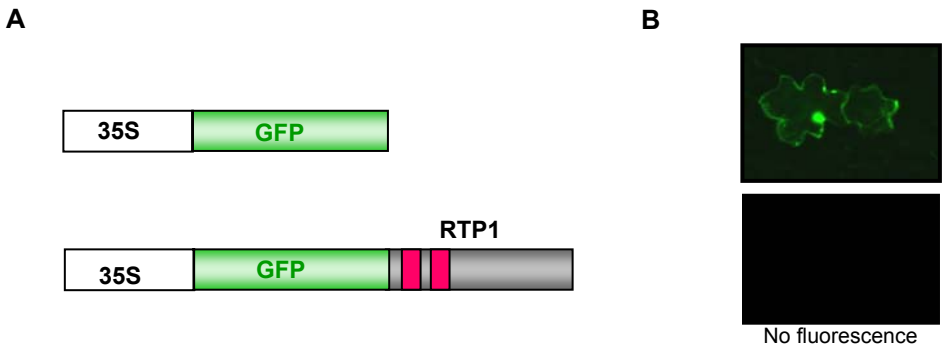

Fig.21 RTP1 transient expression in the host plant *V. faba*. Scheme of the used constructs (**A**)and the corresponding GFP fluorescence pictures (**B**) are shown.

3.4.4 RTP1 contains a PEST-like sequence, which does not destabilise GFP:RTP1

Based on results of the presented work, the RTP1 protein was neither detected neither when stably expressed in *A. thaliana*, nor when transiently expressed in several plant species. This leads to ask whether RTP1 is subjected to degradation. In fact, the analysis of RTP1 primary sequence showed the presence of a putative PEST motif, which is known to be a signal for proteolytic degradation (Rechsteiner and Rogers 1996). In the present study, the role of the predicted PEST-like sequence in the stability of RTP1 has been analysed.

The screen for a putative PEST domain in RTP1 protein sequence was carried out using PESTfind analyses webtool [http://www.at.embnet.org/toolbox/pestfind/]. This algorithm searches for hydrophilic regions of 12 or more amino acids that contain at least one P (proline), one E (glutamic acid) or D (aspartic acid), and one S (serine) or T (threonine), flanked by K (lysine), R (arginine), or H (histidine) residues. The algorithm assigns a score to each possible PEST sequence found. The score ranges from -50 to +50, with a score above zero indicating a possible PEST region while a value greater than +5 being of particular interest. Using the PESTFind algorithm, a potential PEST motif within RTP1 was detected (**Fig.22**). The RTP1 PEST-like region (residues 79-99) scored +9.38 and had a hydrophobicity index of 43.59. Within the 21 residues PEST-like region, 11 are polar (1 K, 1 H, 5 T, 3 S and 1 D), and 10 are nonpolar (5 P, 2 L, 1 V and 2 A). The RTP1 PEST-like sequence is recognised as a low complexity region by bioinformatic programs, which supports that this region may be surface accessible to proteases and/or functions in the interaction with other proteins.

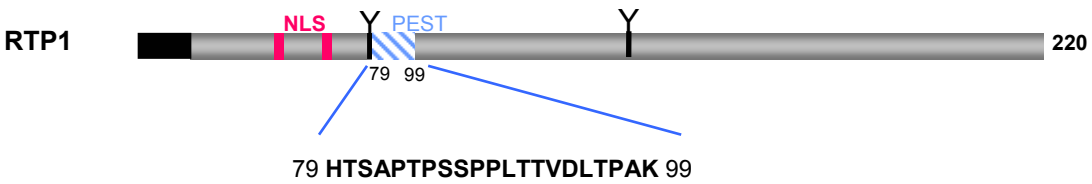

Fig.22. A PEST-like region in RTP1.

3.4.4.1 Construction of PEST mutants

In order to evaluate the role of the PEST sequence and examine whether it affects the stability of RTP1, two sets of RTP1 mutants were generated, either by in frame deletion or by alanine substitution of residues within the PEST-like region (**Table.6**). In the poly-alanine mutant ($RTP1_{PESTala7}$), 7 consecutive polar/charged residues (83-89 aa), forming the longest contiguous sequence of PEST residues, were mutated each to alanine, a small neutral and hydrophobic residue. This increased the hydrophobicity of the PEST-like region and removed the majority of significant PEST residues. The in frame deletion mutant ($RTP1_{\Delta PEST}$) was generated by deletion of the entire longest contiguous PEST sequence (83-89 aa), and was replaced by *Sma*I restriction site which allowed verification of the construct during the cloning (**Fig. 23**). All constructs were additionally confirmed by sequencing.

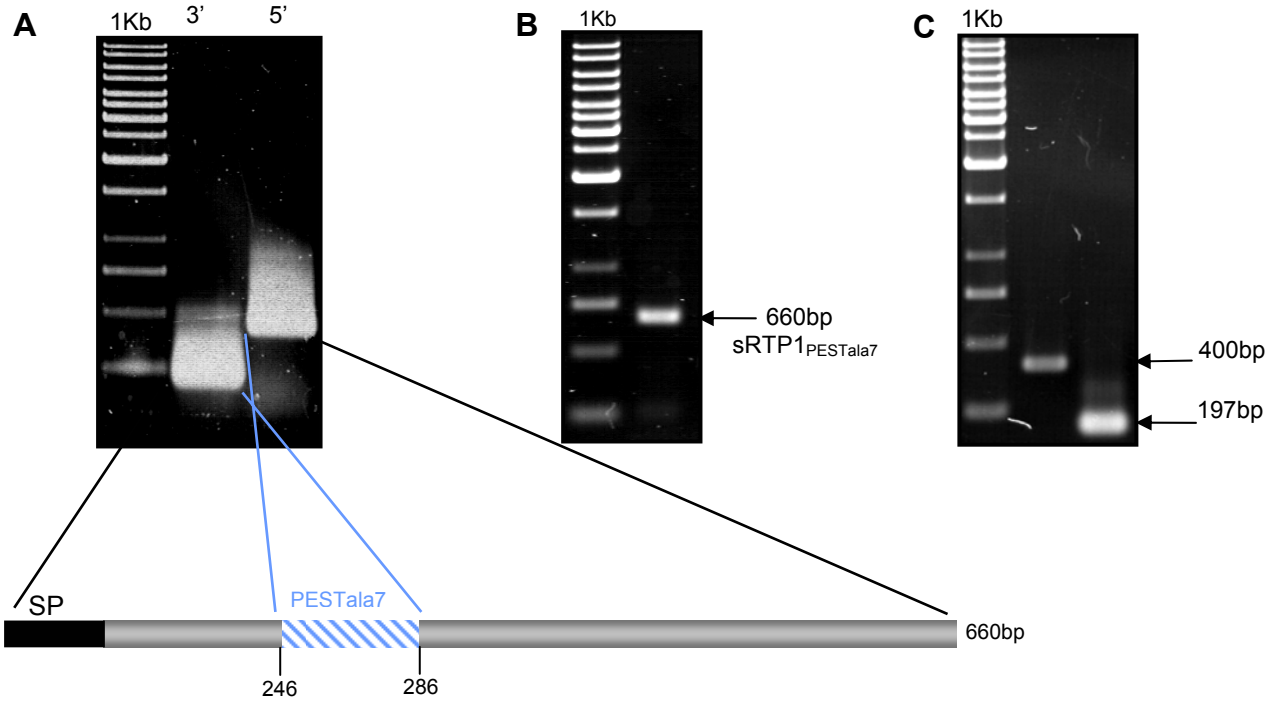

Fig.23. PCR amplification of $sRTP1_{PESTmutant.}$ (**A**) First round PCR to amplify *$sRTP1_{PESTala7}$*. Amplification of the first 286bp fragment at the *3'* end of *sRTP1* which contains 42 bp overlaps with the 415bp *5'* end of *sRTP1* fragment . The overlapping sequence introduced site directed mutations within the PEST-like region aiming to substitute the longest contiguous PEST residues with 7 alanines (Chapter 3.3). (**B**) Second round PCR to amplify *$sRTP1_{PESTala7}$*. The purified fragments shown in panel A were used as DNA template in the second round PCR to generate the overlap extension product corresponding to $RTP1_{PESTala7}$. (**C**) Generation of *$RTP1_{\Delta PEST}$* . PCR amplified *3'* (197bp) and *5' RTP1* (400bp) *RTP1* fragments were fused, using *SmaI* in pCHS-GFP to generate *$GFP:RTP1_{\Delta PEST}$*, in which the longest contiguous PEST-like motif was in frame deleted and substituted by *SmaI* restriction site. Sequences of RTP1-specific primers as well as primers introducing mutations are listed in Table. 2.

Table. 6. Mutations introduced into the predicted PEST-like sequence of RTP1.

Mutant	PEST-like sequence	PEST score
RTP1 (wild type)	79 HTSA**PTPSSPP**LTTVDLTPAK 99	+9.38
$RTP1_{PESTala7}$	79 HTSA**AAAAAAA**LTTVDLTPAK 99	-14.54
$RTP1_{\Delta PEST}$	79 HTSA**PG**LTTVDLTPAK 95	-2.87

3.4.4.2 Expression of the PEST mutants

To examine whether the disruption of the PEST-like sequence affected the stability of the various mutants, *$RTP1_{PESTala7}$* and *$RTP1_{\Delta PEST}$* cDNAs were fused to *GFP* in pGFP plasmid which was used in the transient expression studies. The resulting constructs *35S:GFP:$RTP1_{PESTala7}$* and *35S:GFP:$RTP1_{\Delta PEST}$* were transiently transfected into *V. faba* leaf cells by particle bombardment. The bombarded leaves were analysed, 18-20 hours after transfection, for detection of GFP by fluorescence microscopy. As illustrated in **Fig.24A**, the polyalanine mutation had no apparent effect on the expression of GFP:RTP1. Both GFP:$RTP1_{PESTala7}$ and GFP:RTP1 constructs suppressed GFP fluorescence in comparison to GFP construct. This indicated that the PEST-like region doesn't seem to be responsible for any presumed instability of RTP1. In contrast, transient expression of GFP:$RTP1_{\Delta PEST}$ showed GFP fluorescence in the nuclei of the transformed cells, although the number of fluorescent cells was much lower than in leaves transformed with GFP alone (**Fig.24**). This result is contradictory to the result obtained from GFP:$RTP1_{PESTala7}$, and is likely due to the deletion of the entire 7 amino acids within the studied motif, which might have caused a significant structural disruption in the protein. To further verify that RTP1 PEST-like sequence is not acting as a proteolytic signal, a construct was generated that fused the PEST-like motif to the C-terminus of GFP in pGFP plasmid. The expression of the latter construct did not affect GFP stability, which argues against the role of RTP1 PEST-like motif as a degradation signal.

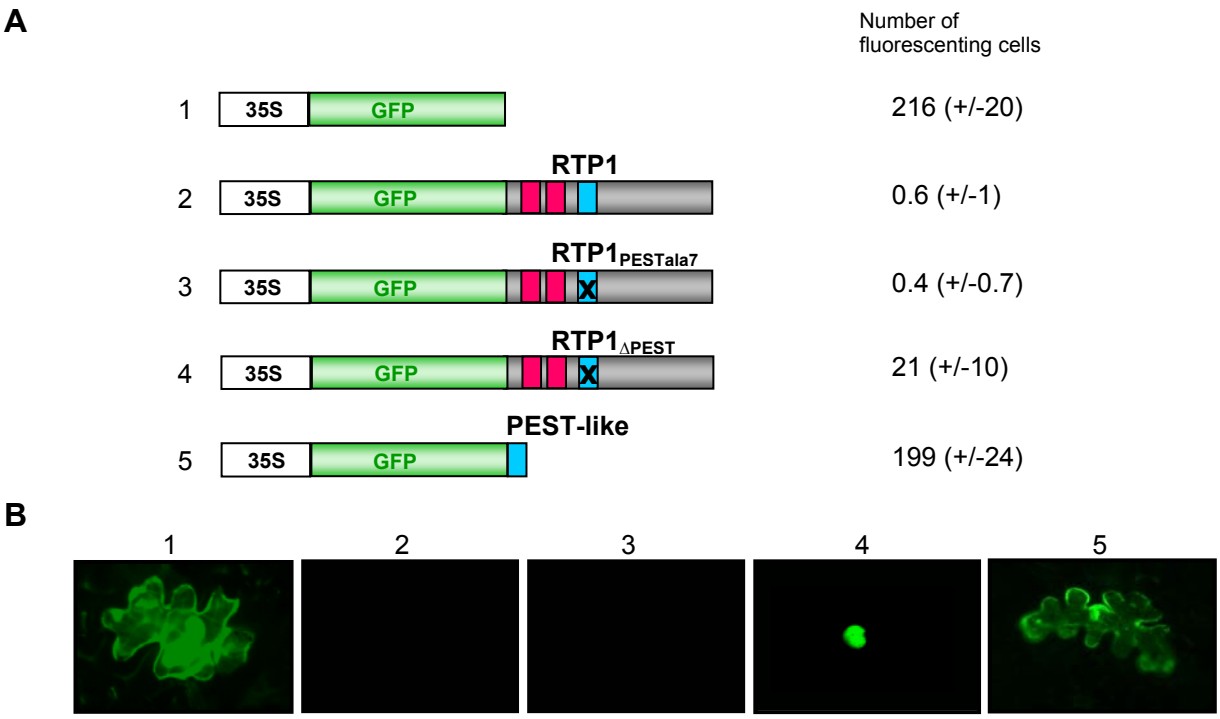

Fig.24. Expression of RTP1$_{PESTmutant}$ constructs. (**A**) Fusion protein constructs used to study RTP1 PEST-like sequence (blue) and mean numbers of the corresponding fluorescenting cells. The original and the mutated sequences are shown in **Table. 6**. (**B**) fluorescence microscopy images of *V. faba* epidermal cells expressing the constructs shown in A.

3.4.5 Coexpression with RTP1 suppresses GFP expression

As reported above, disruption of the RTP1 PEST-like motif by polyalanine mutation (ala7) did not disable RTP1 to suppress GFP fluorescence in plant cells. This observation prompted us to investigate whether the GFP:RTP1 fusion protein itself was responsible for the suppression of GFP fluorescence by having an effect on the folding of GFP. Therefore, a coexpression experiment was performed, in which GFP and RTP1 were coexpressed as separated cassettes. To this end, pGFP plasmid was used to express a second cassette; *35S:RTP1* (see materials and methods). Thus, the resulting plasmid expressed both *35S:GFP* and *35S:RTP1*. Transfection of this plasmid in *V. faba* cells led to similar results as obtained with 3*5S:GFP:RTP1*, namely no GFP fluorescence (**Fig.25**). Collectively, these data indicate that RTP1, likely, interferes with plant cell vitality, possibly by suppressing gene expression in plant cells. Additionally, these data support the use of GFP as a

marker for cell vitality to study RTP1 function in plants. Similarly, GFP has been used to indicate and quantify HR triggered by *Avr* genes from the bacterium *P. syringae* (Leister et al. 1996), the oomycete *Hyaloperonospora parasitica*, and the rice blast fungus *Magnaporthe grisea* (Jia et al., 2000).

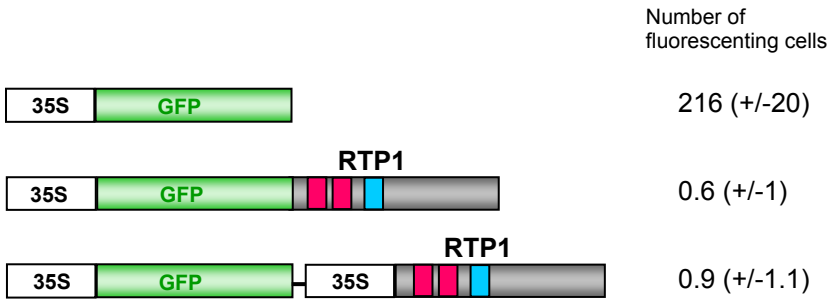

Fig.25. Coexpression of RTP1 and GFP leads to suppression of GFP fluorescence . Fusion protein constructs and the mean number of the corresponding fluorescenting cells are shown.

3.4.6 Identification of a functional domain in RTP1 necessary for interference with plant cell vitality

Based on the results described in the previous chapters, *RTP1* expression in plant cells is likely to interfere with gene expression and cell vitality. To get more insights into RTP1 biological role in plant cells, we first sought to better define the RTP1 region which is required for this function. Defining RTP1's functional domain should shed light on important amino acids and motifs necessary for the function of the protein besides allowing structural studies. Therefore, a series of deletion mutants were constructed that expressed portions of *RTP1* when transfected into *V. faba* cells by particle bombardment. The deletion constructs were analysed for interference with plant cell vitality, using GFP as a vitality marker.

3.4.6.1 Construction and characterization of truncated GFP:RTP1 fusion proteins

RTP1 deletion mutants were created by sequential removal of various numbers of aa from the N- and C-termini of the protein, creating 6 mutant proteins in total (**Fig.26**). These deletions, along with full-length RTP1, were cloned into a pGFP

plasmid driving their expression as C-terminal fusions with GFP. PCR primers directed to the respective sequences contained at their 5´end and 3´end respectively, an *Eco*RI and a *Bam*HI site, and thus the PCR products could easily be inserted into the MCS of pGFP plasmid, allowing direct fusion to GFP. All transformation assays were repeated at least 4 times, and GFP alone was used to normalize for transformation efficiency.

3.4.6.2 Identification of functional domain in RTP1

Interestingly the RTP1 N-terminal region of 50 acid residues ($RTP1_{20-69}$), which contains the NLS with a few flanking aa, showed GFP fluorescence localized in cell nuclei and therefore did not interfere with GFP expression. Deletion of the N-terminal 113 aa ($RTP1_{114-220}$) also resulted in GFP expression, distributed uniformly in all fluorescent cells. In contrast, deletions of the C-terminal 44 aa and N-terminal 69 aa regions ($RTP1_{69-176}$) had no effect on GFP suppression (**Fig.26**). Overall, these deletion analyses clearly indicated that an intact region between 69-176 aa is required for the interference of RTP1 with plant gene expression as illustrated by GFP fluorescence suppression.

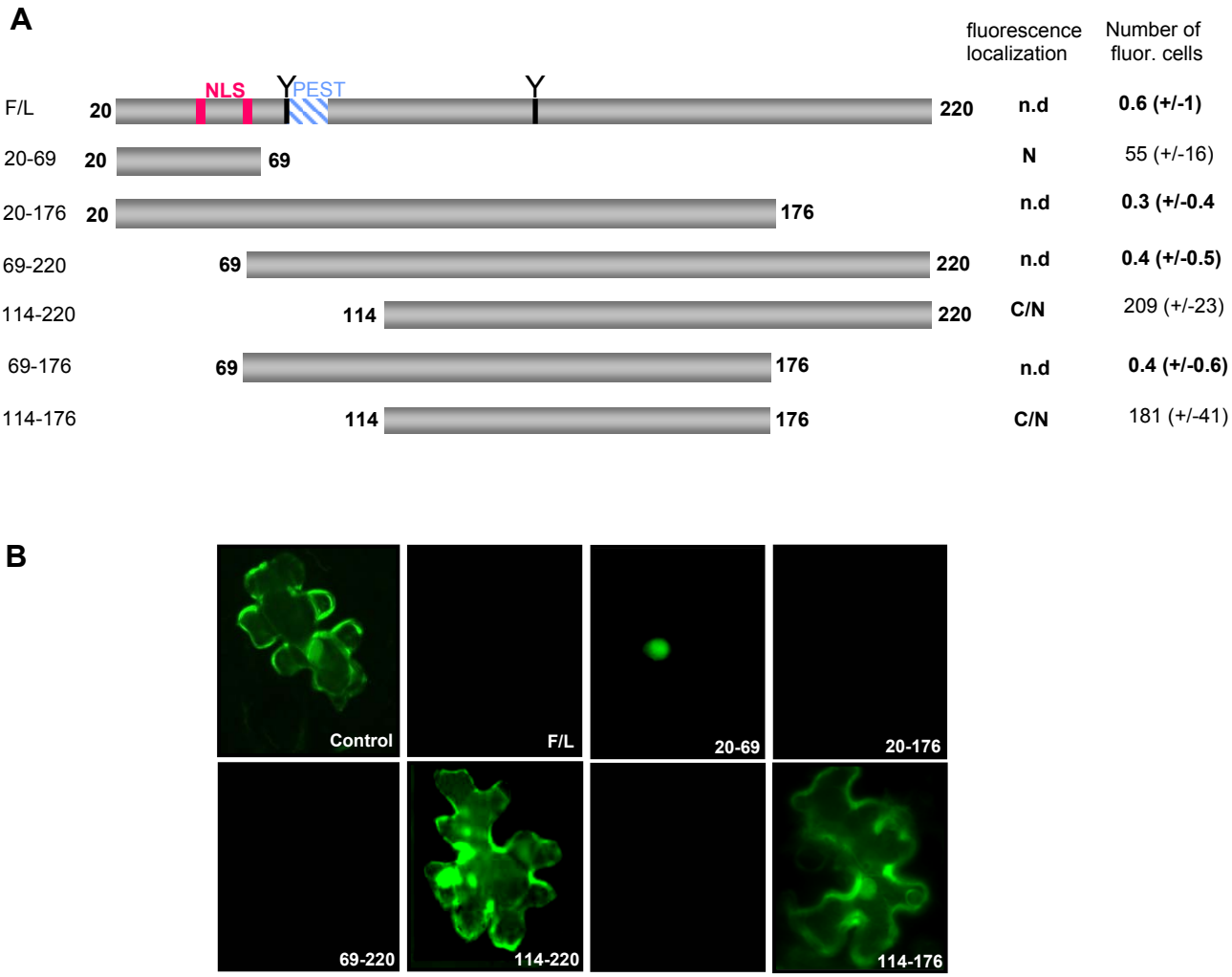

Fig.26. Functional analyses of RTP1 deletion mutants, part 1. (**A**) RTP1 deletion constructs are shown in comparison to the mature full-length of the mature RTP1 protein (F/L) lacking the signal peptide. The amino acid coordinates at the start and end of each deletion protein version are marked. All these sets of RTP1 mutants are fused to the C-terminus of GFP in pGFP plasmid. The average number of GFP expressing cells and the subcellular pattern of fluorescence is indicated on the right. C, cytoplasmic, N, nuclear; C/N, both cytoplasmic and nuclear, n.d, GFP not detected. (**B**) GFP fluorescence images corresponding to the analysed constructs. The studies were carried out in *V. faba* epidermal cells by particle bombardment.

3.4.6.3 Definition of the minimal functional domain of RTP1

The previously identified RTP1 functional domain was subjected to further deletion analyses in order to determine the minimal functional core protein. The data obtained from the second series of the deletion constructs (**Fig. 27**), demonstrate that the domain starting at L100 up to the G145 including the second N-linked

glycosylation site and excluding the identified PEST-like sequence, is required for the functional activity of RTP1 within plant cells. Deletions of 11 more aa up to Q111 from the N-terminal or 6 aa up to Y139 from the C-terminal renders the construct partially inactive. BLAST searches at the amino acid level showed no obvious homology for RTP1 functional domain in the data bases.

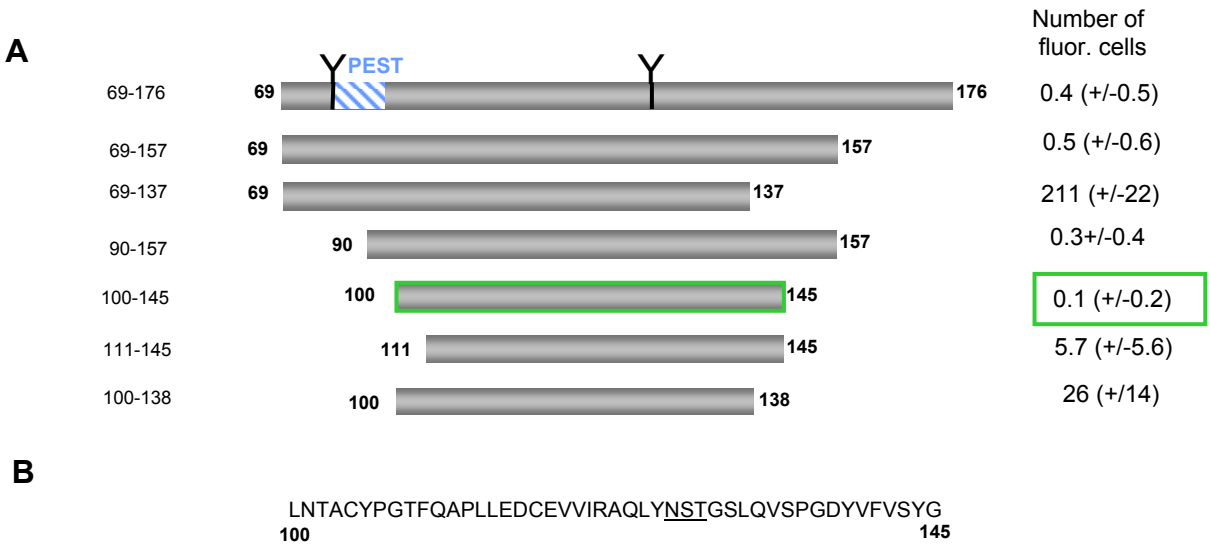

Fig.27. Functional analyses of RTP1 deletion mutants, part 2. (**A**) Constructs used for the deletion analyses of the previously obtained RTP1$_{69\text{-}176}$ active domain. (**B**) Sequence of the minimal RTP1 functional domain.

3.5 Investigation of RTP1 translocation into plant host cells

This work has indirectly confirmed, through biolistic and *Agrobacterium*-mediated transient expression analyses, that RTP1 interferes with plant cell vitality. Expression of truncated forms of RTP1 in plants has identified a central domain which is responsible for this function. These data indicate that RTP1 biological function consists, likely, in modulating the host plant cells vitality during the biotrophic growth of the rust fungus. The key question of this chapter is: How does RTP1 cross the plasma membrane and gain entry into the host plant cell? RTP1 primary sequence does not contain any known translocation motif. However, two possibilities could be suggested for the translocation of RTP1 from the rust haustoria into the host cell: RTP1 is transferred by an unknown specialized translocation apparatus produced by the rust fungus itself (like the bacterial T3SS). Alternatively, RTP1 entry

depends on a plant cell transport mechanism. The second possibility has been studied using transient expression assays.

3.5.1 RTP1 enters the plant cytoplasm in the absence of the rust pathogen

To determine whether RTP1 is able to reenter the plant cell after secretion through the ER secretory pathway, *35S:sRTP1* was coexpressed with *35S:GFP* and transfected into *V. faba* cells by particle bombardment. Plasmids expressing *35S:GFP* alone or coexpressed with 3*5S:RTP1* were used as negative and positive controls for interference with plant cell vitality, respectively. Fluorescence microscopy revealed that, s*RTP1*, similar to *RTP1*, also suppresses GFP expression in transfected cells (**Fig.28**). This indicates that the secreted RTP1 is possibly reentering plant cells after secretion, and subsequently suppressing GFP fluorescence.

To further confirm that GFP suppression is a result of RTP1 reentry, it was necessary to first verify that *35S:sRTP1* directs the secretion of RTP1 through the ER secretory pathway. To this end, the tetrapeptide ER retrieval signal HDEL (Denecke et al., 1992, 1993) was used. HDEL signal was C-terminally fused to sRTP1 expressed under *35S* promoter, the resulting cassette *35S:sRTP1:HDEL* was coexpressed with *35S:GFP* and transiently expressed in *V. faba* cells via particle bombardment. The ER retention signal is expected to prevent the secretion of RTP1 into the apoplast and consequently its reentry into the plant cytoplasm. In fact, addition of the HDEL signal rendered the *35S:sRTP1* construct inactive regarding GFP suppression (**Fig.28**). These results showed that the RTP1 signal peptide is also functional in plants, and that after secretion, RTP1 reenters the cytoplasm from the apoplast.

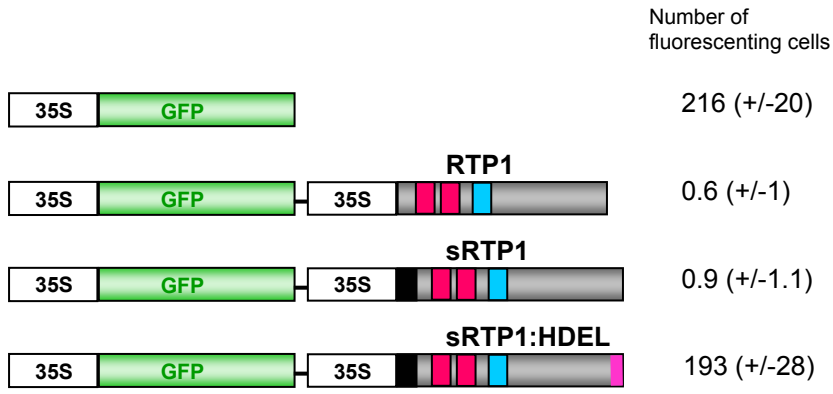

Fig.28. Functionality of the RTP1 signal peptide in plant cells. Fusion protein constructs used to study secretion of RTP1 in plant cells and average number of the corresponding fluorescent cells are shown.

3.5.2 RTP1 PEST-like sequence plays a role in RTP1 reentry into plant cells

As shown in Chapter 3.4.4, the functional role of the PEST-like sequence is not clear, as it does not seem to destabilise RTP1. Additionally, this region has been detected by bioinformatic programs as a region of low compositional complexity. This prompted us to investigate whether RTP1 PEST-like motif would play a role in the reentry of RTP1, probably by interacting with a potential receptor at the plant plasma membrane which would promote endocytosis of the protein. For this, a plasmid was constructed in which *35S:GFP* was coexpressed with *35S:sRTP1*$_{PESTala7}$. Transfection of this plasmid into *V. faba* cells did not suppress GFP, clearly indicating that the PEST-like region plays a role in the entry of RTP1 through the plasma membrane into the plant cell.

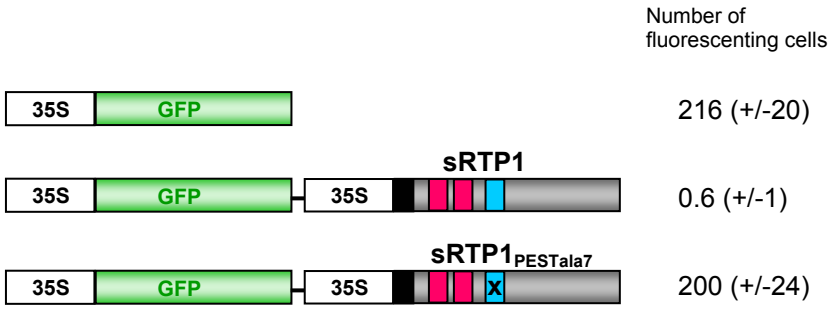

Fig.27. Role of the PEST-like region in the internalization of RTP1. Coexpression constructs, used to study the role of the PEST-like region in reentry of the secreted RTP1 into plant cells, and average number of the corresponding fluorescent cells are shown.

3.6 Establishment of a delivery model to study RTP1 translocation mechanism

Although the biolistic transient expression system has been efficiently used to rapidly analyse RTP1 expression and reentry in plant cells, it presents some limitations: First of all, it does not allow biochemical analyses, due to the restricted number of transformed cells within a detached leaf sample. Furthermore, it is difficult to study RTP1 delivery mechanism into the plant cells in the native pathosystem *U. fabae*/*V. faba* by gene disruption and loss of function analyses, as there is no reproducible transformation method for rust fungi. Therefore, it has been important to develop a recombinant delivery system to facilitate structural and functional studies on the mechanism of RTP1 translocation.

3.6.1 Heterologous expression of *sRTP1* by *Colletotrichum lindemuthianum*

During infection of bean (*Phaseolus vulgaris*), the hemibiotrophic anthracnose fungus, *Colletotrichum lindemuthianum*, initially establishes a biotrophic phase, for 3 to 4 days, associated with large intracellular primary hyphae, followed by a necrotrophic phase associated with narrower inter- or intracellular hyphae. In an attempt to study recombinant RTP1 secretion from *C. lindemuthianum* during the biotrophic phase, the strain UPS9 was transformed to constitutively express *sRTP1* under the control of the strong *oliC* promoter from *Aspergillus nidulans*. The

oliC:sRTP1 transformants were analysed for infection and for RTP1 expression (**Fig.28**). Although *sRTP1* mRNA could be amplified from *oliC:sRTP1* transformants, only a very weak RTP1 band could be detected among proteins recovered from the liquid culture of UPS9 transformants (not shown). Failure in recovering recombinant RTP1 protein did not allow the use of this expression system as a delivery model.

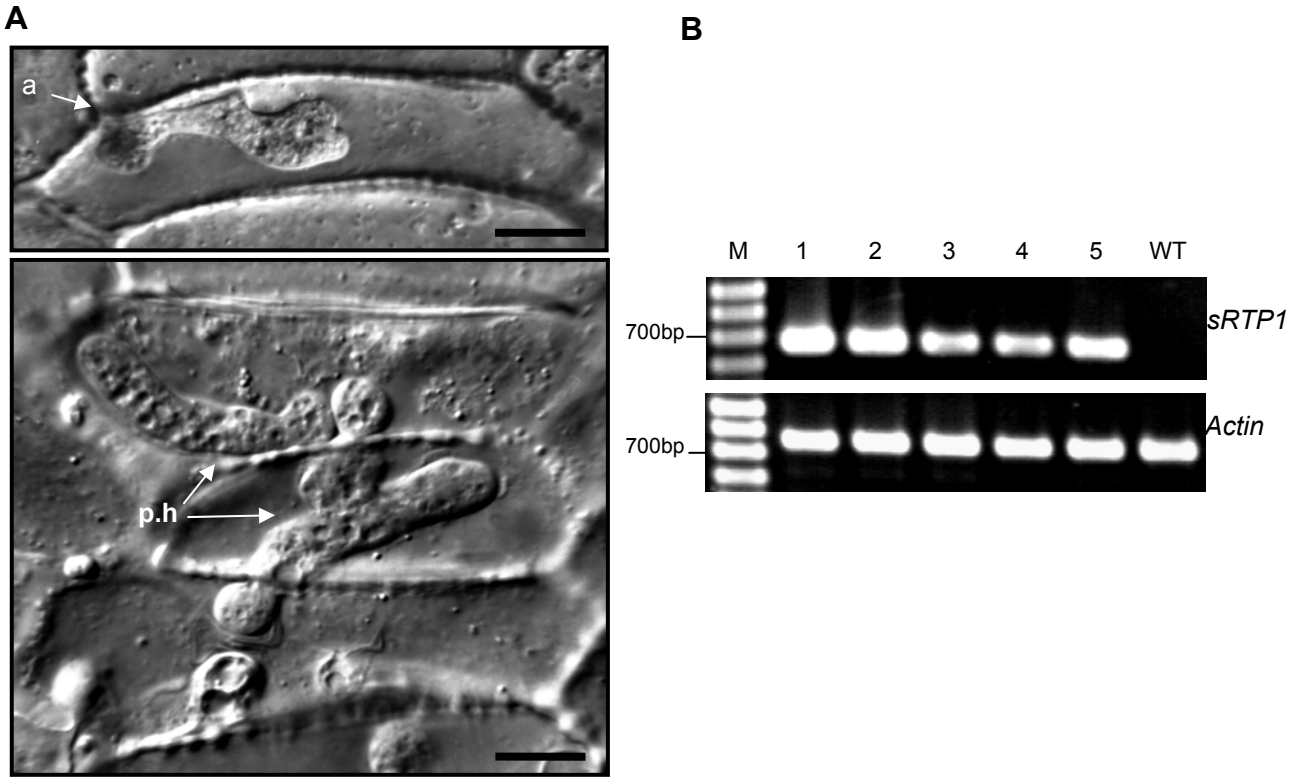

Fig.28. Analyses of *C. lindemuthianum oliC:sRTP1* transformants. (**A**) Cytological examination showed normal pathogenicity of a *oliC:sRTP1* transformant on cotyledons of La Victoire, a susceptible cultivar of common bean. Photographs were taken 4 days after infection. a, appressorium, i.v, infection vesicle, p.h, primary infection hyphae. Scale bar =10µm. (**B**) Semi-quantitaive RT-PCR to analyse *sRTP1* transcript (660bp) in 5 different *oliC:sRTP1* transformants, using the gene encoding actin (750bp) as an internal control. M:1-kb DNA ladder.

3.6.2 *Ustilago maydis/Zea mays* pathosystem as a model to study RTP1 delivery

U. maydis, like *U. fabae*, is a biotrophic fungus that belongs to the class of Basidiomycetes. *U. maydis* does not form haustoria in host plant cells. Instead, it proliferates intra- and intercellular hyphae through plant tissue and maintains a

biotrophic relationship with its host during growth *in planta* (Kahmann et al, 2000). *U. maydis,* similar to *U. fabae,* has also been found to express several *in planta* induced genes clusters, encoding small secreted proteins lacking homology to proteins from other organisms (Kämper et al., 2006). *U. maydis* SG200 haploid strain, in which pheromone signalling is activated, carries a hybrid *b* locus composed of the compatible *bE1* and *bW2* genes necessary to trigger pathogenic development. As a consequence, SG200 is solopathogenic and shows filamentous growth on charcoal-containing plates. This yeast like strain of *U. maydis* can be cultivated on artificial media making it amenable to genetic and molecular analysis (Bölker et al., 1995).

In this approach, recombinant expression of RTP1 in *U. maydis*, has the goal of establishing an expression system in which RTP1 could naturally be delivered from *Ustilago* infection hyphae into maize cells (**Fig.29**). Establishing such expression system would allow to test different mutant and truncated versions of RTP1 and to follow up their delivery to the plant cells, and consequently identify RTP1's putative motif (s) which mediates its translocation from the fungus to the plant cell.

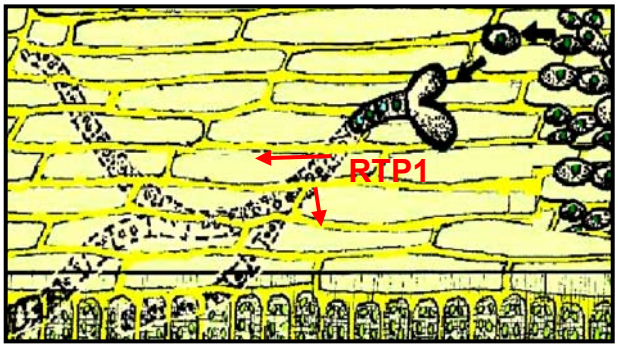

Fig.28. **Scheme showing mated *U. maydis* sporidia developing on maize epidermis.** Formation of inter- and intracellular hyphae within the plant tissue is shown. Red arrows denote potentially secreted recombinant RTP1.

3.6.2.1 Efficient *in vitro* secretion of RTP1 from transgenic *U. maydis*

The plasmid p123 was used to clone *sRTP1* and *sRTP1:GFP* under the constitutive control of *o2tef* promoter (**Fig.29**). The resulting plasmids were linearized

with *AgeI* restriction enzyme and transformed into SG200 protoplasts by PEG mediated transformation (see materials and methods). Two independent transformants, corresponding to each construct, were selected on carboxin-containing HA plates and used in immunoanalyses for detection of RTP1 and RTP:GFP fusion protein, using polyclonal anti-RTP1 antibodies. Western blotting of cell-free supernatant proteins, isolated from the growth medium of o*2tef:sRTP1* transgenic strains, showed a strong signal by a distinct protein band whose size (24 - 26 kDa) is very similar to that of RTP1. This demonstrated efficient expression of *sRTP1* in *U. maydis*, as well as the functionality of RTP1 signal peptide. The RTP1 band was not accompanied by any obvious degradation. Additionally, the size of the signal, 24 to 26 kDa instead of 23 kDa as is predicted for the mature secreted protein, suggested that the processed recombinant RTP1 is glycosylated similarly to the native RTP1 secreted from rust haustoria. No band was detected in the control lane corresponding to the cell-free supernatant proteins recuperated from the non-transformed SG200 strain.

Western analysis of the cell-free supernatant proteins obtained from *o2tef:sRTP1:GFP* expressing strains, detected multiple bands for RTP1:GFP fusion protein: The major band has an apparent molecular mass of about 50 kDa, which is of about the size of the expected recombinant RTP1:GFP fusion protein (~49 kDa). The sizes of the three other bands were about 32, 28 and 25 kDa. The smallest band likely corresponds to RTP1 spliced from most of GFP. The intermediate bands seem to represent partial degradation products of GFP in the RTP1:GFP fusion protein. Such multiple banding has also been observed with other GFP-fusion proteins targeted to the secretory pathway (Kenny et al. , 2005).

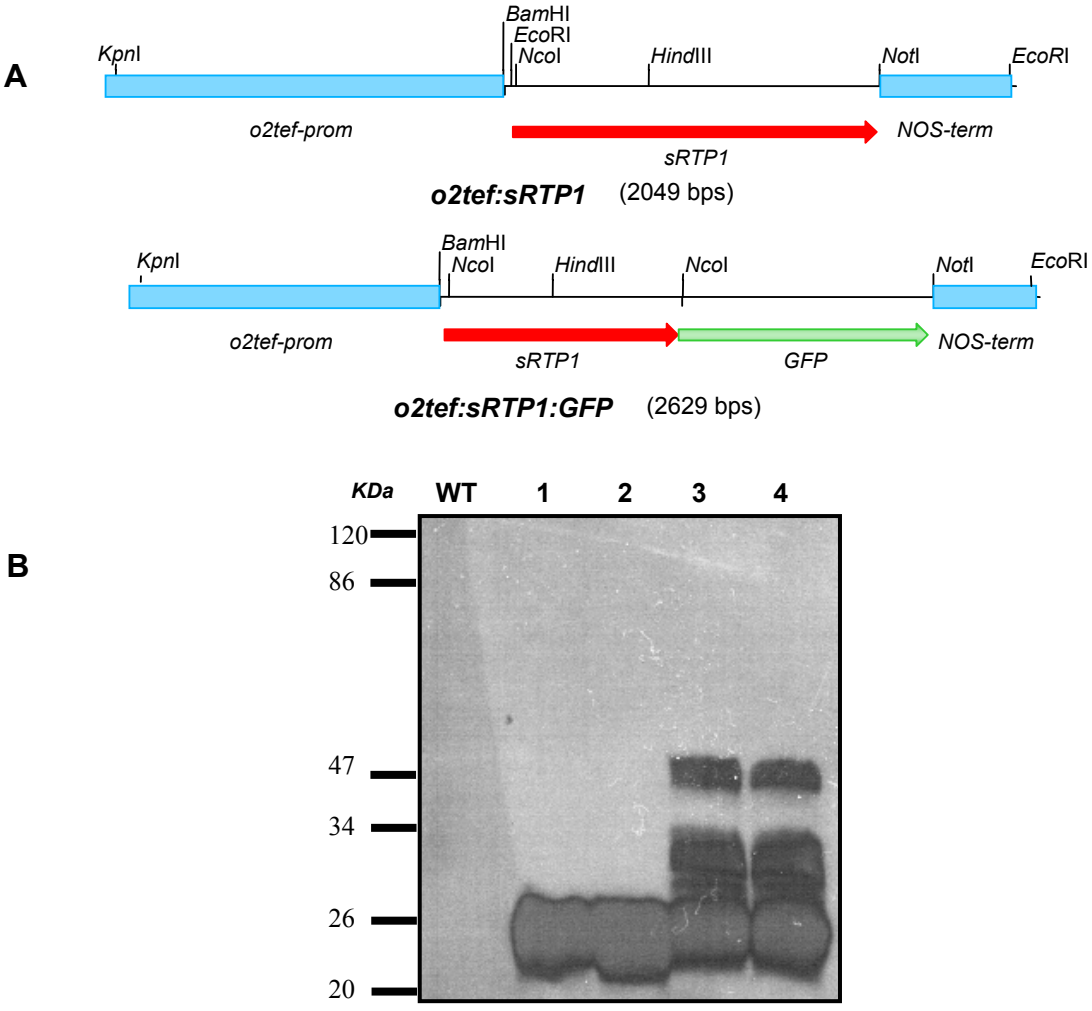

Fig.29. *U. maydis* as a secretion system for RTP1. (**A**) Constructs used to constitutively express s*RTP1* and *sRTP1:GFP* in *U. maydis* SG200 strain. (**B**) Western blotting of cell-free supernatant proteins to detect secreted RTP1 and RTP1:GFP, using anti-RTP1 antibodies. Lanes 1, 2, 3 and 4 correspond to protein samples from two different *o2tef:sRTP1* and *o2tef:sRTP1:GFP* expressing strains, respectively.

Together these results confirm that the signal peptide of RTP1 mediates secretion of RTP1 and RTP1:GFP, and demonstrate that *U. maydis* is an efficient secretion system for these proteins. Once secreted RTP1 remains stable, whereas GFP in RTP1:GFP is most likely subjected to protease degradation. However, GFP molecules were not completely degraded, as it could be observed from the detection of the intact RTP1:GFP signal band. Furthermore the western blot pointed to the presence of several protease-sensitive sites within GFP, making it impossible for the

degraded GFP to be fluorescent. Therefore, any GFP fluorescence would probably come only from the intact RTP1:GFP fusion protein.

3.6.2.2 Recombinant secreted RTP1 shows similar glycosylation as native RTP1

As described above, the size of the secreted recombinant RTP1 protein could be interpreted as a glycosylation form of RTP1. To investigate the N-linked glycosylation patterns in recombinant RTP1 from *U. maydis* and in native RTP1 secreted by *U. fabae* haustoria, deglycosylation experiments were performed. In fact, after treatment with Endo H_f, the heterogeneous 24 kDa to 26 kDa bands, in both *U. maydis* and *U. fabae* samples shifted to a lower molecular weight band of 23 kDa. This is consistent with the shift expected from the removal of the asparagine-linked complex glycans, and hints to the fact that both RTP1 detected bands represented distinct glycoforms of RTP1 protein. All together, these data clearly show that the glycosylation pattern of RTP1 secreted from *U. maydis* is very similar to its glycosylation when secreted in the native pathosystem, which makes *U. maydis* a favorable expression system to study RTP1 translocation into plant cells.

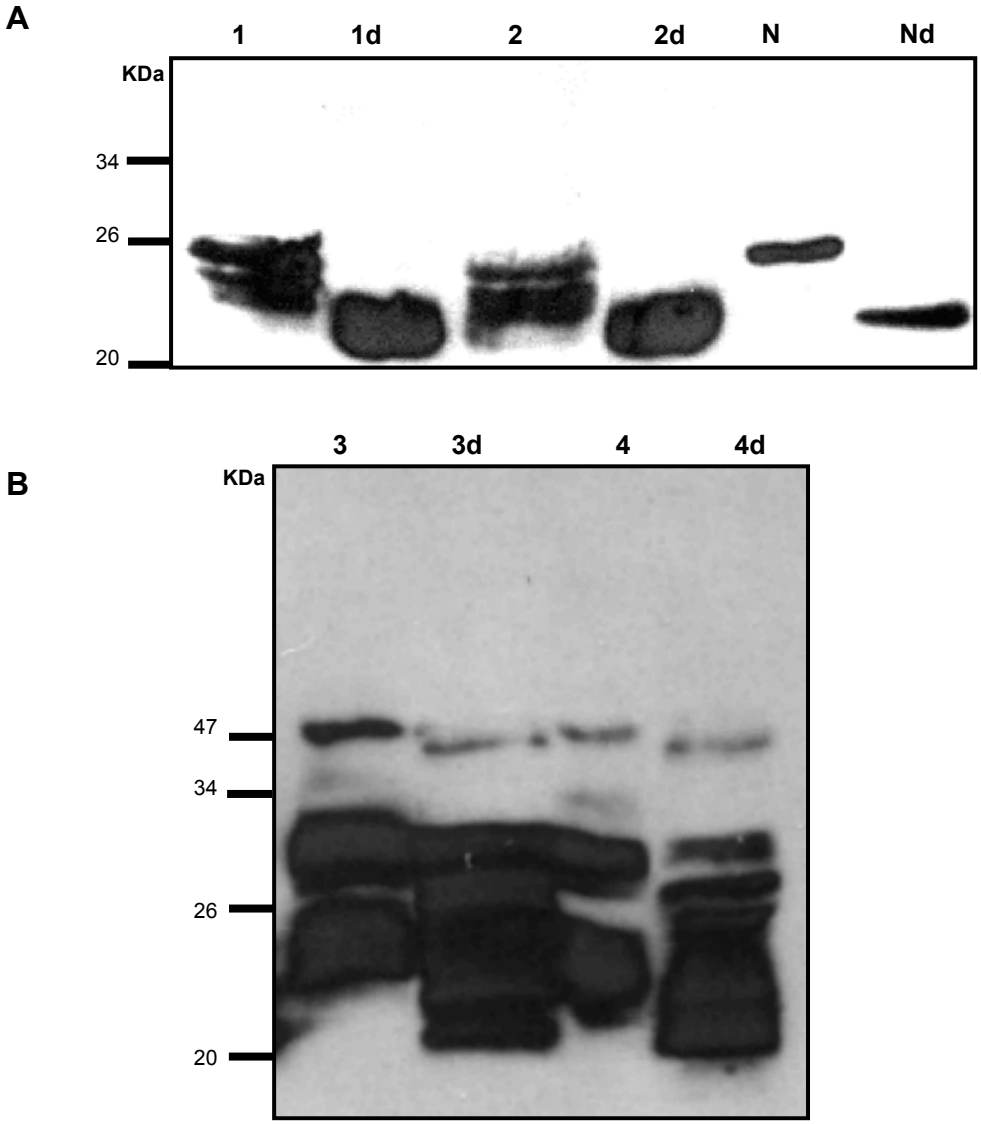

Fig.30. Immunodetection of N-glycosylation of secreted RTP1 and RTP1:GFP by Endo H_f treatment. (**A**) Western blotting revealed the same molecular mass shift, after deglycosylation, for both native (N) and recombinant RTP1 (1 and 2) bands in all tested strains. (**B**) Western blot analysis showing the effect of deglycosylation on bands pattern of RTP1:GFP (3 and 4). Treatment with Endo H_f (d) shifted all bands, including the major polypeptide band corresponding to intact RTP1:GFP fusion protein, to about 2 to 3 K Da lower molecular mass.

3.6.2.3 Expression of *sRTP1* in *U. maydis* under control of *in planta*-induced promoter

Based on the results of the presented work, it has been demonstrated that RTP1 expression and secretion in *U. maydis* is very similar to its secretion from

U. fabae haustoria. To further follow up *in planta* secretion of recombinant RTP1 from transformed SG200 strains and its potential transfer into plant cells, it was important to express *sRTP1* under control of a promoter that displays a strong expression during *in planta* growth of the fungus. However, strains expressing *o2tef:sRTP1:GFP* showed only a weak expression during growth on plant tissue, suggesting that *o2tef* promoter is likely suppressed during the pathogenic growth of the fungus. To ensure strong *in planta* expression, the *mig2-6* promoter was chosen. This promoter has been found to be exclusively and strongly activated during pathogenic growth of *U. maydis* in plants (Farfsing et al., 2005).

A total of 4 plasmids were constructed to express *GFP, sRTP1:GFP*, *sRTP1* or $sRTP1_{PESTala7}$ under the control of *mig2-6* promoter. To this end the previously constructed plasmids expressing *o2tef:sRTP1* and o*2tef:sRTP1:GFP* were used to replace *o2tef* promoter with *mig2-6* promoter (kindly provided by Dr. J. Schirawski, MPI Marburg), using *Sph*I and *Bam*HI restriction sites (see materials and methods). The resulting plasmids (**Fig.31**) were linearized with *Age*I and transformed into SG200 strain.

3.6.2.4 *mig2-6:GFP* resulted in highly bright hyphal cytoplasmic fluorescence

To investigate the regulation of the *mig2-6* promoter, two independent *mig2-6:GFP* expressing transgenic *U. maydis* strains were generated in this study. These strains showed no detectable expression of *mig2-6:GFP* during growth in PD medium. In contrast when these strains were injected into young maize seedlings, GFP was strongly detected in intercellular infection hyphae starting from the second day after infection. GFP activity was further detected in multiply-branched hyphal structures (inter- and intracellular) protruding into plant cells (**Fig.32A**). GFP activity remained strongly detectable in hyphal sections during 8 to 10 days following infection. These data confirmed the strong *in planta*-specific expression of *mig2-6* promoter, which makes it a suitable promoter to analyse RTP1 secretion and potential transfer into the plant cells.

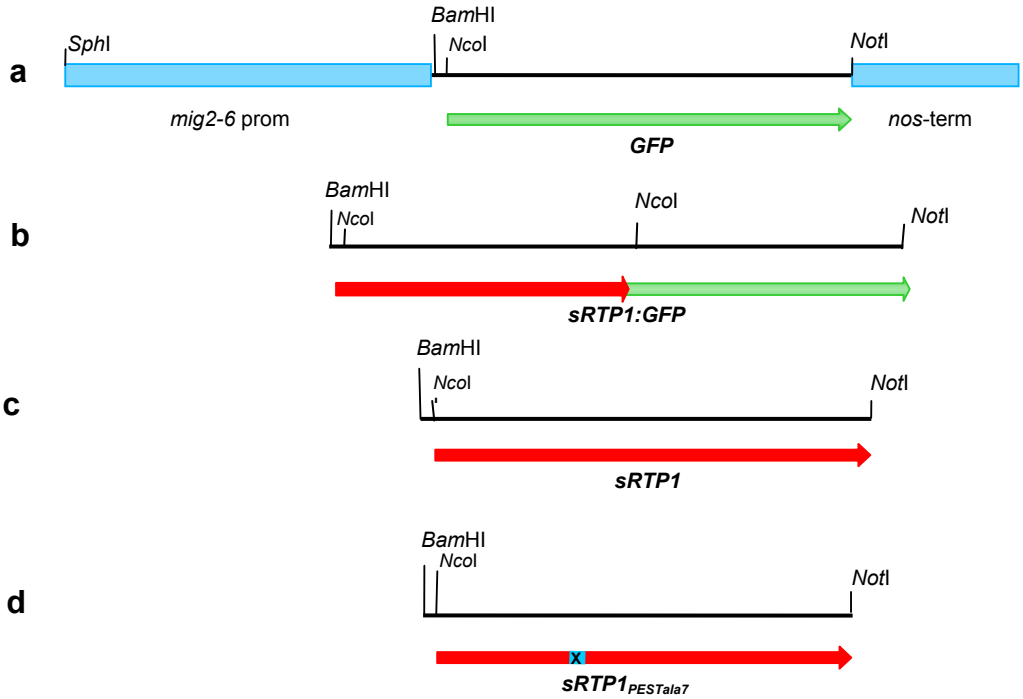

Fig.31. Generated constructs to study RTP1 secretion and translocation from transgenic *U. maydis* strains into maize plant cells. All constructs contained *mig2-6* promoter to differentially drive expression of *GFP* (a), *sRTP1:GFP* (b), *sRTP1* (c) or $sRTP1_{PESTala7}$ (d). Strains expressing constructs (a) and (b) were analysed by fluorescence microscopy, and constructs (c) and (d) were made for immunofluorescence microscopy.

3.6.2.5 Efficient secretion of RTP1:GFP during pathogenic growth of transgenic *U. maydis* hyphae

To determine whether RTP1:GFP is efficiently expressed and secreted from transgenic *U. maydis* infection hyphae, *in vivo* observations of maize leaf sections, infected with two independent strains expressing *mig2-6:sRTP1:GFP,* were carried out with fluorescence and laser scanning microscopes. Strong GFP activity was detected throughout the infection hyphae (**Fig.32B**), indicating that RTP1:GFP fusion protein was successfully processed and secreted from infection hyphae growing on maize plant cells. Bright GFP fluorescence was detected at the hyphal tips and, sometimes, enclosed in vesicle-like structures (data not shown).

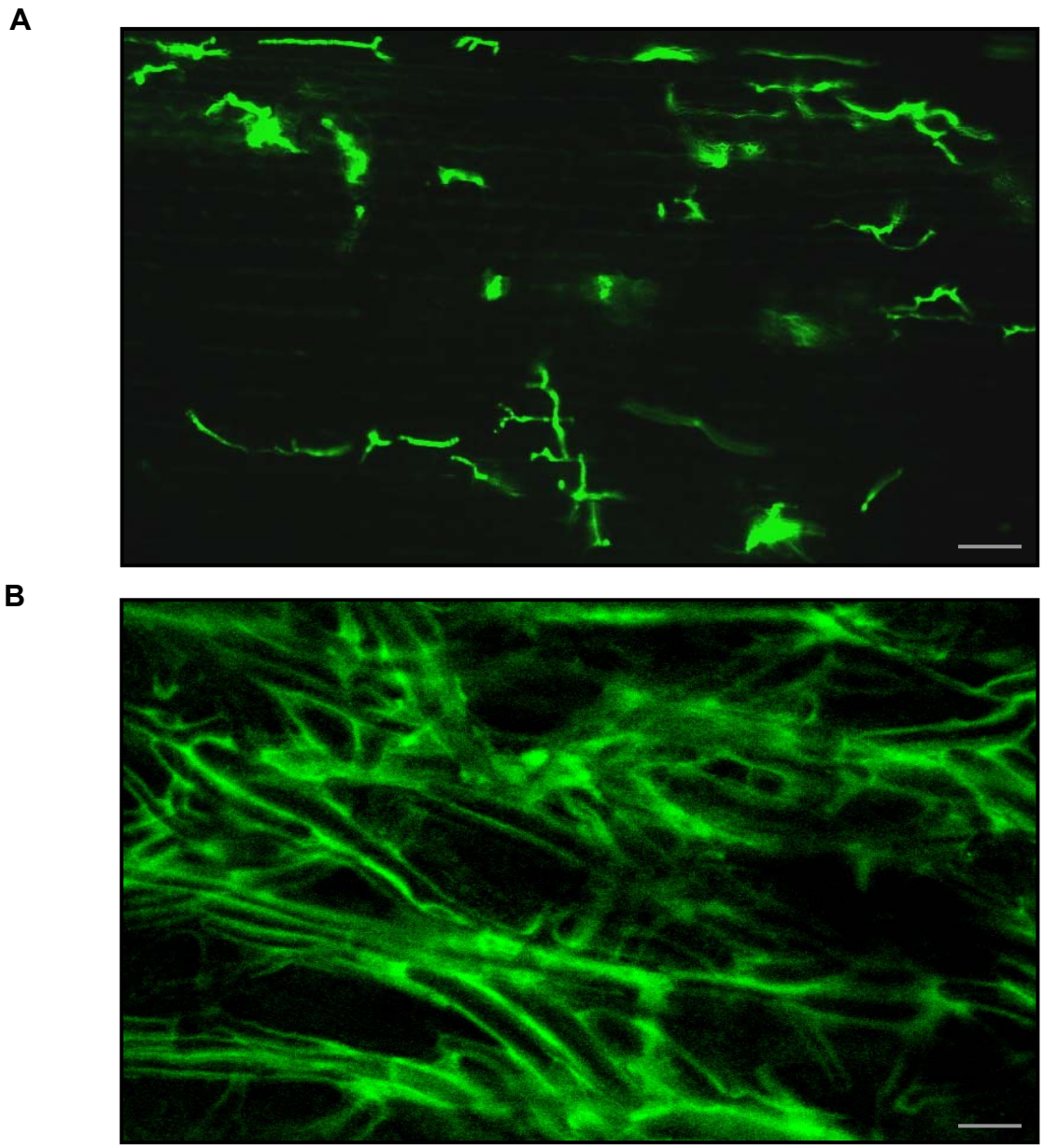

Fig.32. *U. maydis* as a recombinant secretion system to secrete RTP1 into plant cells. Visualisation of secreted RTP1:GFP fusion protein. (**A**) Fluorescence microscopy image of maize leaf section 4 days after infection with *U. maydis* strain SG200 expressing *mig2-6:GFP*. The image is showing GFP signal localization inside infection hyphae. Scale bar =100µm. (**B**) Laser scanning microscopy of a section of a maize leaf infected with *U. maydis* strain expressing *mig2-6:sRTP1:GFP*. Scale bars =10µm.

3.6.2.6 Evidence for RTP1:GFP transfer into plant cells

To investigate whether the secreted RTP1:GFP is further transferred into the plant cells, fluorescence microscopy analyses of infected maize leaves were carried

out. Some plant cells showed intracellular GFP-like fluorescence distributed in the cytosol (**Fig.33**). This intracellular signal, which was difficult to distinguish from background fluorescence, was also detected in few plant cells nuclei. Future immunofluorescence localization experiments are necessary to confirm protein transfer mediated by RTP1.

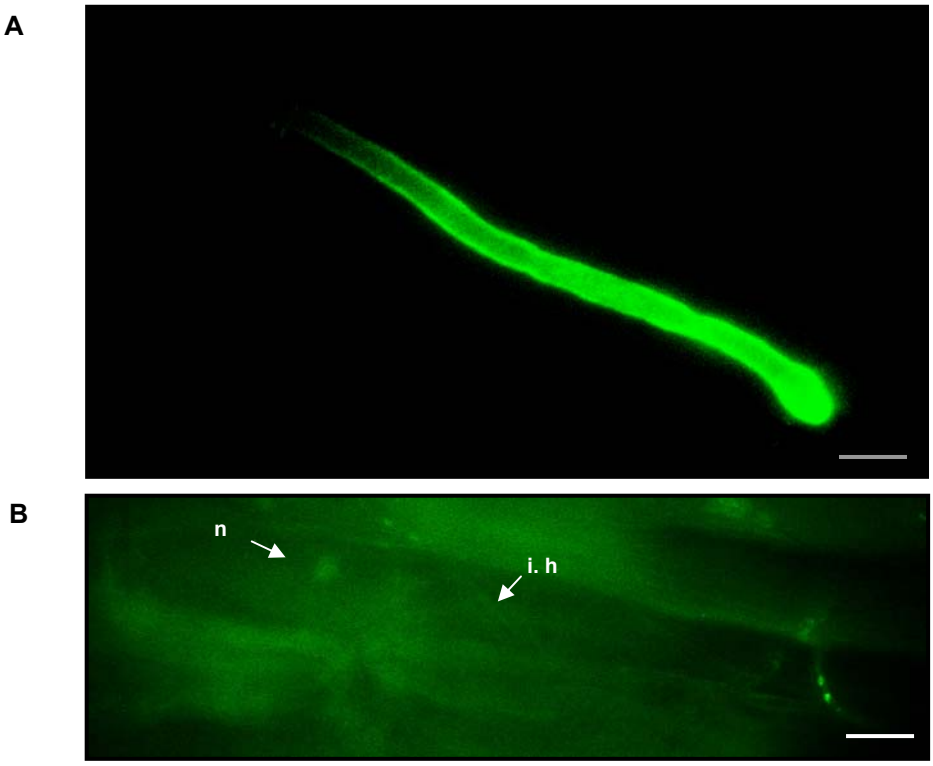

Fig.33. Pursuing hyphal secreted RTP:GFP. (**A**) Laser scanning microscopy image showing fluorescence accumulated towards the hyphal tip. Scale bar =10µm (**B**) and Fluorescence microscopy images showing fluorescence in vesicle-like structures (arrows) within infection hypha, and in the cytosol of an infected plant cell, respectively. i.h, infection hyphae, n, plant nucleus. Scale bar =50µm

4 Discussion

At the time when this work was started, intensive studies towards molecular understanding of the plant–rust fungus pathogen interactions had been initiated.
An important break through has been achieved through differential expression analysis of genes isolated from haustorium-specific cDNA library (Hahn and Mendgen, 1997), with special emphasis towards isolation of haustorium secreted proteins (Dodds et al., 2004; Catanzariti et al., 2006). However, the activity of most isolated haustorial secreted effectors remains elusive, and little evidence exists for their role in virulence. The presented work brings new insights into the mechanisms used by rust fungi to maintain the biotrophic association with plants, through functional and structural analyses of RTP1, the first identified rust protein transferred from the haustorium into the host cells. Different questions have been addressed to discuss both the biological function as well as the translocation process by which RTP1 is delivered.

4.1 What is the final target compartment for RTP1?

Cytological analysis of *U. fabae* infected broad bean leaves described three main stages for the development and expansion of the haustorium inside the host plant cells. An early stage characterized by a small round haustorium, an intermediate stage characterized by a more developed haustorium, and a later stage corresponding to the mature lobed haustorium; towards which the host plant nucleus has migrated. Immunolocalization of RTP1 during these three stages indicated that RTP1 is progressively secreted and delivered first to the EHM, then to the plant cell cytoplasm and finally to the plant nucleus (Kemen et al., 2005). However, the immunocytological analysis did not show a stage where RTP1 signal would be detected exclusively in the plant nucleus. Whether this stage would exist remains unknown. Analysis of RTP1 sequence by several prediction programs revealed the presence of a putative bipartite NLS (RQHHKR X_9 HRRHK) within the N-terminal region of RTP1. This prediction is in accordance with the data obtained from the immunofluorescence studies that showed a strong RTP1 signal inside the plant nucleus in addition to its accumulation in the plant host cytoplasm. To determine the

necessity of the predicted NLS for the nuclear localization of RTP1, mGFP fusion constructs were generated. GFP fuorescence in transformed tobacco protoplast was analysed under a fluorescence microscope. Unlike GFP, which resulted in cytoplasmic and nuclear signals, fusion of GFP to RTP1 fragment containing the NLS [GFP:RTP$_{(36-69)}$] localized exclusively to the nuclei of transformed protoplasts, clearly indicating that RTP1 NLS is functional in plant cells. To verify that RTP1 NLS was crucial for the nuclear localization of GFP:RTP$_{(36-69)}$, GFP:RTPx$_{(36-69)}$ was constructed encoding three point mutations in the putative NLS. In contrast to wild type RTP1 NLS, defective NLS abolished accumulation of GFP:RTPx$_{(36-69)}$ in the nucleus. Intriguingly, GFP:RTP1 didn't exhibit fluorescence in transformed protoplasts. To determine the necessity of the identified NLS for the nuclear localization of full-length RTP1, these constructs were transfected to *V. faba* cells by microprojectile bombardment (**Fig.34**) that allows a higher transformation efficiency. Although GFP:RTP1 rarely resulted in GFP fluorescence in comparison with GFP:RTP$_{(36-69)}$, both constructs accumulated in the plant cells nuclei. With comparable transformation efficiency, NLS mutants, GFP:RTP1x and GFP:RTPx$_{(36-69)}$ respectively, exhibited similar numbers of fluorescent cells when compared to GFP alone. Taken together, these data establish that secreted RTP1 from rust haustorium is likely to be specifically targeted to the plant cell nucleus. Immunocytological analyses, however, showed RTP1 signals both in the cytoplasm and the nucleus of infected cells (**Fig. 6**). Whether nuclear localization is important for RTP1 function remains unclear.

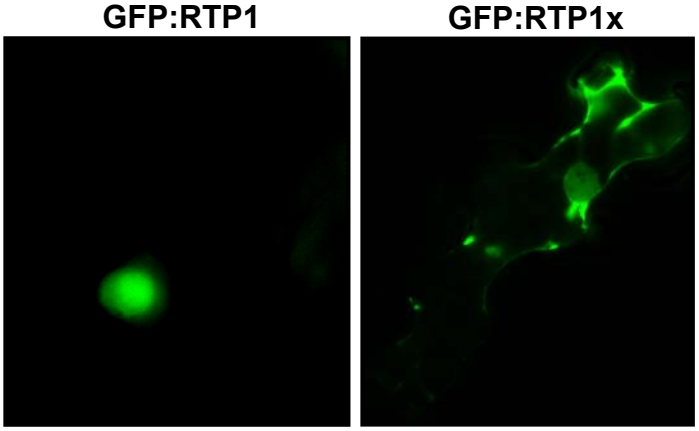

Fig.34. Subcellular localization of GFP:RTP1 and GFP:RTP1x intrnasiently transformed *V. faba* cells

The requirement for NLS motifs had previously been demonstrated for some plant and animal pathogenic bacterial T3SS effector proteins, and has been found to be necessary in activating host transcription machinery. Members of the *Xanthomonas* AvrBs3 effector family, which represents proteins targeted to plant cells by a T3SS (e.g., AvrBs3, AvrXa10, and AvrXa7), contain a C-terminal NLS and an acidic transcriptional activation domain (AAD). Both motifs were found to be necessary for protein activity. The NLS of AvrBs3 has been found to be functional, and the AAD of AvrXa10 is capable of transcriptional activation of reporter genes in *Arabidopsis* and yeast (Zhu et al., 1998). In addition, DNA binding of AvrXa7 could be shown although a defined sequence was not revealed (Yang *et al.*, 2000). These findings have been interpreted as that AvrBs3 effector family alters plant nuclear gene transcription during pathogen infection, likely as a tool to suppress host defences and to cause hypertrophy in susceptible host plants. Similarly, the *Yersinia* effector YopM was also found to contain a functional NLS and is also localized in nuclei of infected host cells suggesting that YopM may bind to the host's transcription machinery (Benabdillah *et al*., 2004)

RTP1 is the first fungal transferred protein that carry a functional NLS. The NLS motif in RTP1 belongs to the class that function in a broad range of eukaryotic cells (Smith and Raikhel, 1999), suggesting that nuclear localization may be necessary for the function RTP1.

4.2 What is the biological function of RTP1 in plants?

The absence of a reproducible transformation method for rust fungi makes it difficult to study RTP1 biological function by gene disruption and loss of function analyses. Use of transgenic plants expressing avr genes has been reported in many studies. HR induction has been observed when stably transformed plants expressing Avr products are crossed to plants containing the corresponding *R* genes, with the progeny showing seedling death or stunted growth phenotypes (Jones et al., 1994; Gopalan et al., 1996; Erickson et al., 1999; Dodds et al., 2004). In some experiments involving avr heterologous expression inside plant cells, Avr proteins were suggested to be deleterious even in the absence of a known cognate *R* gene when expressed

strongly (McNeillis et al., 1998; Nimchuk et al., 2000). Whether these effects result from interaction with susceptibility targets in the host is unknown.

The primary aa sequence of RTP1 does not provide any clue to its intrinsic biochemical function within rust infected plant cells. Therefore, we have chosen to stably transform the model plant *Arabidopsis* (chapter 3.2) as the first approach to get some insights into the biological role of RTP1. Only 3 gluphosinate resistant T1 plants could be obtained that express *35S:RTP1*. The surprising failure to recover transformants likely resulted from lethality during seed production and/or germination. This lethal effect was reduced in *35S:sRTP1* expressing lines in which full length, *sRTP1* including the signal peptide was used. Additionally, the recovered *35S:RTP_T1* plants were retarded in growth when compared to *35S:sRTP1_T1* plants (**Fig.12**), providing a further evidence that RTP1 expression in plants is likely to interfere with plant growth and vitality. However, the growth retardation phenotype was not stable and was partially and completely lost in homozygous T2 and T3 plants respectively, likely due to posttranscriptional gene silencing. In fact, although RT-PCR demonstrated that *RTP1* and *sRTP1* transcripts were expressed, protein analysis by western blotting did not result in detectable amounts of the RTP1 and sRTP1 proteins. Besides silencing, this could also be explained by the instability of the encoded proteins, or RTP1 suppression of its own. Further *in planta* expression analyses negate the first two hypotheses and argue for negative interference of RTP1 with plant gene expression.

4.2.1 Does RTP1 interfere with plant's defence?

To determine whether RTP1 could act as a virulence factor that can modulate plant defense, WT and transgenic *35S:RTP1_T2 and 35S:sRTP_T2* plants were challenged with the necrotrophic fungus *Botrytis cinerea* and the hemibiotrophic bacterium *Pseudomonas syringae*. No significant differences were observed, between all plants, concerning symptoms and disease development caused by both pathogens. These data do not support the hypothesis that RTP1 influences plant defence. This observation was further supported when pathogenicity-related genes (*PR* genes) were analysed in transgenic and WT plants. PR1, PR2 acidic proteins

are known to be regulated by the salicylic acid (SA) signaling pathway, whereas regulation of vacuole-localized basic PR3, PR4, and PDF1.2 are reliant on both ethylene and jasmonic acid (JA) signalling pathway(s) (Feys and Parker, 2000).

In the absence of any stimuli, both *35S:RTP1_T2* and *35S:sRTP1_T2* did not differ significantly from WT plants with respect to induction of the defence genes *PR4, PR3* and *PR2* (not shown). However, *PR* was expressed at lower levels in both *35S:RTP1_T2* and *35S:sRTP1_T2* than it was in WT plants. The decrease in *PR1* expression was accompanied by an increase in *PDF1.2* transcripts (**Fig.35**). This effect was most noticeable in *35S:RTP1_T2* plants, in which *PDF1.2* transcripts were most abundant. One explanation for this result is that RTP1 may interact with SA signaling pathway suppressing therefore *PR1* expression. Suppression of SA could result in an induction of *PDF1.2*. In fact, in *Arabidopsis*, the expression of *PDF1.2* gene is higher in n*ahG* plants in which a bacterial SA-degrading enzyme is overexpressed (Penninckx et al., 1998). If that is the case, other PR genes should be co-regulated. Yet because no evidence was found for such co-regulation, we assume that the changes observed in *PR1* and *PDF1.2* expression are not resulting from a direct interaction of RTP1 with SA or JA signalling pathways. Instead this might be due to a transformation artefact or an indirect effect of RTP1 expression in the plants, e.g., by manipulating plant genes transcriptional activity.

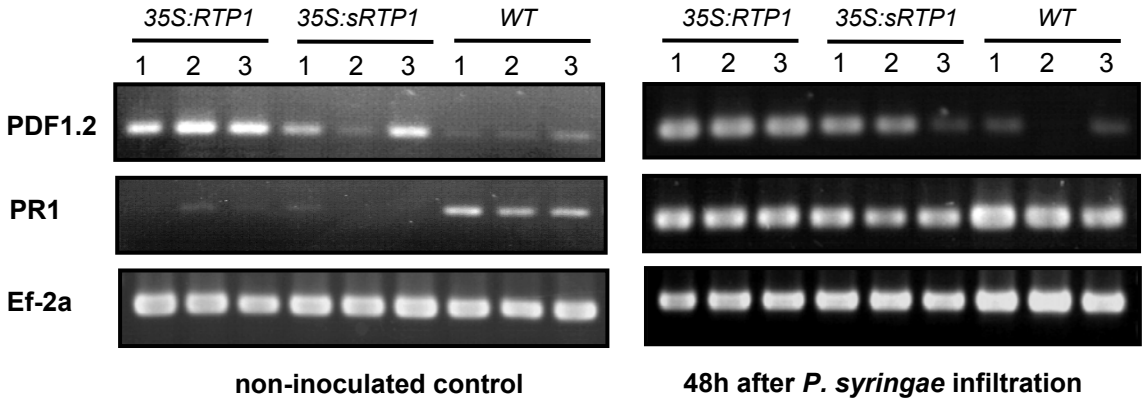

Fig.35. Expression of PR genes in response to inoculation with *P. syringae*. RT-PCR was performed using RNA preparations from 4-5 week-old plants.

4.2.2 Does RTP1 manipulate plant gene expression?

The results, discussed above, have demonstrated that stable and constitutive expression of RTP1 in *Arabidopsis* resulted in limited number and retarded growth phenotype of the obtained transformants. This has been taken as a basis to postulate that RTP1 interferes with plant growth and vitality. To further characterize this effect, we have utilised an ethanol-inducible (*alcA*) gene expression system (Roslan et al., 2001), that allows to conditionally express *RTP1* in stably transformed *Arabidopsis* plants. GUS reporter protein was used to test the efficiency of *alcA* inducible expression system. In fact, the responder cassette in *alcA:UidA* plants was efficiently activated after induction with 2% ethanol. This was monitored by GUS activity, which occurred in a highly responsive manner to ethanol induction. However RTP1 protein could not be detected by western blotting in induced *alcA:RTP1* plants despite repeated attempts. Nevertheless, induction of *RTP1* in the transgenic *alcA:RTP1* seedlings appeared to weaken the seedlings in further growth. Importantly, the observed phenotype associated with ethanol induction was dependent on RTP1 expression because induction of *alcA:GUS* seedlings did not exhibit any symptoms during all the first 8 days after induction. Longer ethanol treatments caused weak chlorosis which is due to ethanol toxicity. It is to note that this phenotype was obtained only when 10-days-old seedlings were induced. 4 weeks-old *alcA:RTP1* soil-grown plants did not show any particular phenotype after induction. This could be explained by the fact that *alcA:RTP1* induction may result in the production of RTP1 protein in the plant sufficiently to trigger suppression of cell vitality. This would affect rather the young seedlings for which *de novo* protein synthesis is more critical.

Quantitative RT-PCR was performed to analyse RTP1 and GUS transcripts in transgenic *alcA:RTP1* and *alcA:UidA* lines, respectively. A clear induction of *RTP1* and *GUS* mRNAs was observed (Chapter 3.3). Interestingly, while *GUS* transcript accumulation increased in the second day after induction in *alcA:GUS* plants, *RTP1* transcript level remained constant in *alcA:RTP1* plants. These results point to a putative role that RTP1 might play in suppressing general gene expression and subsequently its own expression in induced *alcA:RTP1* plants. Similarly, *Agrobacterium*-mediated leaf transient expression assay with *Nicotiana benthamiana*, has revealed that RTP1 is present at the level of the transcript although no protein

could be detected. In contrast, the GUS reporter control, was easily detected in agroinfiltrated leaves expressing *35S:RTP1:GUS* T-DNA. Analysis of GUS transcripts by real time RT-PCR revealed a slight decrease in *RTP1:GUS* transcript when compared to *GUS* transcripts in *35S:GUS* plants. However, this difference in mRNA level was not significant. This could be due to the fact that we measured the transcripts level at one and two days after agroinfiltration. Analysis of multiple transcript over a longer time-course could maybe reflect more significant differences.

Overall, this work clearly showed that RTP1 protein is not detected when heterologously expressed in different plant species (*A. thaliana*, *N. benthamiana*, *V. faba* and onion epidermal cells). The codon usage of RTP1 cDNA sequence expressed in plants does not differ significantly from the codon usage reported for most genes of *A. thaliana* (appendix1 and 2). Several hypotheses may be formulated to explain this discrepancy. Either RTP1 protein is degraded by proteolytic activity immediately following its translation. In this respect, this work reports the presence of a conditional signal for rapid degradation within RTP1 (discussed below). A second possibility is that further *RTP1* mRNA, due to the action of the first produced RTP1 protein molecules, is actually not translated when expressed in plants. This hypothesis is attractive as it is conceivable that translation inhibition would have been selected in rust fungi in order to manipulate host cells vitality and growth, probably for better control of nutrient uptake and disease development.

Although it is too early to conclude that RTP1 manipulates plant gene expression, as no DNA/protein binding site could be identified in its primary sequence, the ability of RTP1 to reversibly suppress host cell gene transcription/translation may provide a mechanism to prolong the biotrophic parasitism. For example, this could occur by slowing the synthesis rate, or mediating degradation of host nuclear and/or cytoplasmic proteins important for metabolism or plant defence. Recently, a conserved *P. syringae* virulence protein, HopM1, has been shown to target 21 plant proteins named AtMINs (*A. thaliana* HopM interactors). HopM1 has been found to mediate destruction of AtMINs via the host proteasome degradation pathway (Nomura et al., 2006). One of the AtMINs, encodes one of the eight members of the *Arabidopsis* adenosine diphosphate ribosylation factor (ARF) guanine nucleotide exchange factor (GEF) protein family. The ARF GEF proteins are

key components of the vesicle trafficking system in eukaryotic cells. Therefore it has been suggested that HopM1's virulence function is to inhibit host vesicle trafficking pathway, as an effective strategy of suppressing the extracellular cell wall–associated host defence.

It is important to mention that until now, the biochemical activity has been characterized only for a few bacterial and fungal effector proteins. Recently, Avr_{K1} and its paralogue Avr_{a10} of barley powdery mildew fungus, *Blumeria graminis f sp hordei* have been found to contribute to parasite virulence in susceptible host plants (Ridout et al., 2006). However, the biochemical activity of Avr_{K1} and Avr_{a10}, like most identified Avr effectors, remains elusive. The few identified biochemical functions for Avr proteins have been predicted relying on the conservation of either catalytic amino acids or predicted secondary structures between isolated effectors and known enzyme families. Some of such functions include sumo- and cysteine-proteases, tyrosine phosphatases and ADP-ribosyltransferases (Mudgett. 2005)**.** Recently, determination of the crystal structure of type III effectors from *P. syringae* provided some clues about their function in plants (Desveaux et al., 2006).

4.3 Structure-function deletion analyses of RTP1

The three dimensional structure of RTP1 is still highly in demand, but the production of large quantities of purified protein for structural studies is a problem (A. Kemen, 2007). To determine the minimal functional domain of RTP1 that would allow structural studies, we performed RTP1 functional domain boundary analyses. Prediction of the precise domain boundaries is difficult due the absence of sequence similarities. Through structure-function deletion analyses, we could show that the 45 aa central region of RTP1 (100-145 aa) was sufficient to suppress GFP expression (**Fig.36**), indicating that this region is likely to be responsible for interaction with plant gene expression. The suppression ability of the construct expressing the 45-amino-acid region was similar to the suppression obtained with full length RTP1.

Fig.36. Location of RTP1 functional domain

The RTP1 minimal functional domain excludes the NLS motif. However we can not rule out the necessity of nuclear localization for RTP1 functionality, since all RTP1 deletion mutants localized partially to the nucleus in our plant transient expression assay. Attempts to fuse a nuclear export signal (NES) to GFP:RTP1 mutant constructs could not clarify this point, because the NES used was not functional in our system and the control GFP:NES was still partially detected in the nucleus of transformed plant cells (not shown).

RTP1 minimal functional domain also excluded the PEST-like region, which corroborates that this region is not necessary for RTP1's activity. Interestingly, the identified functional domain does not contain any lysine residue, making it unlikely to be subjected to proteasomal degradation.

The minimal functional domain contained one of the two putative glycosylation sites of RTP1 (NST). However the functional domain as well as all generated deletion mutant constructs were cytoplasmically expressed and subsequently not glycosylated. Therefore, it is likely that glycosylation is not important for RTP1 function inside the plant cell. Yet, we can't rule out a potential important role for oligosaccharides allowing correct folding of RTP1 protein, necessary for its secretion, translocation through the EHM to plant cell surface, or for interaction with a plant plasma membrane receptor. In fact, heterologous expression of RTP1 mutants in *Pichia pastoris* revealed that at least the second putative N-glycosylation site of RTP1 (NST), also included in the minimal functional domain, is necessary for RTP1 secretion from the used yeast strain (A. Kemen, 2007). Whether this is true for RTP1 secretion from the rust haustorium is still unclear.

The RTP1 functional domain contains two cysteine residues at positions 104 and 117. To test if these residues are important for RTP1 function, we tested mutant constructs where the C104 and C117 were replaced by serine residues. None of both cysteines appeared to be important for the ability of RTP1 to interfere with plant gene expression (not shown).

4.4 What is the role of the RTP1 PEST-like sequence?

Among peptide motifs identified in rapidly degraded proteins that target proteins for rapid degradation are: lysosome-targeting KFERQ motifs (Dice. 1988) , PEST regions (Rechsteiner and Rogers. 1996) and the cyclin destruction box responsible for eukaryotic cell cycle (Tyers and Jorgensen 2000). We could identify a PEST-like motif within RTP1 sequence. Although presence of PEST motifs does not necessarily lead to constitutive degradation of the protein, there were a number of reasons why we thought it was worth investigating. Besides its proteolytic roles, PEST motifs have also been found to be involved in protein-protein interactions. For example, the PEST motif of c-Myb transcription factor (a highly regulated nuclear protein regulating the proliferation, differentiation, and apoptosis of hematopoietic cells) was found to directly interact with Ubc9, a ubiquitin-like protein (Bies et al., 2002).

The PEST sequence identified in RTP1, with a significant score of 9.38 lies within its half N-terminal domain and is recognised by bioinformatic programs as a low complexity region. Location of the PEST-like sequence towards RTP1 N-terminus is consistent with earlier findings highlighting the N-terminal location of PEST motifs (Rogers S et al., 1986). To test if the identified PEST-like motif affects the stability of the RTP1 protein, mutant constructs were made either via alanine substitution or by in frame deletion of the contiguous PEST residues (83-89aa) aiming to disrupt the PEST-like region. Contribution of the PEST-like motif to the stability of RTP1 would allow the visualisation of GFP in plant cells expressing GFP:RTP1$_{\text{PEST mutants}}$. GFP:RTP1$_{\text{PESTAla7}}$ retained GFP fluorescence suppression, suggesting that RTP1-PEST like sequence is unlikely to act as a degradation signal. This is consistent with the result got from a construct in which RTP1 PEST-like motif

was fused to the C-terminus of GFP, this construct did not affect GFP expression and stability. However, when GFP:RTP1$_{\Delta PEST}$, in which RTP1 residues 83-89 aa were deleted, was tested , fluorescence was detected in the nuclei of transformed cells. That GFP:RTP1$_{\Delta PEST}$ showed GFP fluorescence was unexpected and different to the results got from GFP:RTP1$_{PESTAla7}$. We assume that GFP:RTP1$_{\Delta PEST}$ results are likely due to a deleterious effect of the removal of the 7 amino acids within the PEST-like domain. This deletion might have changed the secondary and tertiary structure of the protein, rendering RTP1 inactive. The hypothesis that PEST-like motif of RTP1 is not functioning as a degradation signal is supported by the results obtained from the coexpression of *RTP1* and *GFP*, that retained GFP suppression property, confirming that failure in detecting RTP1 protein expressed in plants is likely due to a putative function of RTP1 in interfering with plant gene expression. However, we cannot completely rule out the possibility that RTP1's PEST-like motif is contributing to the instability of RTP1. In fact, PEST regions, which may vary considerably in sequence and length, have been found in a number of proteins such as yeast proteins: Gnc4, Fos, G1 cyclins, phytochrome A, MAT_2, p53 and fructose-1,6-bisphosphatase. All these proteins have been shown to be substrates of ubiquitin-dependent degradation (Deshaies, 1995, Rechsteiner and Rogers, 1996). Furthermore, for a number of diverse proteasome substrates, phosphorylation within PEST sequences often precedes and serves to instigate subsequent ubiquitination (Rechsteiner and Rogers, 1996). In this respect RTP1 carries potential casein kinase II phosphorylation site within the PEST-like motif at aa position 91.

Overall, three different roles could be attributed to the PEST-like region identified in RTP1: Besides putative roles in the stability and in the interaction with other proteins, as discussed above, the PEST-like region of RTP1 might play a third role during the translocation of RTP1 from the haustorium into the host plant cell. In fact there are a number of studies that demonstrated that the PEST motif mediates not only ubiquitination, but also subsequent internalisation of some plasma membrane proteins. For example, the N-terminal acidic PEST-like sequence has been reported to participate in the constitutive endocytosis of a number of yeast proteins such as Fur4p (Marchal et al., 1998), maltose permease Mal61p (Medintz. et al., 2000) and mating factor receptor (Roth et al., 1998).

PEST sequences have not been previously described neither in *U. fabae* nor in other plant pathogenic fungi secreted effectors. RTP1 PEST-like sequence identified during this study appears to be very similar to those known in other organisms. A bioinformatic work performed with *Plasmodium falciparum* genome has revealed that typical PEST sequences are present in 13% of the proteins on chromosome 2, including a large number of cell-surface exposed proteins and DNA binding proteins (Mitchell and Bell, 2003).

4.5 How does secreted RTP1 enter the plant cell?

Despite the important progress achieved in the last years to clone fungal effectors delivered from the haustoria to the host plant cells, nothing is known yet about how they enter the host cells. In addition, none of the cloned rust delivered effectors, including RTP1, seem to contain the recently identified transport motif (RXLR) of oomycete effectors (Rehmany et al. 2005). We suggest two possibilities for the mechanism of translocation of RTP1 from the haustorium into the infected host cell across the plant membrane: Either it may be mediated by a specialized translocation apparatus produced by the rust fungus, like the bacterial T3SS, or it may be dependent on the plant cell membrane transport machinery.

Coexpression studies of RTP1 and GFP in transiently transformed plant cells showed that RTP1 suppressed GFP fluorescence even when it was secreted. This is consistent with the hypothesis that RTP1 reenters the cell from the apoplast, even in the absence of the rust pathogen. This observation could also be explained by the retention of some RTP1 molecules in the cytoplasm as a result of inefficient secretion. However, the addition of an ER retrieval signal to the full-length sRTP1 abolished RTP1 activity and resulted in GFP fluorescence, confirming that sRTP1 is directed through the secretory pathway *in planta* and that the secreted RTP1 is able to reenter the host cytoplasm from the apoplast in the absence of the pathogen. Similar results were obtained when secreted flax rust effectors AvrM and AvrP4, from *Melampsora lini,* were transiently expressed in plant cells. Secreted AvrM and AvrP4 induced necrotic responses, and necrosis was inhibited when the ER retention signal was added, indicating that both Avr proteins can reenter plant cells after secretion

(Katanzariti et al., 2006). Furthermore, secretion of $RTP1_{PESTAla7}$ did not suppress GFP, suggesting a possible role for the PEST-like motif in the uptake of RTP1 by plant cells. But how does RTP1 reenter the plant cell across the plasma membrane?

Translocation of effector proteins has been mostly studied in bacterial pathogens. Apart from the well characterized T3SS, pathogenic bacteria use other mechanisms to deliver bacterial effectors. Some gram-positive bacteria appear to construct large pores within the plasma membrane of target cells that function as portals for direct effector delivery (Blanke. 2006). In other cases, bacterial AB-toxins are not injected into host cells by the bacterium. Instead, they are secreted and mediate their own entry to access their targets. AB-toxins bind to specific receptor molecules at the host cell surface as the first step in cellular entry, these receptors can be proteins, glycoproteins, or glycolipids. The toxin-receptor complex is subsequently internalized either by clathrin-dependent endocytosis (e.g. Shiga toxin and *Pseudomonas* exotoxin A), similarly to the way eukaryotic cells take proteins and lipids up from the cell surface, or by one of several clathrin- independent endocytic pathways (**Fig.37**) (Falnes and Sandvig, 2000). Members of this second group of toxins have been shown to exploit the ER-associated degradation pathway (ERAD) to target their final compartment within the host cell. The ERAD system recognizes misfolded proteins in the ER and exports them to the cytosol for ubiquitination and proteasomal degradation (Perlmutter, 1999). Hazes and Read (1997) proposed that an exposed hydrophobic stretch within the A13 subdomain of A1 cholera toxin (CTA1) identifies the toxin as a misfolded protein and thereby triggers ERAD activity. After transfer to the cytosol, CTA1 is thought to escape proteasomal degradation because it has a low number of lysine residues that are required for ubiquitination.

A similar scenario could be proposed for the entry of RTP1 from the EHM into the host plant cells. But how is it then that RTP1 can exploit a cellular system whose primary function is to send misfolded proteins to the proteasome for degradation? The answer to this question may derive from some structural properties of RTP1. First, the identified PEST-like sequence studied in this work, is defined as a low complexity region by bioinformatic programs. This region might interact with a receptor at plant cell plasma membrane, thereby stimulating its internalization. Once endocytosed, either the PEST-like motif itself or another domain within RTP1 protein

could stimulate the retrotranslocation by masquerading RTP1 as misfolded proteins. A similar situation was described for some AB-toxins where -KDEL, an ER retention motif, at the C-terminus of the A subunit, likely interacts with the KDEL receptor. This receptor recycles between the trans-Golgi network, Golgi cisternae and the ER, scavenging itinerantly soluble ER components and returning them to the ER.

But how does potential retrotranslocated RTP1 escape proteosome-mediated degradation? Proteins destined for degradation typically are posttranslationally decorated with ubiquitin on their lysine residues. RTP1 contains remarkably 7 lysine residues, two of them are nearby the PEST motif. One possibility is that effectively internalized RTP1 undergoes proteasome degaradation and only some RTP1 molecules reach the nucleus and exert their function. A second possibility would be that RTP1 uses other mechanisms to escape ubiquitination mediated targeting to host proteasomes, for example by folding in a structure that would hide the PEST-like sequence.

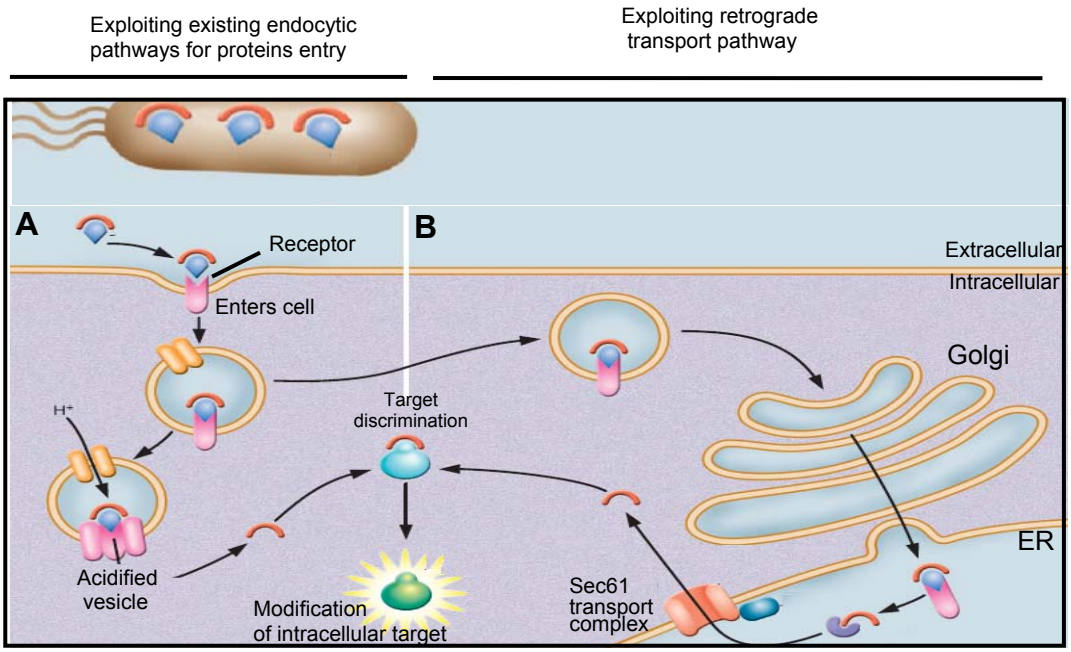

Fig.37. Pathogen-independent entry of AB toxins into target cells. (picture modified from Blanke. 2006)). Bacteria release AB toxins into the host cell surface. (**A**)Some toxins use existing endocytic pathways to enter host cells. (**B**) Other AB toxins exploit the ERAD pathway to enter the cytosol through the ER complex whose primary protein is Sec61.

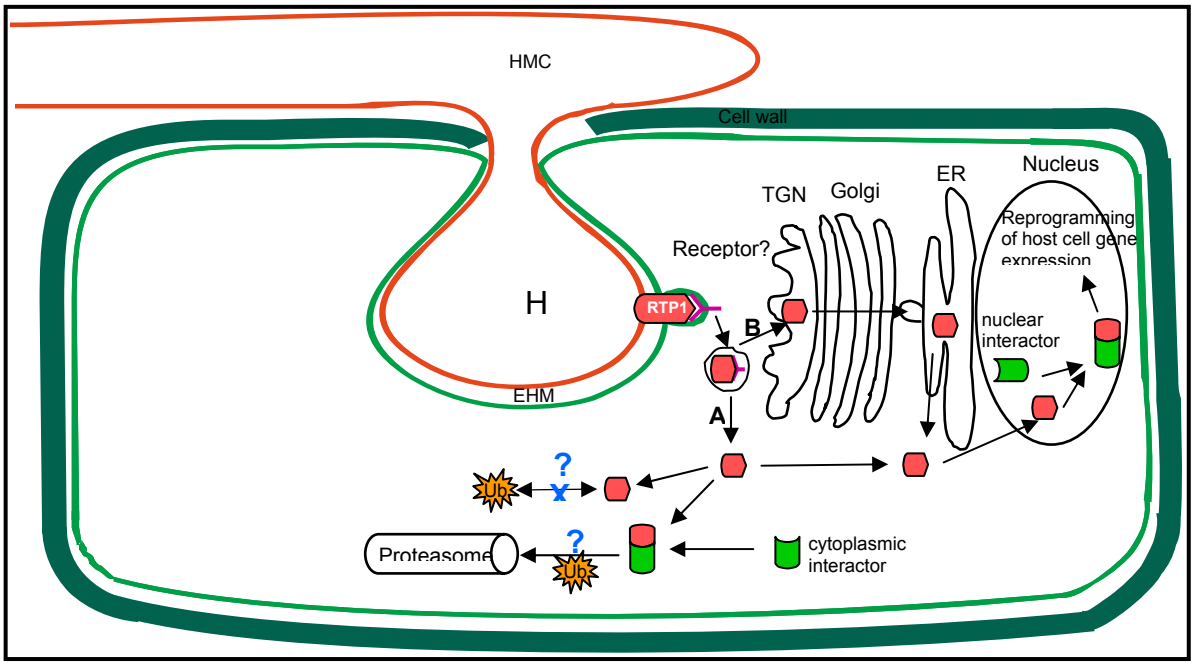

Fig.38. Model for RTP1 translocation from the haustorium into host cell nucleus. We suggest that haustorially secreted RTP1 binds to a cell surface receptor (**Y**). RTP1 enters the host cell cytosol either from endosomes, or via the retrograde transport to the ER where it might be recognized as a misfolded protein and subsequently released into the cytosol. Once in the cytosol, RTP1 might escape proteasomal degradation and reach its target plant protein(s) in the cytoplasm or/and in the nucleus. Alternatively RTP1 alone or RTP1/interactor complex might be subjected to degradation by the host proteasome.

Altogether, it appears that sRTP1 protein is composed of different domains that can be organized in two groups: Domains located towards the N-terminus, involved in the targeting process (signal peptide, NLS, PEST-like sequence) and a further domain where the biological function of RTP1 resides (**Fig.40A**). The proposed sRTP1 domain organization is comparable to several oomycetes RXLR effectors such as ATR1NdWsB and ATR13 of *Hyaloperonospora parasitica* Avr1b-1 of *Phytophthora sojae*, and AVR3a of *P. infestans* (**Fig.40B**).

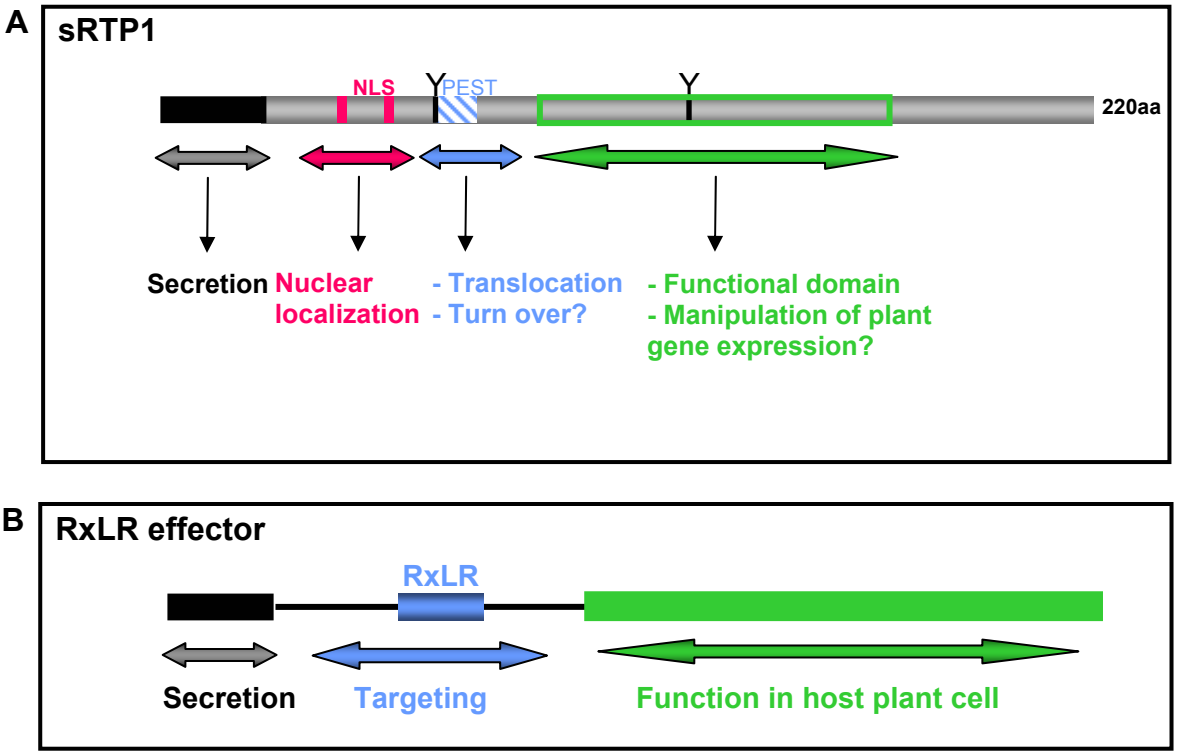

Fig.40. Domain organization in sRTP1 and RxLR effectors. (**A**) Proposed domain structure of RTP1. The N-terminal domain is responsible for targeting (secretion from the haustorium, translocation and nuclear targeting), while the functional domain resides at the C-terminal half of the protein. (**B**) Domain structure of delivered oomycetes RXLR effectors. N-terminal regions are involved in secretion and targeting, while domains involved in effector activity are located within the C-terminal region (Kamoun, 2006).

Another motif within RTP1 (aa 139-151) has been studied by E. Kemen (2007), and has been found to be composed of mostly hydrophobic residues. This motif is predicted by TANGO program as a potential ß-aggregation domain. Synthetic peptides with 21 residues containing the predicted aggregation domain (135-155aa) revealed spontaneous aggregation into amyloid-like filamentous structures (Kemen, E, 2007). These data in contrast to our finding that deletion construct GFP:RTP1$_{(114-220)}$, in which the predicted aggregartion domain is included, showed normal distribution of GFP fluorescence in transformed plant cells, similar to that obtained with GFP alone, and did not give any evidence for filamentous structures formation. A. Kemen (2007) found that secretion of RTP1 from transformed *P. pastoris* results in aggregates and amorphous plaques formation, and attributed this effect to the ß-aggregation domain. However, it is not yet clear if RTP1 aggregates are formed *in planta*, or whether this property is specific to the used yeast secretion system. Furthermore, expression in *P. pastoris* revealed that RTP1 is N-terminally processed at amino acid R54. This cleavage decreased the molecular size of the deglycosylated protein from 22 to 18 kDa. In contrast, our heterologous expression assays using *Ustilago maydis* (discussed below) did not support the presence of this processing, and the size of recombinant secreted RTP1 from *U. maydis* (24-26 kDa) was the same as native RTP1 secreted from *U. fabae*. Finally, E. Kemen (2007) postulated two roles for the RTP1$_{(139-151)}$ hydrophobic domain: a functional role consisting of RTP1 filaments-mediated blocking cyclosis of the host cell, and a potential role during RTP1 translocation process. Other *in vivo* cytological results will be needed to verify both hypotheses.

4.6 RTP1 in other rust species?

Using polyclonal antibodies raised against RTP1 secreted from *U. fabae*, other RTP1 homologues could be identified in a number of *Uromyces* species: *U. striatus*, *U. appendiculatus* and *U. vignae* (Kemen, K, 2006). Other *sRTP1* homologue genes were cloned from *Melampsora medusae f.sp. deltoidae* and *M. larici-populina* (Unpublished, Dr. D Joly, University of Laval, Canada). Alignment of RTP1 amino acids sequences from *U. fabae* (UfRTP1), *U. striatus* (UsRTP1) and *M. medusae* (MmRTP1) showed that MmRTP1 is more distinct from UfRTP1, UaRTP1 and

UsRTP1 (**Fig.41A**). Considering molecular phylogenetic studies, *M. medusae* (infecting Salicaceae) is taxonomically distant to the legume pathogens *U. fabae*, *U. striatus* and *U. appendiculatus* (Maier et al., 2003). Therefore it is likely that the *RTP1* gene has evolved differently in all these rust species. However, despite their diverse phylogenetic distribution, all proteins encoded by *sRTP1* homologues share some degree of sequence similarity; showing a predicted molecular mass of about 24 kDa. The highest degree of conservation resides in the half C-terminal of the proteins (**Fig.41B**).

The domain organization of RTP1 seems to be conserved, the signal peptide is present in all 4 homologue proteins. The bipartite NLS motif is conserved in UfRTP1 and UaRTP1 but hardly recognised in UsRTP1 and absent in MmRTP1. Attempts to identify a functional NLS in UsRTP1, using GFP fusion studies did not show nuclear localization (not shown). The PEST-like sequence, separating the N-terminal domain (containing the NLS) from the C-terminus containing RTP1 functional domain, is recognised in all proteins with different scores (UfRTP1-PEST= +9.38, UaRTP1-PEST= +0.30, UsRTP1-PEST= 3.71, MmRTP1= -6.08). It is recognized by bioinformatic programs as a low complexity region for all the four homologues. Most residues of the functional domain of UfRTP1 are conserved in the other RTP1s (**Fig.41B**). RTP1 functional domain has been found to suppress plant cell vitality for both UfRTP1 and UsRTP1 (not shown). These striking similarities suggest that RTP1 biological role might be conserved in all proteins. This is in accordance with the results obtained from the transient expression of *35S:GFP:RTP1* in different plant species. In fact the fusion protein suppressed GFP in all tested plants (Chapter 3). Conserved RTP1's activity in different plant species argues in favour of a general virulence function for RTP1.

A

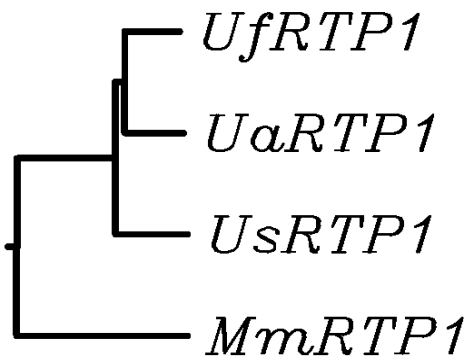

B

```
UfRTP1      1   -MSNLRLLFTIISLAAIARAQLVGSDVVLVRTSHQSMGKASVSYCREMT-------RQHH
UaRTP1      1   ------------------------SEVVLVRTAHESMGEASVSYCRALDSHSTYTAHQLR
UsRTP1      1   MLFNPNLRVFLTIIILAAVARALTPGVVLVRTHHETMGLASVSICRAEKDIHLGHPNVRL
MmRTP1      1   --------------LLGCCWSAFDYSNGSLKAQDVSVGGSKTAKGPINMKTVQGNLKSEY

UfRTP1     53   KRELDQDANPGHRRHKSEPEGVKPSNHTSAPTPSSPPLTTVDLTPAKLN-TACYPGTFQA
UaRTP1     37   KRELDSEATLRHKHHKQKLEDVKSSNHTTNPTHSSPSLTTVDLTPAKLI-TSCYPGTFQA
UsRTP1     61   RKRDMDKFANTPQHSKLELEDAKDSNYLSKATPSSPSLTTVDLTPAKLK-SSCYLGTFQA
MmRTP1     47   KIGLNEMVTVRIYEYKNDFNLVRREANVSATKSN---LTTIDLTPADCDGAQCYPGAFDK

UfRTP1    112   PLLEDCEVVIRAQLYNSTGSLQVSPGDYVFVSYGTCATVFQNPQYSKYSLQYNWAELGYV
UaRTP1     96   PSLEDCEVVIRAQLYNSTGSLQVSPGEYVFVSYGTCATVFQNPHYSNYSLEYNWAELGYV
UsRTP1    120   PLLEDCEVVIRAQLYNSTGSLQASPGDYVFVSYGTCATVFQNPQNSNYTIQYNWAELGYL
MmRTP1    104   PNTTDCDAVWNAQLYNSTGSLTAFPGTFVYVFSGNCAVVFQNPQNQGYAIQFNWAKLGAV

UfRTP1    172   GGKLAGRCLLPEDHSMGGTAVFDTYLGRTYPDVIISLQRFDDRDFIIPE----------
UaRTP1    156   GGKLAGRCLLPEDHSMGGTAVFDTYLGGTYPE
UsRTP1    180   GGKLAGRCLLPEDHSMGGTAVFDTYLGHTYPDVIISLQRFDDRDFIIPE----------
MmRTP1    164   GVKIADKCLAPKTNSIGGICQYTKYLTWTFNDVLISVQKHVEETQKPAEAEKPKAEDPK
```

Fig.41. Comparison of sRTP1 protein in four rust species. (**A**) RTP1 Neighbor-Joining tree. Midpoint rooted dendrogram based on aa sequences of sRTP1 homologues from *U. fabae*, *U. appendiculatus*, *U. striatus* and *M. medusae*. (**B**) Alignment of RTP1 homologues. Amino acids identities are shaded. UfRTP1 domains, studied in the presented work, are outlined, the NLS in pink, the PEST-like region in blue and the minimal active domain in green, respectively.

4.7 *Ustilago maydis* as a model system to study RTP1 delivery into host cells

As it is difficult to study RTP1 translocation mechanism in the native pathosystem *U. fabae*/*V. faba* by gene disruption and loss of function analyses, a suitable recombinant secretion system had to be chosen, that would allow structural and functional studies of RTP1 delivery process. In attempts to purify recombinant RTP1, the yeast strains *Saccharomyces cerevisiaie* and *P. pastoris* have been used

to heterologously express *sRTP1*. This has resulted in hyperglycosylation of the secreted RTP1, showing molecular sizes largely exceeding RTP1's molecular weight, and resulting in insoluble aggregates at high protein concentrations (Hempel, 2005; Kemen. A, 2007). Althought it is not yet known which specific glycosylation pattern is necessary for RTP1 delivery, the hyperglycosylation of RTP1 expressed in yeast may cause improper folding. Another disadvantage of using yeast as secretion system is that it does not allow *in vivo* studies of RTP1 delivery into plant cells.

The presented thesis suggests the use of a new strategy to study not only the secretion, but also the translocation of RTP1 into plant cells. The proposed expression system consists of a biotrophic filamentous fungus that secretes and naturally delivers recombinant RTP1 into plant cells. Besides mimicking the situation in the native pathosystem *U. fabae*/*V. faba*, this novel approach, in contrast to yeast, should not result in extensive hyperglycosylation (Maras et al., 1999).

4.7.1 *U. maydis*: a suitable secretion system

Filamentous fungi, like yeast, have a high capacity for producing large amounts of extracellular proteins (Punt et al., 2002). Use of filamentaous fungi for production of a wide range of hererologous products has been made possible by developed molecular techniques. In the first attempt we used the ascomycete *Colletotrichum lindemuthianum* to constitutively express *oliC:sRTP1*. However only very weak RTP1 bands could be detected among proteins recovered from the liquid culture of UPS9 transformants (results not shown). Failure of RTP1 secretion from UPS9 transformants is likely due to the potential weak activity of the used *Aspergillus nidulans oliC* promoter.

In a second attempt, we used the biotrophic basidiomycete *U. maydis* as a secretion system. We took advantage of the available solopathogenic SG200 strain to express either sRTP1 or sRTP1:GFP under the control of *o2tef* promoter. Immunoanalysis of cell-free supernatant's proteins detected a high amount of secreted RTP1 and RTP1:GFP proteins. While GFP in RTP1:GFP protein fusion was most likely subjected to protease degradation, RTP1 was intact and showed the

exact expected size. Through deglycosylation experiments, we could show that recombinant RTP1 glycosylation pattern is very similar to its glycosylation when secreted by rust haustoria.

4.7.2 Pursuing RTP1 delivery

To follow the *in planta* secretion and the potential transfer of recombinant RTP1, we used transformed SG200 strains expressing either *GFP*, or *sRTP1:GFP* under the inducible control of *mig2-6* promoter. *mig2-6:GFP* expressing strains showed strong GFP fluorescence found only during pathogenic growth, confirming the *in planta* specific activity of *mig2-6* promoter (Farsing et al., 2005). Using fluorescence and laser scanning microscopy, we could clearly visualize secreted RTP1:GFP fusion protein throughout infection hyphae. Location of bright fluorescence towards the hyphal tips is consistent with the “bulk flow hypothesis” (Wessels, 1990), which proposes that protein secretion in filamentous fungi is limited to the growing hyphal tips. Fluorescence was sometimes detected in vesicle-like structures that could be organelles and/or intermediate components of the secretory pathway.

Some infected plant cells showed GFP-like fluorescence located in the cytosol including the nucleus, suggesting that RTP1:GFP might have been internalized. However, despite the strong GFP fluorescence detected throughout the infection hyphae, only very few plant cells showed intracellular fluorescence. An explanation for this could most likely be attributed to the presence of GFP, which either would hamper the internalization of RTP1:GFP fusion protein into plant cells, or would, in case GFP is degraded, not allow fluorescence visualization inside the plant cell cytosol.

Overall, these data support once more the hypothesis that RTP1 transfer is depending rather on the plant cell transport machinery, than on a presumed rust specific translocation apparatus. These findings are very similar to those obtained from ToxA, a host selective toxin delivered from *Pyrenophora tritici-repentis* into wheat cells. Like RTP1, ToxA protein internalization has been found to occur

independently from the pathogen, suggesting that ToxA contains all of the informations required for its internalization by host plant cells. ToxA tanslocation process has been shown to be sufficiently robust to still function despite increasing the size of ToxA by N-terminal fusion to GFP (Manning and Ciuffetti. 2005).

The development of a *U. maydis* expression system for RTP1 is desirable for structural studies as it allows production of a high amount of recombinant RTP1 that is, compared to any other expression system, most similar to native RTP1 secreted from *U. fabae* haustoria. Although secreted RTP1:GFP from *mig2-6:sRTP1:GFP* expressing strains exhibited a low level of fluorescence in the cytosol of infected plant cells, it is expected that this system may have a great potential as a protein delivery system to target tissue. However, since we showed that secreted GFP is subjected to proteolysis, the use of smaller tags (e.g. Myc-tag) for immunological detection, or the direct immunocytological detection of RTP1 appears to be necessary in order to pursue the transfer process of RTP1.

5 Outlook

To finally understand the exact biochemical function of RTP1 in plant cells, we will need to get structural and molecular insights from the identified functional core of RTP1. It is, therefore, crucial to determine the 3D structure of RTP1's functional domain. To this end, the developed *U. maydis* expression system could be used to produce the protein fragment to be crystallized.

This work supports the hypothesis that RTP1 is internalized into plant cells through a receptor and endocytosis-mediated process, and propose the use of *U. maydis* / *Zea mays* pathosystem to pursue the translocation events. However, because of the instability of GFP, immunocytological analyses will be needed to localize RTP1 during the transfer process. Here are some questions arising from the present study and which would be relevant to address:

- Which domains are necessary for the interaction with a potential receptor and which ones are necessary for the translocation from the plant plasma membrane into the cytosol? This question could be answered by immunocytological analysis of *U. maydis* transformants secreting different RTP1 mutants. In this respect SG200 strain expressing *mig2-6:RTP1*$_{PESTAla7}$ has been generated.
- Role of the PEST-like sequence in the RTP1 translocation process could be investigated by generating *U. maydis* expressing *mig2-6:PESTavrX*, in which the PEST motif of RTP1 is fused to a a bacterial T3SS effector AvrX that is causing cell death in maize cells. In this case, transmembrane transfer of the chimeric protein could be monitored by the death of infected plant cells.
- Does RTP1 suppress gene transcription or translation? Microarray analyses of induced *alcA:RTP1* and *alcA:UidA* plants, in addition to *in vitro* translation experiments could answer this question.
- What is (are) the plant interacting partner(s) of RTP1? Answers to this question could be obtained by the screening of an *Arabidopsis* cDNA library using the RTP1$_{100\text{-}145}$ functional domain and full-length RTP1 as baits in a yeast two-hybrid assay.

6 Summary

Haustoria of the rust fungus pathogen *Uromyces fabae* deliver RTP1 (Rust Transferred Protein1) into host plant cells. In this work, different heterologous expression systems were used to study RTP1 biological function as well as RTP1 transfer mechanism.

The first part of this thesis focused on the identification of the subcellular target compartment of RTP1 in plant cells. In this respect we could identify a functional bipartite nuclear localization signal within RTP1. However, stable and transient expression studies of RTP1 in different plant species, including the host plant *Vicia faba*, interfered with plant cell vitality but did not result in detection of RTP1 protein. These findings led us to propose that RTP1 interferes with plant gene expression. However, the molecular basis of this interference remains unclear. By deletion studies, we could localize the active region of RTP1 within a 45 amino acid central domain.

In the second part of this study, two different lines of approaches were taken to study RTP1 transfer mechanism. First, transient expression of secreted RTP1 (sRTP1) also interfered with plant cell vitality. Addition of an endoplasmic reticulum retention signal abolished sRTP1 interference with plant cell vitality, suggesting that RTP1 can reenter the plant cell from the apoplast after secretion in the absence of the pathogen. We have identified a PEST-like region within RTP1, however, contribution of this region to the stability of RTP1 is not clear. Site directed mutagenesis analysis showed that the PEST-like region is likely to play a role during the transfer of RTP1 through plant plasma membrane. In the second line of approach, we established a recombinant delivery model, using *Ustilago maydis*/*Zea mays* pathosystem, to pursue RTP1 translocation into the plant cell. Our results indicate that *U. maydis* is capable of secreting high amounts of recombinant RTP1, showing similar glycosylation pattern as RTP1 secreted from rust haustoria. Our data propose the use of this model system to study RTP1 domains mediating its entry into the plant cell.

ZUSAMMENFASSUNG

Haustorien des pathogenen Rostpilzes *Uromyces fabae* sekretieren das RTP1 Protein (Rust Transferred Protein1) in die Wirtspflanzenzelle. In dieser Arbeit wurden verschiedene heterologe Expressionsysteme genutzt um sowohl die biologische Funktion von RTP1 als auch dessen Transfermechanismus zu studieren.

Der erste Teil der Arbeit beschäftigte sich mit der Identifikation der subzellulären Lokalisation von RTP1 in der Pflanzenzelle. Hierbei konnten wir ein funktionelles zweigeteiltes Kernlokalisierungssignal (NLS) innerhalb von RTP1 identifizieren. Die stabile und transiente Expression von RTP1 in verschiedenen Pflanzenspezies, inklusive der Wirtspflanze *Vicia faba,* führte zu einer reduzierten Vitalität der Pflanzenzellen, obwohl das RTP1 Protein nicht nachweisbar war. Diese Beobachtung führte uns zur Annahme, dass RTP1 die pflanzliche Genexpression unterdrückt. Der molekulare Mechanismus dieser Suppression bleibt weiterhin unklar. Mit Hilfe von Deletionsanalysen konten wir die aktive Region von RTP1 in einer zentralen, 45 Aminosäure langen Domäne lokalisieren.

Im zweiten Teil dieser Arbeit wurden zwei verschiedene Ansätze verfolgt, um den Transfermechanismus von RTP1 zu studieren: Zum einen unterdrückte die transiente Expression des sekretierten RTP1 (sRTP1) die Vitalität der Pflanzenzellen. Die Hinzufügung eines ER-Rententionssignals neutralisierte die Unterdrückung der Pflanzenzellvitalität durch sRTP1, was zur Annahme führte, dass RTP1 nach der Sekretion in den Apoplasten erneut in die Pflanzenzelle eindringt, und zwar in Abwesenheit des Pathogens. Eine PEST-ähnliche Region wurde in RTP1 identifiziert, aber ein Beitrag dieses Motivs zur Stabilität von RTP1 ist unklar. Durch gezielte Mutagenese konnte jedoch gezeigt werden, dass die PEST-ähnliche Region wahrscheinlich eine Rolle bei dem Transfer von RTP1 über die Pflanzenmembran spielt. In einem zweiten Ansatz wurde ein rekombinantes Übertragungssystem etabliert, unter Nutzung des *Ustilago maydis- Zea mays* Pathosystems, um die Translokation von RTP1 in die Pflanzenzelle zu studieren. Die Ergebnisse zeigen dass *U. maydis* fähig ist, eine große Menge an rekombinantem RTP1 zu sekretieren, mit einem ähnlichen Glykosylierungsmuster wie das sekretierte RTP1 von Rost-Haustorien. Unsere Daten unterstützen die Eignung dieses Modellsystems, um damit die Domänen zu untersuchen, die den Transfer von RTP1 in die Pflanzenzellen vermitteln.

7 Appendix

Codon Usage of sRTP1 in *A. thaliana*

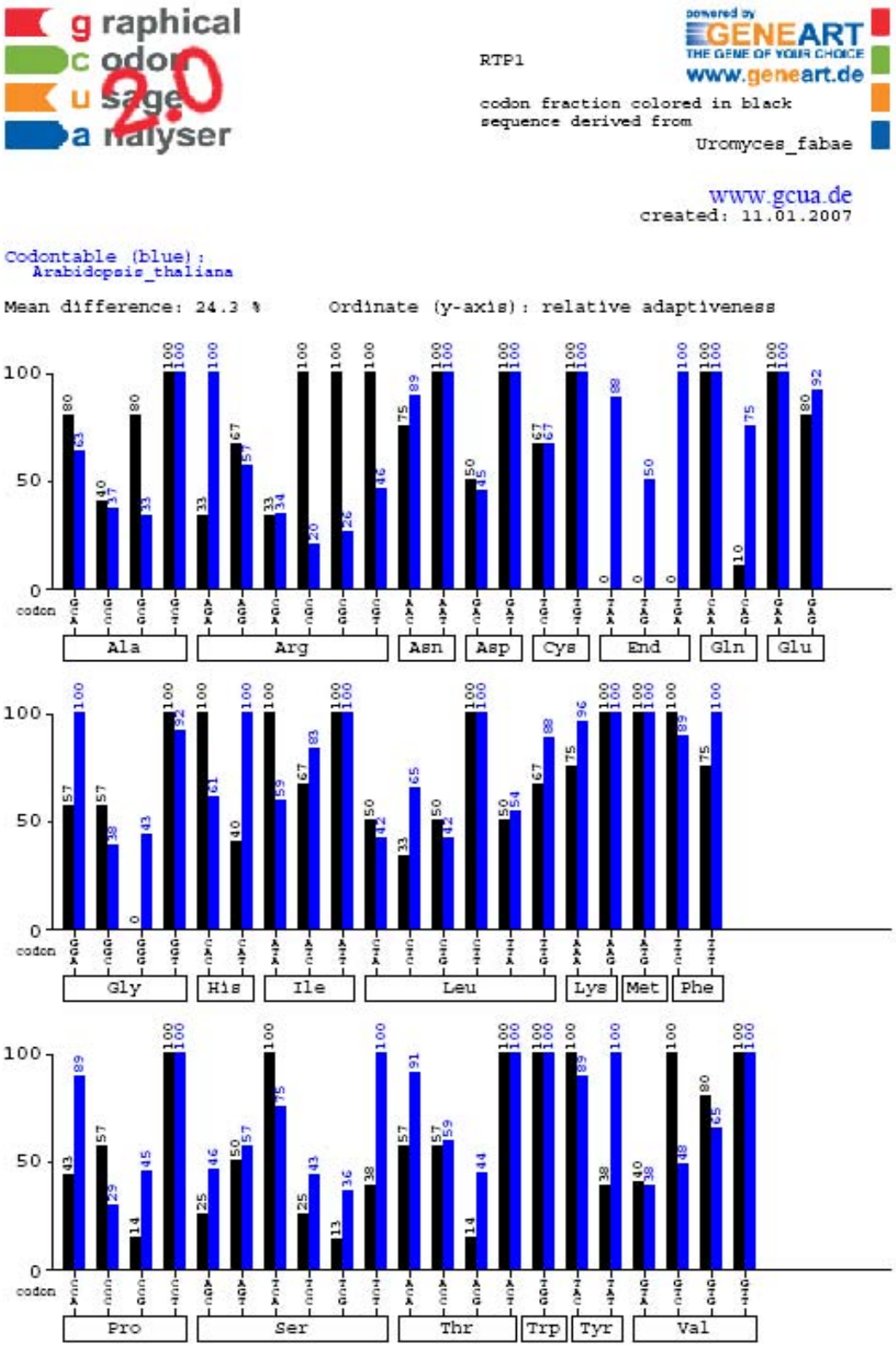

8 References

Allen, E.A., Hazen, B.E., Hoch, H.C., Kwon, Y., Leinhos, G.M.E., Staples, R.C., Stumpf, M.A., and Terhune, **B.T. (**1991) Appressorium formation in response to topographical signals by 27 rust species. *Phytopathology* **81**:323-331.

Allen, R.L., Bittner-Eddy, P. D., Grenville-Briggs, L.J., Meitz, J.C., Rehmany, A.P., Rose, L.E., and Beynon, J. L. (2004) Host-parasite co-evolutionary conflict between *Arabidopsis* and downy mildew *Science*. **306:**1957–1960.

Amy F. Roth, Daniel M. Sullivan, and Nicholas G.D. (1998) A Large PEST-like equence Directs the Ubiquitination, Endocytosis, and Vacuolar Degradation of the Yeast a-Factor Receptor. *J. Cell Biol*. **142** (4):949-961.

Banuett, F.(1992) *Ustilago maydis*, the delightful blight. *Trends Genet*. **8:**174-180.

Benabdillah, R., Jaime Mota, L., Lutzelschwab, S., Demoinet, E., and Cornelis, G.R. (2004) Identification of a nuclear targeting signal in YopM from *Yersinia* spp. *Microb Pathog* **36:**247–261.

Bies J, Markus J, and Wolff L. (2002) Covalent attachment of the SUMO-1 protein to the negative regulatory domain of the c-Myb transcription factor modifies its stability and transactivation capacity**.** *J Biol Chem.* **277**(11):8999-9009.

Blanke, S.R. (2006) Portals and Pathways: Principles of Bacterial Toxin Entry into Host Cells. *Microbe*. **1**(1):26-32.

Bölker M, Urban M, and Kahmann R. (1992) The *a* mating type locus of *Ustilago maydis* specifies cell signaling components. *Cell*. **68:**441–450.

Bölker,M. (2001) *Ustilago maydis* – a valuable model system for the study of fungal dimorphism and virulence. *Microbiol*. **147**:1395–1401.

Caddick, M.X., Greenland, A.J., Jepson, I. *et al*. (1998) An ethanol inducible gene switch for plants used to manipulate carbon metabolism. *Nature Biotech.* **16**:177–180.

Cantrell, L.C., and Deverall, B.J (1993) Isolation of haustoria from wheat leaves infected by the leaf rust fungus, *Physiol. Mol. Plant Pathol*. **42**:337-343.

Catanzariti, A.M., Dodds, P.N., Lawrence, G.J., Ayliffe, M.A., and Ellis, J.G. (2006). Haustorially Expressed Secreted Proteins from Flax Rust Are Highly Enriched for Avirulence Elicitors. *The Plant Cell* **18:**243-256.

Chen, H., Nelson, R.S. and Sherwood, J.L. (**1994**) Enhanced recovery of transformants of *Agrobacterium tumefaciens* after freeze-thaw transformation and drug selection. *Biotechniques* **16:**664-668.

Clough, S.J. and Bent, A.F. (**1998**) Floral dip: a simplified method for *Agrobacterium*-mediated transformation of *Arabidopsis thaliana. Plant J*. **16**:735-. 743

Corbett, **A.H. and Silver, P.A.** (1997). Nucleocytoplasmic transport of macromolecules. *Microbiol. Mol. Biol. Rev.* **61**:193-211.

Cornelis, G.R. (2005) The V-antigen of Yersinia forms a distinct structure at the tip of injectisome needles. *Science* **310:**674-676.

Cornelis, G.R. (2006) The type III secretion injectisome. *Nat Rev Microbiol* **4**:811-825.

Dangl J.L, and McDowell J.M (2006) Two modes of pathogen recognition by plants. *Proc Natl Acad Sci USA* **103:**8575–8576.

Deising H, Jungblut P.R, and Mendgen K. (1991) Differentiation-related proteins of the broad bean rust fungus *Uromyces viciae-fabae*, as revealed by high resolution two-dimensional polyacrylamide gel electrophoresis. *Archives of Microbiol.* **155:**191–198.

Denecke, J., DeRyk, R., and Botterman, J. (1992). Plant and mammalian sorting signals for protein retention in the endoplasmic reticulum contain a conserved epitope. *EMBO J*. **11**:2345–2355.

Denecke, J., Ek, B., Caaspers, M., Sinjorgo, K.M., and Palva, E.T. (1993). Analysis of sorting signals responsible for the accumulation of soluble reticuloplasmins in the plant endoplasmic reticulum. *J. Exp. Bot*. **44**:213–221.

Deshaies R.J. (1995) Make it or break it: The role of ubiquitin-dependent proteolysis in cellular regulation. *Trends Cell Biol*. **5**: 428–434.

Desveaux, D., Singer, A.U., and Dangl, J.L.(2006) Type III effector proteins: doppelgangers of bacterial virulence. *Curr. Opi. Plant Biol*. **9**:376-382.

Dice J.F. (1988) Microinjected ribonuclease A as a probe for lysosomal pathways of intracellular protein degradation. *J Protein Chem*. **7**:115-127.

Dickinson, L.A., Gulizia, R.J., Trauger, J.W., Baird, E.E., Mosier, D.E., Gottesfeld, J.M., and Dervan, P.B. (1998) Inhibition of RNA polymerase II transcription in human cells by synthetic DNA-binding ligands. *Proc. Natl. Acad. Sci. USA* **95:**12890-12895.

Dodds P.N, Lawrence G.J, Catanzariti A.M, Ayliffe M.A and Ellis J.G. (2004)The Melampsora lini AvrL567 avirulence genes are expressed in haustoria and their products are recognised inside plant cells. *Plant Cell* **16:**755–768.

Dodds, P.N., Lawrence, G.J., Catanzariti,A.M., Ayliffe, M.A., and Ellis, J.G. (2004) The *Melampsora lini AvrL567* Avirulence Genes Are Expressed in Haustoria and Their Products Are Recognized inside Plant Cells. *Plant Cell*. **16**(3):755–76.

Eckardt, N.A. (2006). Identification of Rust Fungi Avirulence Elicitors. *Plant Cell*. 2006 **18**(1): 1–3
Ellis,J., Catanzariti, A.M., and Dodds,P (2006) The problem of how fungal and oomycete avirulence proteins enter plant cells. *Trends Plant Sci*. **11**(2): 61-63.

Erickson, F.L., Holzberg, S., Calderon-Urrea, A., Handley, V., Axtell, M., Corr, C., and Baker, B. (1999). The helicase domain of the TMV replicase proteins induces the *N*-mediated defence response in tobacco. *Plant J.* **18:**67–75.

Falnes. P and Sandvig. K. (2000) Penetration of protein toxins into cells. *Curr. Opin. Cell Biol*. **2**:407–413.

Farfsing JW, Auffarth K and Basse CW. (2005) Identification of cis-active elements in *Ustilago maydis* mig2 promoters conferring high-level activity during pathogenic growth in maize. *Mol Plant Microbe Interact*.**18**(1):75-87.

Feys, B.J., and Parker, J.E. (2000) Interplay of signaling pathways in plant disease resistance. *Trends Genet*. **16:**449–455.

Haasen, D., Kohler, C., Neuhaus, G., and Merkle, T. (1999) Nuclear export of proteins in plants: AtXPO1 is the export receptor for leucine-rich nuclear export signals in *Arabidopsis thaliana*. *Plant J.* **20:**695-705.

Hahn, M. (2000) The Rust Fungi. Cytology, Physiology and Molecular Biology of Infection. In Fungal Pathology, ed. JW Kronstad, pp. 267-306. *Dordrecht: Kluwer Academic Publishers*.

Hahn, M., and Mendgen, K (1997). Characterization of in planta-induced rust genes isolated from a haustorium-specific cDNA library. *Mol Plant–Microbe Interact*. **10**:427–437.

Harder, D.E, Chong, J. (1984) Structure and physiology of haustoria. In: Bushnell WR, Roelfs AP, eds. The cereal rusts origins, specificity, structure, and physiology. *Orlando, FL, USA: Academic Press*, Inc, 431–476.

Hazes, B., and Read, R.J. (1997) Accumulating evidence suggests that several AB-toxins subvert the endoplasmic reticulum-associated protein degradation pathway to enter target cells. *Biochemistry* **36:**11051-11054.

Heath, M.C (1990) Influence of carbohydrates on the induction of haustoria of the cowpea rust fungus *in vitro*. *Exp. Mycol.* **14**:84–88.

Hempel, U. (2005). Genes expressed during the biotrophic phase of the rust fungus *Uromyces fabae*. Dissertation, University of Konstanz.

Hiller, N.L., Bhattacharjee, S., van Ooij, C., Liolios, K., Harrison, T., Lopez-Estrano, C., and Haldar, K (2004) A host-targeting signal in virulence proteins reveals a secretome in malarial infection. *Science*. **306:**1934-1937.

Hoch, H.C., Tucker, B.E., and Staples, R.C. (1987) An intact microtubule cytoskeleton is necessary for mediation of the signal for cell differentiation in *Uromyces. Eur.J.Cell Biol*. **45:**209-218.

Hofte, H., and Chrispeels, M.J. (1992). Protein sorting to the vacuolar membrane. *Plant Cell* **4:**995-1004.

Holliday, R (1974) *Ustilago maydis*. In King,R.C. (ed.), *Handbook of Genetics*, Vol. 1. *Plenum Press*, *New York, NY*, pp. 575–595.

Horton, R.M., Hunt, H.D., Ho, S.N., Pullen, J.K., and Pease, L.R. (1989) Site-directed mutagenesis by overlap extension using the polymerase chain reaction. *Gene* **77**(1): 61-8.

Jia, Y., McAdams, S.A., Bryan, G.T., Hershey, H.P., and Valent, B.(2000) Direct interaction of resistance gene and avirulence gene products confers rice blast resistance. *The EMBO J*. **19**:4004-4014.

Jones, D.A., Thomas, C.M., Hammond-Kosack, K.E., Balint-Kurti, R.J., and Jones, J.D.G. (1994) Isolation of the tomato Cf-9 gene for resistance to *Cladosporium fulvum* by transposon tagging. *Science* **266:**789–793.

Joosten, M., Hendrickx, L. and De Witt, P (1990) Carbohydrate composition of apoplastic fluids isolated from tomato leaves inoculated with virulent or a virulent races of *Cladosporium fulvum* (syn. *Fulvia fulva*). *Neth. J. Plant Pathol.* **96**:103– 112.

Kaemper et al., (2006) Insights from the genome of the biotrophic fungal plant pathogen *Ustilago maydis Nature.* **444**(2): 97-101

Kahmann, R., Steinberg G., Basse, C., Kämper, J. (2000) *Ustilago maydis*, the causative agent of corn smut diseas. In: Fungal Pathology. *Kronstad, J.W. (ed.) Kluwer academic publishers, Dodrecht, The Netherlands*, pp. 347-371

Kahmann, R., Steinberg, G., Basse, C., Feldbrügge, M., and Kämper, J.(2000) *Ustilago maydis*, the causative agent of corn smut disease. In Fungal Pathology *(J.W. Kronstad, ed.) Kluwer Academic publishers, Dordrecht*, pp.347-371

Kamoun, S. (2006) A Catalogue of the Effector Secretome of Plant Pathogenic Oomycetes. *Annu. Rev. Phytopathol*. **44**:41-60.

Kapila, J., De Rycke, R., Van Montagu, M., and Angenon, G.(1997). An *Agrobacterium*-mediated transient gene expression system for intact leaves. *Plant Sci*. **122**:101-108.

Katagiri, F., Thilmony, R., and He, S.Y. (2002) in The *Arabidopsis* Book, eds. Somerville, C.R. and Meyerowitz, E.M. *(Am. Soc. Plant Biologists, Rockville, MD)* doi/10.1199/tab. 0039.

Kemen, A.C. (2006) RTP1p, eine neue Familie amyloid-ähnlicher Proteine. Dissertation, University of Konstanz.

Kemen, E. (2006) Cytologie und Funktion eines amyloidähnlichen Proteins aus Rostpilzen. Dissertation, University of Konstanz.

Kenny, A.P., Enver,T., Ashworth, A. (2005) Receptor and secreted targets of Wnt-1/β-catenin signalling in mouse mammary epithelial cells. *BMC Cancer*. **5**:3.

Klein, T.M., Wolf, E.D., Wu, R., and Sanford, J.C. (1987). High-velocity microprojectiles for delivering nucleic acids into living cells. *Nature* **327**:70 – 73.

Koncz, C., and Schell, J. (1986). The Promoter of TL-DNA Gene 5 Controls the Tissue-Specific Expression of Chimeric Genes Carried by a Novel Type of *Agrobacterium* Binary Vector. *Mol. Gen. Genet.* **204:**383-396.

Kronstad J.W., and Leong S.A. (1990)The *b* mating-type locus of *Ustilago maydis* contains variable and constant regions. *Genes Dev*. **4**:1384–1395.

Lazo G.R., Stein P.A., and Ludwig R.A. (1991) A DNA transformation-competent *Arabidopsis* genomic library in *Agrobacterium*. *Bio-Technology*. **9**:963–967.

Leister, R.T., Ausubel, F.M. and Katagiri, F. (1996) Molecular recognition of pathogen attack occurs inside of plant cells in plant disease resistance specified by the *Arabidopsis* genes RPS2 and RPM1. *Proc. Natl. Acad. Sci. USA.* **93:**15497–15502.

Link, T., Lohaus, G., Heiser, I., Mendgen, K., Hahn, M. and Voegele, R.T. (2005) Characterization of a novel NADP+-dependent D-arabitol dehydrogenase from the plant pathogen Uromyces fabae. *Biochemical Journal* **389:**289-295.

Maier, W., Begerow, D., WeiB, M., and Oberwinkler, F. (2003) Phylogeny of the rust fungi: an approach using nuclear large subunit ribosomal DNA sequences. *Can J Bot*. **81** (1): 12–23.
Maizel, A. and Weigel, D. (2004) Temporally and spatially controlled induction of gene expression in *Arabidopsis thaliana*. *Plant J.* **38**:164–171.

Manning, V.A., and Ciuffetti, L.M. (2005) Localization of Ptr ToxA Produced by Pyrenophora *tritici-repentis* Reveals Protein Import into Wheat Mesophyll Cells. *Plant cell*. **17**:3203-3212

Maras, M., van Die, I., Contreras, R., and van den Hondel, C.A. (1999) Filamentous fungi as production organisms for glycoproteins of bio-medical interest. *Glycoconj* **16:**99–107.

Marchal, C., Haguenauer-Tsapis, R., and Urban-Grimal, D. (1998) A PEST-like sequence mediates phosphorylation and efficient ubiquitination of the yeast uracil permease, *Mol. Cell. Biol*. **18**:314-321.

McNellis, T.W., Mudgett, M.B., Li, K., Aoyama, T., Horvath, D., Chua, N. H. and Staskawicz, B. J. (1998) Glucocorticoid-inducible expression of a bacterial avirulence gene in transgenic *Arabidopsis* induces hypersensitive cell death**.** *Plant J.* **14:**247-257.

Medintz, I., Wang, X., Hradek, T., and Michels, C.A. (2000) A PEST-like sequence in the N-terminal cytoplasmic domain of Saccharomyces maltose permease is required for glucose-induced proteolysis and rapid inactivation of transport activity., *Biochemistry* **182**:518-4526**.**

Mendgen K (1981) Nutrient uptake in rust fungi. *Phytopathology* **71**: 983–989.

Merkle, T., Leclerc, D., Marshallsay, C. and Nagy, F. (1996) A plant *in vitro* system for nuclear import of proteins. *Plant J*. 10:1177-1186.

Mills, L.J, and Kotzé, J.M. (1981) Scanning electron microscopy of the germination, growth and infection of *Ustilago maydis* on maize. *Phytopathol Z*. **102:**21–27.

Mitchell, D., and Bell, A. (2003) PEST sequences in the malaria parasite *Plasmodium falciparum*: a genomic study. *Malaria J.* **2** (16): [5 pp].

Mota, L.J., and Cornelis, G.R. (2005) The bacterial injection kit: type III secretion systems. *Ann. Med.* **37**: 234–249.

Mota, L.J., Sorg, I., and Cornelis, G.R (2005b) Type III secretion: the bacteria-eukaryotic cell express. *FEMS Microbiol Lett*. **252:**1-10.

Mudgett, M.B (2005) New insights to the function of phytopathogenic bacterial type III effectors of plants. *Annu Rev Plant Biol*. **56:**509-531.

Mueller, C.A., Broz, P., Mueller, S.A., Ringler, P., Erne-Brand, F., Sorg, I., Kuhn, M., Engel, A., and Cornelis, G.R. (2005). The V-Antigen of Yersinia Forms a Distinct Structure at the Tip of Injectisome Needles. *Science* **310:**674-676.

Negrutiu, I., Shillito, R., Potrykus, I., Biasini, G., and Sala, F. (1987). Hybrid genes in the analysis of transformation conditions. I. Setting up a simple method for direct gene transfer in plant protoplasts. *Plant Mol. Biol.* **8:** 363-373.

Nimchuk Z., Marois E., Kjemtrup S., Leister R.T., Katagiri F., Dangl J.L. (2000)Eukaryotic fatty acylation drives plasma membrane targeting and enhances function of several type III effector proteins from *Pseudomonas syringae*. *Cell*. **101**:353–363.

Nomura K., DebRoy S., Lee Y.H., Pumplin N., Jones,J., He S.Y (2006) A bacterial virulence protein suppresses host innate immunity to cause plant disease. *Science* **313**:220-223.

Panstruga.**R** (2004) A golden shot: how ballistic single cell transformation boosts the molecular analysis of cereal-mildew interactions. *Mol. Plant Pathol.* **5**(2):141-148.

Penninckx, I.A.M.A., Thomma, B.P.H.J., Buchala, A., Metraux, J.P., and Broekaert, W.F. (1998). Concomitant activation of jasmonate and ethylene response pathways is required for induction of a plant defensin gene in *Arabidopsis*. *Plant Cell* **10:**2103–2113.

Perlmutter, D.H. (1999). Misfolded proteins in the endoplasmic reticulum. *Lab*. *Investig*. **79:**623–638.
Punt, P. J., van Biezen, N., Conesa, A., Albers, A., Mangnus, J., and van den Hondel, C. (2002) Filamentous fungi as cell factories for heterologous protein production. *Trends Biotechnol*. **20:**200–206.

Rechsteiner M, Rogers S.W (1996) PEST sequences and regulation by proteolysis**.** *Trends Biochem Sci.* **21:**267-271.

Rechsteiner, M., and Rogers, **S. W.** (1996) PEST sequences and regulation by proteolysis. *Trends Biochem. Sci.* **21:**267–271.

Rehmany,A.P., Gordon, A., Allen, R.L., Armstrong, M.R., Whisson, S.C., Kamoun, S., Tyler, B.M., Birch, P.R.J., and Beynon, J.L (2005) Differential recognition of highly divergent downy mildew avirulence gene alleles by RPP1 genes from two *Arabidopsis* lines. *Plant Cell* **17**(6): 1839–1850.

Ridout, C.J., Skamnioti, P., Porritt, O., Sacristan, S., Jones J.D., and Brown, J.K. (2006) Multiple avirulence paralogues in cereal powdery mildew fungi may contribute to parasite fitness and defeat of plant resistance. *Plant Cell*. **18**(9):2402-14.

Rogers, S., Wells, R and Rechsteiner, M. (1986) Amino acid sequences common to rapidly degraded proteins: the PEST hypothesis *Science* **234:**364-368.

Roslan, H.A,. Salter, M. G., Wood, C.D., White, M.R.H., Croft, K.P., Robson, F., Coupland, G., Doonan, J., Laufs, P., Tomsett, A.B., and Caddick, M.X. (2001) Characterisation of the ethanol-inducible alc gene expression system in *Arabidopsis thaliana*. *Plant J*. **28**:225-235.

Sambrook, J., Fritsch, E.F., and Maniatis, T. (1989). *Molecular cloning: a Laboratory Manua*l, 2nd edn. *Cold Spring Harbor Laboratory Press, Cold Spring Harbor, New York*.

Smith, H.M.S., and Raikhel, N.V. (1999) Protein targeting to the nuclear pore. What can we learn from plants? *Plant Physiol.* **119**:1157-1163.

Snetselaar, K.M., and Mims, C.W. (1993) Infection of maize stigmas by *Ustilago maydis*: light and electron microscopy. *Phytopathol.*. **83**:843–850.

Somers, D.A., Samac, D.A., and Olhoft, P.A. (2003) Recent Advances in Legume Transformation. *Plant Physiol*. **131:**892–899.

Steinmann, T, Geldner, N., Grebe, M., Mangold, S., Jackson, C.L., Paris, S., Galweiler, L., Palme, K., and Jurgens, G (1999) Coordinated polar localization of auxin efflux carrier PIN1 by GNOM ARF GEF. *Science*. **286:**316-318.

Tiburzy, R., Martins, E.M.F.M., and Resener, H-J (1992) Isolation of haustoria of puccinia graminis f. sp. tritici from wheat leaves. *Exp. Mycol*. **16:**324-328.

Tsuji, G., Fujii, S., Fujihara, N., Hirose, C., Tsuge, S., Shiraishi, T., and Kubo, Y (2003) *Agrobacterium tumefaciens*-mediated transformation for random insertional mutagenesis in *Colletotrichum lagenarium*. *J Gen Plant Pathol* **69:**230-239.

Tyers, M., and Jorgensen, P. (2000) Proteolysis and the cell cycle: with this RING I do thee destroy. *Curr Opin Genet Dev.* **10:**54-64.

Van der Hoorn, R.A.L., Laurent, F., Roth, R. and De Wit, P.J.G.M. (2000). Agroinfiltration is aversatile tool that facilitates comparative analyses of *Avr9/Cf-9*-induced and *Avr4/Cf-4*-induced necrosis. *Mol. Plant Microbe Interact*. **13**:439-446.

Voegele, R.T. (2006) Uromyces fabae:development,metabolism, and interactionswith its hostVicia faba. *FEMS Microbiol Lett.* **259**:165–173.

Wessels, J.G.H. (1990) Cell wall architecture and fungal tip growth, p. 1-29. *In*In I. B. Heath (ed.), Tip growth in plants and fungal cells. *Academic Press, San Diego, Calif*.

Xiang, C., Han, P., Lutziger, I., Wang, K., and Oliver, D.J (1999) A mini binary vector series for plant transformation. *Plant Mol Biol***. 40:**711–717.

Yang, B., Zhu, W., Johnson, L.B. and White, F.F. (2000) The virulence factor AvrXa7 of *Xanthomonas oryzae* pv. *oryzae* is a type III secretion pathway-dependent nuclear-localized double-stranded DNA-binding protein. *Proc. Natl Acad. Sci. USA*, **97**:9807– 9812.

Zhu, W., Yang, B., Chittoor, J.M., Johnson, L.B., and White, F.F. (1998) AvrXa10 contains an acidic transcriptional activation domain in the functionally conserved C terminus. *Mol. Plant Microbe Interact*. **11**:824–832.

9 Acknowledgements

I would like to express my gratitude to Prof. Matthias Hahn for the opportunity to carry out my thesis in his laboratory, for his continuous support and our fruitful discussions in the course of my research work. I would like to thank Prof. Ekkehard Neuhaus for his scientific advice and his contribution in financing the third year of my PhD work.

I am grateful to Prof. Jörg Kämper and Dr. Jan Schirawski at Max Planck Institute, Marburg, for providing plasmids, promoters and help with *Ustilago* transformation. Many thanks for the fruitful collaboration of Prof. Kurt Mendgen laboratory in Konstanz, special thanks to Dr. Ralf Vögele, Ariane Kemen and Eric Kemen for our continuous scientific discussions and their critical point of view and interest in my work.

My lab members Christa Jung, Matthias Kretschmer, Klaus Klug, Annette Fuchs and Astrid Bickmann deserve a special mention of thanks for always lending a helping hand. I wish to thank all present and past members of the Hahn lab: Sandra Grille, Oli Rui, Nele Ilmberger, Sara Mazzotta, Andreas Böhm, Gunther Döhlemann, Holger Reis, Michaela Leroch, Andreas Mosbach, Astrid Schamber, Janine Diwo, Manti Schwarzkopf, Melanie Wiwiorra, Steffi Pfiffi and Steffi Treitschke. I am thankful to members of Prof. Neuhaus lab for letting me use their supplies and equipments.

My special regards go to family Raab and family Heydt for their friendship offered to me during my stay in Kaiserslautern.

Last, but not the least, I cannot express in words how grateful I am to my wonderful family for their constant encouragement and support from so far away.

CURRICULUM VITAE

Name Maryam Rafiqi
Date of birth 25/02/1977
Nationality Moroccan

Professional Education

2003-2007	PhD. University of Kaiserslautern, Germany .
1999-2002	Master Degree in Horticultural Genetics and Biotechnology. MAICH, Greece .
June 1999	BSc in Agronomy, Institut Agronomique et Vétérinaire Hassan II. Rabat, Morocco.

Research Experience

2003-2007	PhD Research Project "Functional and structural analyses of RTP1, a rust haustorial protein transferred into host plant cells", in the laboratory of Prof. Dr. Matthias Hahn at the Department of Phytopathology, University of Kaisreslautern, Germany.
2002-2003	Training project "The diversity of Arbuscular Mycorrhizal Fungi in the Swiss Alps" at the University of Basel, Switzerland.
2002	Training project "Chloroplast gene expression" at Ruhr University, Bochum, Germany.
1999-2002	Master Degree Research Project "*Agrobaterium*-mediated transformation of carnation", in the laboratory of Dr. Panagiotis Kalaitzis. Mediterranean Agronomic Institute, Chania, Greece
2001	Training Project in "*Agrobaterium*-mediated transformation of carnation" in the laboratoty of Dr. Tineke Creemers, Plant Research International, Wageningen, Netherlands
1996	Training project "Integrated Pest Management", Agricultural company. Agen, France.

Publications

Kemen, E., Kemen, A.C., Rafiqi, M., Hempel, U., Mendgen, K., Hahn, M. and Voegele Ralf, R.T. (2005) Characterization of a protein from rust fungi that is transferred from haustoria into the plant host cell. *Mol. Plant-Microbe Interact*. **18**: 1130-1139.

Other results of my PhD work are pending on publication.

Other experiences

Oct 2006	Oral presentation "Structural and functional studies of a protein transferred from rust haustoria into the host plant cell". 1st Meeting of Biology of Yeasts and Filamentous Fungi, 2006, Frankfurt
2003-2006	Part-time supervising at the University of Kaiserslautern. Practical course in Plant Physiology (3^{th} semester students), practical course in Plant Molecular Pathology (8^{th} semester students).